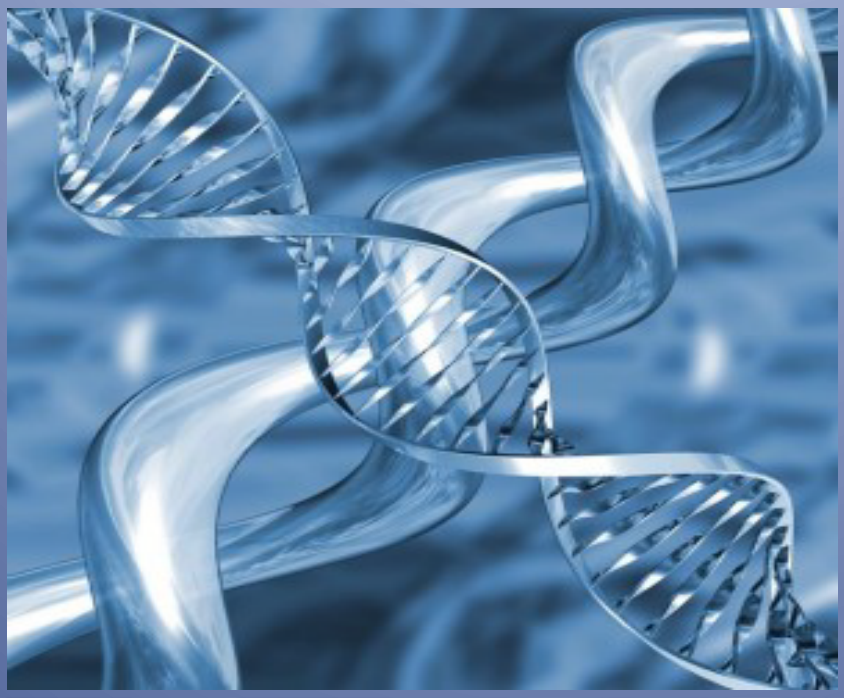

Epigenetic control of antioxidant gene expression

Tesis Doctoral Brigitte Wild Madrid 2015

Universidad Autónoma de Madrid

Departamento de Biología Molecular

Universidad Autónoma de Madrid
Departamento de Biología Molecular
Facultad de Ciencias

Epigenetic control of antioxidant gene expression

Memoria de Tesis Doctoral presentada por

Brigitte Wild

Licenciada: DEA Biologie moleculaire et cellulaire IGBMC Strasbourg

Para optar al grado de Doctor por la
Universidad Autonoma de Madrid

Directora de Tesis: Dr. María Monsalve Pérez

MADRID 2015

Instituto de Investigaciones Biomédicas “Alberto Sols”


EVERY
JOURNEY
NEEDS
A FIRST
STEP

Acknowledgments

There are many people who you connect with during a thesis.

Some will support you with the scientific part and some just make your journey more enjoyable which also means a lot. To all of them I want to give my thanks. For those who know me well, they will already know how much I appreciate them.

First, of course, I would like to thank my parents; without them, I would not be where I am nor would I be who I am. You aroused my scientific curiosity that brought me to where I am today. Thank you.

For Maria Monsalve (MM), I reserve a special acknowledgement. I learned a lot during these years of research. I believe, in many ways, I've grown a lot, and much of this has been from your example.

There have been many colleagues with whom I shared many hours, weeks and weekends and all of MM's lab has been there for me, when needed.

To Alberto, always to the point with his comments, a really inspirational character and my first Spanish teacher, I still have the post it! To Nieves, with her special microscopy skills and humor. To Yoli, for teaching me "paciencia" among other things. To Cris for transferring her knowledge on Hepatocytes to me and her positive energy. And to Nacho for the special WB summer.
Thank you all for having made these years a nice and enjoyable trip.

A special thanks for all the help and support to all of the CNIC and IIB members that have been involved and took part in this project from near and far: Melissa, Raphael, Alicia, Julie, Alberto, Carlos, Fatima,…

Thanks to everyone around during the drafting. Thank you all for your input, hours, "sonrisas" to overcome desperation.
Stephen (big big thanks for everything), Marjolain, Marta, Claudia, Carole, Andrès, Paul, Jaume, Stephanie, Mélanie, Chantal, Jochen, Laure,…

I hope our paths keep on crossing again and again and hope we will be able to share these nice memories over and over.

Thank you all for being part of this special ADVENTURE of once in a life time!!!!!!

Summary

To respond to exogenous and endogenous stimuli, organisms have developed a variety of mechanisms to modulate the quantity, duration and the type of response to these stimuli. Of these mechanisms, one of the most important is the regulation of gene expression. This regulation of gene expression occurs at various levels but especially by the employment of different transcription factors and cofactors. Transcription factors interact with specific sequences within the regulated genes. The way in which co-factors act can be very diverse and are generally less known.

The present work aims to analyse the mechanisms used by cells to regulate gene expression for reactive oxygen species (ROS) detoxification genes, and in particular, the mechanisms controlling the activity of the two co-factors SirT1 and PGC-1α on those genes. PGC-1α was first discovered as a regulator of biogenesis and mitochondrial activity. Later, it was demonstrated that PGC-1α operated as an expression coordinator of a group of genes controlling ROS levels and therefore prevented the accumulation of oxidative stress due to its binding to the transcription factor FoxO3a. Moreover, SirT1 was first discovered as a Histone deacetylase, involved in the regulation of genomic stability. Later on, SirT1 was shown to regulate activity of other proteins, specifically transcription factors or cofactors such as PGC-1α.

The first aim of the work presented in this thesis was to determine if SirT1 collaborates with PGC-1α in regulating antioxidant genes and to find out through which mechanisms this regulation is mediated. The results demonstrate not only that SirT1 deacetylates PGC-1α and FoxO3a, but also that all three proteins together form an efficient ternary transcription elongation complex recruited to the regulating regions of the target antioxidant genes. After recruitment to the regulating regions, SirT1 deacetylates the nearby histones; this specific deacetylation does not lead to a gene silencing. However the exact mechanism of regulation is still not clear and remains to be elucidated. These results show for the first time that SirT1 can not only lead to a general silencing of chromatin, but can also induce specific gene expression when involved in a specific transcription complex.

PGC-1α has a RNA recognition motif (RRM) whose deletion abolishes some of the transactivation capacity of PGC-1α. The second aim of this work was to study the functionality of this motif in the specific context of regulating antioxidant genes. The results showed that some genes are more sensitive to the absence of RRM than others. To have a global overview of the genomic functionality of the RRM, a complete genome microarray expression analysis comparing wild-type PGC-1α protein to the PGC-1α protein lacking the RRM was performed. The observation that the deletion of the PGC-1α RRM differentially affects genes regulated by PGC-1α suggests that the RRM could be involved in selection of 3'UTR and as a consequence modify RNA transcripts.

The final aim of this study was to confirm and identify RNA species binding to PGC-1α RRM. The technique applied to confirm and identify these RNA species was high throughput cross-linked immuno-precipitation (HITS-CLIP). The use of HITS-CLIP confirmed binding of RNA to PGC-1α. The presence of RRM suggests preferential transcription of some protein isoforms. The combination of the obtained results from array and RNA sequencing support this hypothesis.

In summary, this study not only gives detailed information about ROS detoxification gene regulation by PGC-1α but also allowed the identification of new mechanisms of action for SirT1 and PGC-1α.

Presentación

Para responder de manera adecuada a estímulos exógenos y endógenos, los organismos han desarrollado diversos mecanismos los cuales permiten variar tanto la cantidad como el tipo de repuestas. Entre estos mecanismos se encuentran aquellos que permiten regular la expresión génica. Esta ocurre a varios niveles y a través de distintos tipos de factores, siendo los más importantes los factores de transcripción y los cofactores. Los factores de transcripción actúan reconociendo secuencias específicas en los genes regulados. Los cofactores operan a través de mecanismos muy variados y, en general, estos son más desconocidos.

La presente Tesis analiza los mecanismos por los cuales la célula regula la expresión de los genes implicados en la destoxificación de especies reactivas de oxígeno (ROS). En primer lugar se determinaron los mecanismos que median la actividad de los cofactores SirT1 y PGC-1α sobre estos genes. Inicialmente el cofactor PGC-1α se describió como regulador de la biogénesis y de la actividad mitocondrial. Posteriormente, se demostró que PGC-1α regula de manera coordinada la expresión de un grupo de genes encargados de controlar los niveles de ROS y prevenir la aparición de estrés oxidativo a través de su interacción con el factor de transcripción FoxO3a. Por otra parte, el cofactor SirT1 se describió primeramente como una desacetilasa de histonas, responsable de la regulación de la estabilidad genómica, pero después se determinó que SirT1 puede también regular la actividad de otras proteínas, y en concreto, de factores de transcripción como PGC-1α. El primer objetivo de este trabajo fue determinar si SirT1 colaboraba con PGC-1α en la regulación de genes antioxidantes y a través de que mecanismo.

Este estudio ha permitido demostrar que SirT1 no solo desacetila PGC-1α y FoxO3a, sino que forma con ellos un complejo ternario de elongación transcripcional más eficiente que es reclutado a las regiones reguladoras de los genes diana. Tras su reclutamiento, SirT1 desacetila las histonas próximas, pero esta desacetilación no va asociada a silenciamiento génico, el cual ocurre a través de un mecanismo desconocido. Estos resultados muestran por primera vez que más allá de la capacidad de SirT1 de inducir un silenciamiento general de la cromatina, puede además tener un efecto inductor en la expresión de genes específicos cuando forma parte de complejos de regulación transcripcional.

PGC-1α contiene un dominio de unión a RNA (RNA recognition motif; RRM) cuya deleción compromete la capacidad transactivadora de PGC-1α. El segundo objetivo de este trabajo fue estudiar la funcionalidad de este dominio en el contexto específico de la regulación de genes antioxidantes. Se concluyó que algunos genes son más sensibles a la deleción de este dominio y que el coactivador TLS es capaz de activar PGC-1α solo en algunos de ellos.

Con el fin de tener una visión global a nivel genómico de la funcionalidad del RRM, se realizó un análisis de expresión con microarrays de genoma completo, comparando la actividad de la proteína WT con el mutante en la region RRM. Se observó que la deleción del dominio afecta de forma diferencial a los genes regulados por PGC-1α, sugiriendo así que el dominio RRM podría afectar a la selección del 3'UTR y alterar la estabilidad del transcrito.

El último objetivo de esta Tesis fue el de confirmar e identificar qué especies de ARN se unen al RRM de PGC-1α. Para ello, se utilizó la inmunoprecipitación con entrecruzamiento covalente apareada de alto rendimiento (HITS-CLIP), la cual confirmó la unión del ARN a la proteína PGC-1α. La presencia del RRM sugiere la transcripción preferencial de ciertas isoformas de la proteína. La combinación de los resultados obtenidos mediante arrays de ARN y la secuenciación de ARN apoyan esta hipótesis.

En conclusión, los resultados obtenidos en este trabajo no solo proporcionan información detallada sobre la regulación de la expresión de genes antioxidantes, sino que también han permitido identificar dos nuevos mecanismos de acción para los cofactores SirT1 y PGC-1α.

Content

List of Acronyms

List of Acronyms

Ac: acetylation
Ad: adenoviruses
ADP: adenosine diphosphate
AMP: adenosine monophosphate
AMPK: AMP kinase
ANOVA: analysis of variance
aRNA: anti-sense RNA
ATP: adenosine triphosphate
BAEC: Bovine aortic endothelial cells
BAT: brown adipose tissue
BLAST: basic local alignment search tool
BlastN: nucleotide database alignment tool
bp: base paire
cAMP: cyclic
CAR: constituve active/androstane receptor
casiRNA: *cis*-acting siRNA
CBP: CREB binding protein
cDNA: complementary DNA
CEBPB: CCAAT/enhancer binding protein β
ChIP: Chromatin Immunoprecipitation
CLIP: cross-linked immuno-precipitation
CLIP: Crosslinking Immunoprecipitation
ClustaW: multisequence alignement tool
co-IP: co-immunoprecipitate
CREB: cAMP-response element binding protein
CTD: carboxyl-terminal domain
CTDS2P: CTD serine-2 phosphorylated of DNA-dependent RNA polymerase II
CTDS5P: CTD serine-5 phosphorylated of DNA-dependent RNA polymerase II
CUT: cryptic unstable transcripts
DBE: DNA binding elements
diRNA: DSB-induced small RNA
DNA: Deoxyribonucleic acid
dNTP: desoxynucleoside triphosphate
DPE: downstream core promoter element
dsDNA: double stranded DNA
DUB: deubiquitinases
endo-siRNA: endogenous siRNA
EtBr: Ethidium bromide
ETC: electron transport chain
exo-siRNA: exogenous siRNA
FAO: rat hepatoma cell line
FoxO3a
GAF: GAGA associated factor
GAPDH: glyceraldehyde 3-phosphate dehydrogenase
GCN5
GNAT: Gcn5-related N-acetyltransferases
GST: Glutation S-transferase
H4K16Ac: H4 on lysine 16
HA: hemagglutinin
HAT: histone acetyl transferases
hc-siRNA: heterochromatic siRNA
HDAC: histone deacetylases
HEK-293A: human embryonic kidney cell line
HITS-CLIP: high throughput sequencing cross-linked immuno-precipitation
HNF4, GR and FOXO1
Inr: initiator
IP: immunoprecipitation
IR: insulin receptor
IRE: insulin response element
ISWI: imitation (SWI) switch-based complexes
K: lysine
KO: knock out
Me: methylation
MEF: Mouse Embryonic Fibroblasts
miRNA: microRNA precursors
MMLV: Moloney murine leukemia virus
Moi: multiplicity of infection
mRNA: messenger RNA
MYST: named after its founding members MOZ, Ybf2/Sas3, Sas2, and Tip60
NaMN: nicotinic acid mononucleotide
natsiRNA: natural antisense transcript siRNA
NR: nuclear receptor

nt: nucleotides

PARG: poly-ADP-ribose glycohydrolases

PARP: poly(ADP) ribose polymerase

PARP: poly-ADP-ribosyltransferases

PDH: pyruvate dehydrogenase

PFU: plaque-forming units

PGC-1α: peroxisome proliferator-activated receptor gamma (PPARγ)-co-activator 1 alpha

Ph: phosphorylation

PI3K: phosphatidylinositol 3-kinase

PIC: pre-initiation complex

piRNA: Piwi-associated small RNA

PKA: protein kinase A

PRC: PGC-1-related coactivator

pre-rRNA: precursor ribosomal RNA

Prx3: peroxiredoxins 3

Prx5: peroxiredoxins 5

P-TEFb: positive transcription elongation factor b

PTM: post translational modification

PVDF: polyvinyliden fluoride

PXR: pregnane X receptor

qiRNA: QDE-2-interacting small RNA

qRT-PCR: real time PCR of reverse transcribed cDNA

R: arginines

RNA: ribonucleic acid

RNAP: DNA-dependent RNA polymerases: RNAP I, II, II, IV.

RNA-seq: RNA sequencing

ROS: reactive oxygen species

RRM: RNA recognition motif

rRNA: ribosomal RNA

RS domain: Arginine Serine domain

RT: reverse transcriptase

S: serine

sbRNA: stem bulge RNA

scnRNA: small scan RNA

SD: standard deviation

SDS-PAGE: sodium dodecyl sulfatepolyacrylamide gel electrophoresis

shRNA: silencing RNA

SIM: SUMO interaction motifs

siRNA: small interfering RNA

SirT1: sirtuin 1

snoRNA: small nuclear RNAs

snoRNA: small nucleolar RNA

snRNA: spliceosomal small nuclear RNAs

sod2-MnSOD*:* mitochondrial Mn^{2+} superoxide dismutase

ssRNA: single stranded RNAs

SUMO: small ubiquitin-related modifier

SWI/SNF: switch genes/sucrose non-fermentors family

T: threonines

tasiRNA: *trans*-acting siRNA

TBP: TATA-binding protein

TCA: tricarboxylic acid cycle

TF: transcription factor

TLS: Translocated in liposarcoma

TR2: thioredoxin reductase 2

tRNA: transfert RNA

Trx2: thioredoxin 2

UCP-2: uncoupling protein 2

UCPs: uncoupling proteins

UTR: 5' untranslated region

UV: ultraviolet

vtRNA: vault RNA

WB: Western blot

WCE: whole cell extracts

WT: wild type

Introduction

Introduction

1. Regulation of chromatin structure and gene expression

In 1958 Francis Crick introduced the Central Dogma of Molecular Biology as the key concept behind gene expression regulation (Crick F 1970; Thieffry D and Sarkar S 1998, Figure 1.1).

Figure 1.1: Concept of gene expression

Deoxyribonucleic acid (DNA), the blueprint of life, produces molecules called ribonucleic acid (RNA) by a mechanism called transcription. RNA translates the genes encoded in DNA (genotype) into proteins and regulation of RNA levels is determinant in the modulation of protein levels and the cellular response to extracellular and intracellular stimulus.

There are several classes of RNA, all of which undergo transcription via specific transcription complexes in which RNA polymerases play a central role. In eukaryotic cells there are different RNA polymerases, of which RNA polymerase II (RNAP II) is responsible for the transcription of a class of RNAs called messenger RNAs (mRNA) that include most protein coding RNAs. The concept of mRNA as the intermediate carrier of information in protein synthesis was first proposed by F. Jacob and J. Monod (Jacob 1961) and experimentally confirmed by S. Brenner, F. Jacob and M. Meselson (Brenner *et al.* 1961).

The complete process of gene expression regulation is complex, highly dynamic and discontinuous involving modulation of three main checkpoints, transcription initiation, elongation, and termination. The transcription cycle will be described in detail in Introduction Section 1.2.3. Due to the complex nature of DNA packaging (chromatin structure), a multitude of transcription factors (that bind specific DNA sequences) and co-activators (do not bind DNA or do so in a non-sequence specific manner) with a multitude of different activities are needed for efficient and specific transcription.

The presented work will focus on the mechanisms of transcriptional regulation by two transcriptional co-activators, peroxisome proliferator-activated receptor gamma (PPARγ)-co-activator 1 alpha (PGC-1α), and sirtuin SirT1, and their role in the regulation of target gene expression via transcription factors, histone code regulation and their interactions with the transcriptional machinery.

1.1. Chromatin structure

The enormous length of the eukaryotic genome requires for its stability that it is packaged in structures that can be replicated and propagated during mitosis. Furthermore, it is essential that this packaged structure remains sufficiently malleable and modifiable to enable access to genetic

information. Such a structure is acquired by the formation of chromatin, which contains DNA and its associated proteins.

The structured DNA is packed into a cellular structural unit located in the nucleus called the nucleosome. The nucleosome is a nucleoprotein complex consisting of 147 base pairs of DNA wrapped in a left-handed superhelix 1.7 times around an octamer of core canonical histones proteins H2A, H2B, H3 and H4 (2 molecules of each, Richmond TJ *et al.* 1984), arranged as an octamer in a "bead-on-a string" configuration (11 nm fiber) and stabilised by linker histones (H1, H1a, and H5, 40-70 bp of linker DNA). Nucleosomes are fundamental in gene expression control (Kornberg RD 1974). The different degrees of compaction are shown in Figure 1.2.

It is known that nucleosomes form a chromatin fiber (Finch J.T. and Klug A 1976), which can further compact into structures increasingly complex. Compactation reaches its peak during cell division with the formation of mitotic chromosomes (Felsenfeld and Groudine 2003).

Cytological examination of mitotic chromosomes distinguishes two types of chromatin known as euchromatin and heterochromatin. Heterochromatin is thought to be tightly condensed and thus inaccessible to DNA binding factors, unlike euchromatin which adopts a more relaxed conformation (Grewal SI and Moazed D 2003). Most highly transcribed genes are found in euchromatin regions.

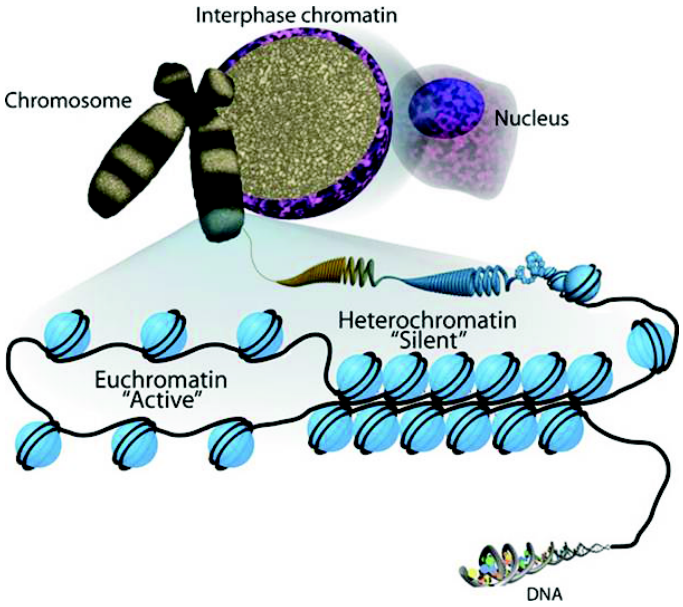

Figure 1.2: Hierarchical organisation of nuclear DNA structure in eukaryotes.

Chromatin structure can be altered by nucleosome remodeling enzymes, replacement of the core histones with specialised histone variants or by covalent modification of histones within the nucleosome. Covalent modification of histones will be discussed in further detail below.

The term "Epigenetic", first used by Conrad H. Waddington (1905–1975), as the junction of *epigenesis* and genetics has become a central concept of gene regulation in more recent years. The term "Epigenetic modifications" is now used to define all functionally-relevant modifications to the genome that do not alter the underlying DNA sequence, and which aim mainly to regulate gene

expression, but also DNA stability, replication and repair, and include not only histone modifications but also DNA modifications such as methylation.

1.1.1. DNA Modification: DNA methylation, CpG island, DNA methylases

Methylation is the main and first described DNA modification in vertebrates. DNA methylation occurs on the fifth carbon position of cytosine residues to yield 5-methylcytidine. This occurs almost exclusively within CpG dinucleotides. In the mammalian genome, approximately 70–80% of CpG dinucleotides are methylated. However, stretches of CpG-rich sequences with low levels of DNA methylation, known as CpG islands, do exist (Blackledge NP and Klose R 2011, Deaton AM and Bird A, 2011). DNA methylation is typically associated with epigenetic gene repression and many targets of de novo DNA methylation during differentiation (Weber M *et al***.** 2007, Mohn F *et al***.** 2008, Farthing CR *et al***.** 2008). DNA methylation also recruits methyl-CpG-binding proteins, which recruit additional proteins that add silencing modifications to neighboring histones.

Interestingly, CpG islands make up only 0.7% of the human genome but contain 7% of the CpG dinucleotides. CpG islands often are highly enriched in gene promoters. For example, approximately 60% of all mammalian gene promoters are CpG-rich. CpG islands are typically unmethylated, open regions of DNA with low nucleosome occupancy. As such, CpG islands promote relaxed chromatin structure that favors active transcription, known as euchromatin, and increases accessibility of RNAP II and other components of the basal transcription machinery to the transcription start site (see Section 1.2.3.).

The mechanisms that keep CpG islands free of methylation appear to involve binding of transcription factors and transcriptional machinery itself. However, according to recent studies, CpG islands can become hypermethylated (Meissner A *et al***.** 2008; Mohn F *et al***.** 2008) to silence specific genes during cellular differentiation, genomic imprinting and X chromosome inactivation. DNA methylation is catalyzed by DNA methyltransferases (DNMTs). Two DNMTs, DNMT3A and DNMT3B, are involved in de novo methylation (Okano M *et al***.** 1999) and are targeted to particular genomic regions by specific histone modifications (Pradhan S *et al***.** 1999).

1.1.2. Nucleosomes positioning and modifications

Nucleosome remodeling

In addition to its central structural role, nucleosomes are also key regulators of gene expression (Peterson CL and Laniel MA 1994, Imbalzano AN 1994). Generally speaking nucleosomes inhibit transcription by limiting the access of transcription complexes to DNA. Individual nucleosomes can be disrupted by ATP-dependent chromatin remodelling complexes which use the energy derived from ATP hydrolysis to perform their task (Smith CL and Peterson CL, 2005). A central activity in ATP-dependent chromatin remodelling complexes is performed by a helicase-like protein of the SWI/SNF (switch genes/sucrose non-fermentors) family. This class of helicases has also been divided into three

subfamilies based on primary sequence homology as well as the individual characteristics of the corresponding remodelling complexes: the SWI2/SNF2, ISWI and Mi-2/CHD families (Figure 1.3.; Smith and Peterson, 2005).

- The SWI2/SNF2 complexes have been implicated in the regulation of gene transcription in yeast but also mammalian organisms. The catalytic components contains bromodomains, which mediate interaction with acetylated histone tails. Mutations of SWI2/SNF2 complex components have been associated with tumor progression, in particular lung and gastric cancers. Aside from their role in transcriptional regulation, SWI2/SNF2 complexes have also been implicated in global chromatin structure control during mitosis when chromosomes undergo major structural changes.
- The ISWI (imitation SWI)-based complexes contain ATPases, which are characterised by a different histone-binding domain than SWI/SNF complexes, namely the SANT domain. Although they participate in transcriptional regulation, they have been implicated in global nucleosome assembly and positioning. This is likely to be coupled to replication as ISWI components co-localise with replication foci in mammalian cells. Furthermore, ISWI complexes are thought to be involved in transcriptional repression, as well as the formation of silenced regions on chromatin (Smith CL and Peterson CL, 2005).
- The ATPases of the third class of remodeling complexes, the Mi-2 family, contain another histone binding domain, the chromodomain. Many of the Mi-2 complexes are thought to participate in transcriptional repression by virtue of their association with histone deacetylases (Section 1.1.3.1.).

Histone variants

Gene regulation is controlled by changes in histones isoforms that make up the nucleosome. The several different histone isoforms can vary by a small number of amino acids or include large insertions (Sarma K and Reinberg D, 2005). Variants for all histones except H4 have been identified and are thought to have occurred through gene duplication (Gilbert N and Ramsahoye B 2005).

1.1.3. Covalent histone modifications

The covalent modification of the N-terminal tails of histones is an important mechanism used to regulate eukaryotic transcription and to fine-tune chromatin structure.

The Grunstein group lay the first cornerstone in the eventual description of this mechanism by showing that histone tails have specific functions. They found that between 14 and 38 amino terminal residues of each core histone extend outside the disk-shape complex as N and C terminal `tail' domains of histones. Various studies have shown that these tails are substrates for a collection of posttranslational modifications that determine whether a gene is on or off or whether its activity is high or low, including acetylation (Ac) and methylation (Me) of lysines (K) and arginines (R), phosphorylation (Ph) of serines (S) and threonines (T), ubiquitylation and sumoylation of lysines, and

ribosylation. At least three of these posttranslational modifications (Ac, Me, Ph) are believed to exert their function primarily by disrupting histone/DNA contacts in the nucleosome, thus altering chromatin structure directly; while there is evidence that modified histone tails serve as platforms for other DNA regulatory complexes via the recruitment of proteins (Jenuwein T and Allis CD 2001). The term "histone code" is used to describe the complex pattern of histone modifications and how different combinations of histone modifications affect transcription levels (Strahl BD and Allis CD 2000, Turner BM 2000, Jenuwein T and Allis CD 2001, Nakayama J *et al.* 2001). Identification of proteins that read, write or erase these marks is critical to help unravel the complexities of epigenetic regulation.

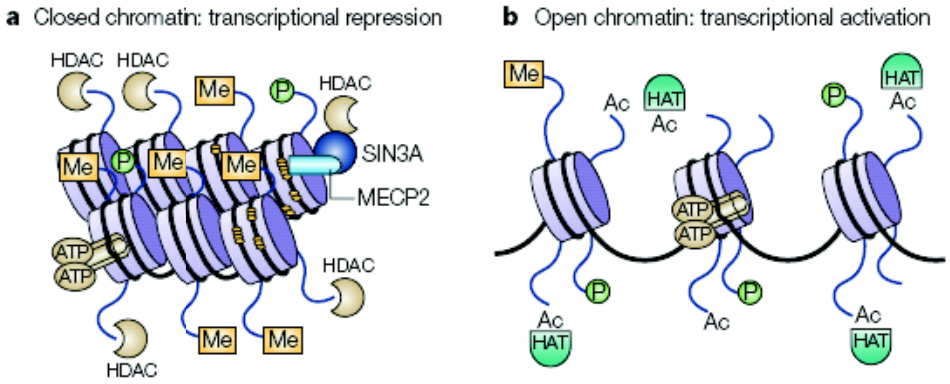

Figure 1.3. Chromatin structure regulates transcriptional activity.

The "Openness" of the chromatin, described as absence of nucleosomes or weak/unstable nucleosome binding, is crucial to allow and modulate the transcription rate of all genes (Figure 1.3.). When the chromatin is in an "open" conformation, the DNA is accessible to transcription factors and polymerase complexes, being a pre-requisite for effective transcription.

1.1.3.1. Histone acetylation and deacetylation

Lysine acetylation occurs on the N-terminal tails of core histones and is controlled primarily by two enzyme families: histone acetyl transferases (HATs) and histone deacetylases (HDACs).

- **HATs** use acetyl CoA as a cofactor to transfer an acetyl group to the epsilon amino group of the lysine side chain. HATs constitute a remarkably diverse class of enzymes that play significant roles in transcriptional regulation (Roth SY *et al.* 2001). Numerous studies have highlighted that this modification is strongly correlated with active gene transcription (Clayton AL *et al.* 2001). They are recruited to specific sites of the genome by sequence-specific transcription factors to regulate gene expression.

These enzymes are grouped into three sub-families: GNAT (Gcn5-related N-acetyltransferases), p300/CBP (CREB binding protein) and MYST (named after its founding members MOZ, Ybf2/Sas3, Sas2, and Tip60). The best characterised being p300/CBP.

- **HDACs** reverse histone acetylation and promote gene silencing. HDACs are often components of large protein complexes. Similarly to HATs, they are recruited to specific sites of the genome by sequence-specific transcription factors to regulate gene expression.

Four classes of deacetylases have been described. Class I, which includes HDAC 1, 2, 3 and 8; Class, II, which includes HDAC 4, 5, 6, 7, 9 and 10; Class III, which includes the NAD^+-dependent **sirtuins** (SIRTs, (Eckwall K 2005, de Ruijter AJ *et al***.** 2003); and Class IV, which includes HDAC11. Sirtuins will be addressed extensively in Section 2.3. Class I HDACs are ubiquitously expressed, whereas Class II HDACs are restricted to specific tissues and thus may be involved in differentiation.

Despite their name, it is now clear that deacetylation of proteins other than histones can be catalysed by HDACs, as is the case of HDAC6 which is associated with microtubules and deacetylates tubulin (Hubbert C *et al.* 2002).

Both HATs and HDACs act in the context of multicellular complexes, which target them to specific genomic sites where they participate in the regulation of gene transcription. Importantly, and in contrast to HATs, recombinant HDACs by themselves do not exhibit robust deacetylase activity, and rely on additional co-factors to catalize deacetylase reactions (de Ruijter AJ *et al*. 2003).

A plethora of studies have highlighted the connection between histone acetylation and transcriptional regulation and facilitated a deep understanding of how histone modifications control chromatin structure and gene expression. (Brownell JE *et al.* 1996, Kuo MH 1996, Taunton J *et al.* 1996). Generally speaking, euchromatin, which is associated with transcriptionally competent regions of the genome, contains high levels of acetylated histones whereas heterochromatin is characterised by histones in a hypoacetylation state (Grewal SI and Moazed D 2003). Importantly, misregulation of HATs and HDACs is often associated with development and progression of cancer and other diseases such as neurodegenerative disorders and cardiovascular diseases, making these enzymes attractive therapeutic drug targets.

1.1.3.2. Histone methylation

Unlike acetylation, which generally correlates with transcriptional activation, histone lysine methylation can signal either activation or repression (Martin C and Zhang Y 2005). Histone methylation occurs at lysine (K) residues, which can be mono-, di- or trimethylated, and arginine (R) residues, which can be mono- or dimethylated (Gilbert N and Ramsahoye B 2005).

To date, researchers have identified over 30 demethylating enzymes (Tsukada Y *et al.* 2006), over 50 protein lysine methyltransferases and over 10 protein arginine methyltransferases, suggesting that protein methylation is a dynamic and complex process (Janzen WP *et al*. 2010).

Histone methylation has different effects on transcriptional activity, depending on the number of methyl groups and on the position of the amino acid being modified. Although H3-K9, H3-K27, H4-K20 methylation usually correlates with silent chromatin, whereas H3-K4, H3-K36, H3-K79 mark

transcriptionally active chromatin, this general rule is subject to exceptions (Sims RJ 3rd *et al*. 2003, Vaquero A *et al*. 2003).

In general, the H3K9me1 mark is activating, whereas H3K9me2 and H3K9me3 are repressive; H3K4me3 and H3K36me3 are associated with active chromatin, whereas H3K9me3, H3K27me3, H3K36me2 and H4K20me1 are often found in transcriptional repressed heterochromatin. H3K4me3 recruits proteins that promote euchromatin formation, whereas H3K9me1, H3K9me2 and H3K27me3 interact with proteins that promote heterochromatin formation.

The downstream effects of histone methylation are largely determined by proteins that bind the modified histones.

1.1.3.3. Other Histone modifications: phosphorylation, ubiquitination, sumoylation, ADP-ribosylation

All histones, including H1, have been shown to be modified by phosphorylation. In particular, histones can be phosphorylated on serine, threonine and tyrosine residues. Many of the serine and threonine phosphorylation events play a role in DNA repair or DNA condensation, segregation and decondensation during mitosis, but some including H3T3ph, H3T6ph, H3T11ph, H2.AS1ph, H3S10ph and H4S41ph are involved in epigenetic regulation of transcription (Pérez-Cadahía *et al*. 2010). In addition to its DNA-restructuring responsibilities during mitosis, H3S10ph seems important for chromatin decondensation associated with transcriptional activation of target genes.

Compared to phosphorylation, histone ubiquitination is a less understood modification. Unlike previous modifications, ubiquitination occurs in the C-terminus of histones and consists of the conjugation of ubiquitin, a 76-amino acid protein, to lysine residues of histone proteins. This can affect transcription activity as well as nucleosome stability and, as a result, gene accessibility. The consequences of histone ubiquitination depend on the histone substrate and on the degree of ubiquitination (Weake VM and Workman JL 2008). Moreover, histone deubiquitination has been associated with both transcription activation (Nakagawa M *et al*. 2008, Draker R *et al*. 2011, Gutierrez-Marcos JF and Dickinson HG 2012) and repression (van der Knaap JA *et al*. 2005, van der Knaap JA *et al*. 2010). Ubiquitination of histones can be reversed by cleaving the peptide bond between ubiquitin and the ubiquitinated protein. Several deubiquitinases (DUBs) have been reported to deubiquitinate histones 2A, 2A.Z and 2B, including USP3, USP10, USP21, USP22 and Bap1.

An additional posttranslational modification that plays an important role in epigenetic regulation is sumoylation, which is the addition of the small ubiquitin-related modifier SUMO (Ouyang J and Gill G 2009). This modification can stabilize proteins, alter subcellular localization, affect enzyme activity and mediate interactions with other proteins. Many transcription factors and cofactors can be sumoylated, which is generally indicative of transcription repression. Many histone-modifying enzymes, nucleosome-remodeling complexes and their associated enzyme cofactors contain one or

more SUMO interaction motifs (SIMs). These motifs allow these proteins to interact with sumoylated transcription factors and cofactors, which can direct these enzymes to specific promoters.

Histone ADP-ribosylation occurs in glutamic acids in a polyglutamate stretch of single arginines (Vaquero A *et al.* 2003). Although mono-ADP-ribosylation can also occur, poly-ADP-ribosylation is relevant to histone function and can comprise more than 100 ADP-ribosyl moieties with extensive branching (Jacobson MK and Jacobson EL 1999). Poly ADP-ribosylation is a highly dynamic process catalyzed by poly-ADP-ribosyltransferases (PARPs) and removed by poly-ADP-ribose glycohydrolases (PARGs). PARP activity requires NAD^+ and one of its enzymatic products is nicotinamide both are features of the enzymatic reaction catalysed by sirtuin deacetylases and related to energy demand (Sections 1.1.3.1. and 2.3.).

1.1.3.4. Histone code

Most of the histones modifications mentioned above work in a coordinated manner. In fact, it has been demonstrated that site-specific combinations of histone modifications correlate well with particular biological functions (Peterson CL and Laniel MA 2004). Histone modifications serve as recognition moieties for specific protein domains that recruit additional chromatin-modifying complexes that regulate gene expression control. Thus, the modification status of histone tails and sequence elements encoded on the DNA can dictate chromatin structure and consequently transcriptional activity. The recognition of this organization lead to the coinage of the term "histone code" which postulates that covalent chromatin modifications are carriers of information that significantly contribute to gene expression control (Jenuwein T and Allis CD 2001). It is therefore of great interest to identify links between specific epigenetic phenomena and associated phenotypes as it becomes apparent that information other than the DNA nucleotide sequence is contained within chromatin.

Examples that highlight the functional relevance of epigenetic control are plentiful, among them aberrant regulation of epigenetic mechanisms occurs in the absence of one of the recognition domains through gene mutation or rearrangement that can cause serious gene misregulation and diseases such as Angelman syndrome and Prader-Willi syndrome. In addition, absence of recognition domain may contribute to the heritability of many forms of cancer; asthma; Alzheimer's disease and autoimmune diseases such as systemic lupus erythematosus, rheumatoid arthritis and multiple sclerosis (Hirst M and Marra MA 2009, Hewagama A and Richardson B 2009, Handel AE *et al*. 2010). Recently, researchers have characterized a translocation in an acute myeloid leukemia patient, involving histone demethylase KDM5A that results in fusion of the H3K4me3-binding PHD finger of KDM5A to the transcriptional activator NUP98, a common leukemia translocation partner (Islam S *et al*. 2011). Mutations that can interfere with epigenetic regulation can occur at many levels, some are inherited, but many accumulate due to environmental factors or with age.

1.2. Gene expression

1.2.1. RNA polymerases

The earliest evidence for the existence of DNA-dependent RNA polymerases (RNAP) was the discovery that the base composition of newly synthesized RNA is complementary to that of the DNA template. Additionally, hybridization experiments revealed that the RNA sequences are complementary to their DNA template (Hall BD and Spiegelman S 1961). The enzyme that produces RNA using a DNA template was discovered independently by Jerard Hurwitz (Hurwitz J *et al.* 1961) and Samuel Weiss (Weiss SB and Nakamoto T 1961). Both researchers named the enzyme "RNA polymerase".

While in prokaryotes, all RNA molecules are synthesized by a single type of RNA polymerase, in eukaryotes, where transcription takes place in the nucleus, there are three types of functionally- and structurally-related RNA polymerases (RNAPs) (Brueckner F *et al.* 2008). The three distinct eukaryotic RNAPs, designated RNAP I, RNAP II and RNAP III, were first distinguished according to their variable sensitivity to α-amanitin, a toxic cyclic octapeptide from the mushroom *Amanita phalloides* (Roeder RG *et al.* 1974, Schwartz LB and Roeder RG 1974).

- RNAP I, which is preferentially localized in the nucleolus, transcribes the abundant array of tandem rRNA genes to produce a long transcript named the precursor ribosomal RNA (pre-rRNA) which is processed into 28S, 5.8S, and 18S rRNAs.
- RNAP II, is located in the nucleoplasm and may cluster in "transcriptional hotspots", transcribes all protein-encoding genes (mRNA), many noncoding RNAs, including all spliceosomal small nuclear RNAs (snRNAs) except U6, as well as small nuclear RNAs (snoRNAs), microRNA (miRNA) precursors and cryptic unstable transcripts (CUTs) (Iborra FJ *et al.* 1996).
- RNAP III, like RNAP II, is located in the nucleoplasm (Lassar AB *et al.* 1983). It transcribes the genes encoding tRNAs, other ribosomal RNA molecules, 5S rRNA and other small, stable RNAs, including U6 RNA (involved in RNA splicing) and the 7S RNA of the signal recognition particle (involved in the transport of proteins into the endoplasmic reticulum).

All DNA-dependent RNA polymerases are able to generate RNA from a DNA template in the 5'→3' direction and do not require primer. The transcription process is generally divided in three main phases, known as initiation, elongation and termination. Each of them can be regulated by transcription factors (Bregman DB *et al.* 2000, Panning B and Taatjes DJ 2008, Arndt KM and Kane CM 2003, Hirose Y and Ohkuma Y 2007, Fuda NJ *et al*. 2009, Nechaev S and Adelman K 2011).

1.2.2. Specificity of the carboxyl terminal domain of RNA P II (CTD)

A unique feature of RNAP II that distinguishes it from the other polymerases is the extended carboxyl-terminal domain (CTD) of its largest subunit, Rpb1. The CTD is essential for cell viability and plays a central role in the regulation of mRNA synthesis *in vivo*. The CTD of Rpb1 consists of a varying

number of tandemly repeated heptapeptides with the consensus sequence YSPTSPS Y1-S2-P3-T4-S5-P6-S7 (Stiller JW and Hall BD 2002, Svejstrup JQ and Reid J 2004). The consensus repeat has been conserved in evolution, although the number of repeats seems to increase with the complexity of the organism, being 26 in yeast, 32 in *C. elegans*, 45 in *Drosophila* and 52 in mammals (Hampsey M 1998, Stiller JW and Hall BD 2002). The unstructured CTD serves as a platform for the assembly and recruitment of various factors involved in initiation, elongation, mRNA maturation, surveillance, and export (Hirose Y and Manley JL 2000, Orphanides G and Reinberg D 2002, Proudfoot NJ *et al.* 2002). Crystal structures indicate a highly versatile nature of CTD folding, depending on its phosphorylation status and binding partner. The CTD can be thought of as a nucleation centre for the multitude of factors that regulate mRNA processing events. Specific modifications of the CTD allow RNAP II to proceed through the transcription cycle (see 1.2.3). These CTD modifications include phosphorylation (mostly on Ser2 and Ser5), glycosylation, and *cis*/*trans* isomerization of prolines (Lin PS *et al.* 2003).

1.2.3. The eukaryotic RNA polymerase transcription cycle

Transcription is a fundamental step in gene expression. As such, it is one of the most regulated and complex processes requiring the functioning of numerous auxiliary factors (Arndt KM and Kane CM 2003, Hirose Y and Ohkuma Y 2007, Fuda NJ *et al.* 2009). The generation of mature mRNA by RNA polymerase involves a myriad of events, some of which occur sequentially and others in parallel. As mentioned above, transcripts are generated through a transcription cycle comprising the following steps: pre-initiation, initiation, elongation, termination and re-initiation (Figure 1.4. Hahn S 2004).

Pre-initiation

DNA sequences located upstream (5') of the gene coding region recruit RNAP II to initiate gene transcription and constitute the pre-initiation complex (PIC). These sequences constitute the core promoter element, which is able to sustain transcriptional initiation by RNAP II. This sequence has to be accessible and must contain a specific epigenetic code as described in the previous chapter. The most common initiation sequence in eukaryotes is the TATA-Box. Initiation by RNAP II-catalysed transcription begins with the recognition of the TATA box element by the TATA-binding protein (TBP) of the transcription factor IID (TFIID) complex. TBP binding causes a dramatic conformational change in the DNA which is thought to contribute to the downstream transcriptional activation events (Orphanides G *et al.* 1996, Orphanides G and Reinberg D 2002). RNAP II transcription initiation can also occur in the absence of TATA elements where other sequences such as the initiator (Inr) or the downstream core promoter element (DPE) take up its role (Butler JE and Kadonaga JT 2002).

A major role in the pre-initiation step is played by sequence specific binding transcription factors to DNA recognition elements that can affect the recruitment and stability of the basal transcriptional complex and may facilitate the unwinding or “opening” of the DNA around the transcription start site. Recognition elements concentrate in the near proximity of the transcription start site,

preferentially in the upstream region, but can be found in other locations, generally grouped in the so called “enhancer” elements (Cosma MP *et al.* 1999, Nechaev S and Adelman K 2011). While in the proximal promoter regions the orientation, relative to the initiation elements, is important, distal enhancers do not have these topological constraints and can promote transcription in a position- and orientation-independent manner.

Transcription factors and associated factors such as GAGA associated factor (GAF) recruit chromatin remodeling complexes, facilitating disruption nucleosome positioning and opening of the DNA double helix to form a “transcription bubble”, rendering it competent as a transcription template (Chen LI *et al.* 1994, Tsukiyama T *et al.* 1994, Cosma MP *et al.* 1999, Peterson CL and Workman JL 2000, Boehm AK *et al.* 2003, Boeger H *et al.* 2004). This process is ATP dependent and requires the action of TFIIE and TFIIH (Goodrich JA and Tjian R 1994, Holstege FC *et al.* 1996, Kim TK *et al.* 2000) in eukaryotes. A large number of factors have been shown to be involved in the initiation of transcription and recruitment of polymerase and the list of members of the pre-initiation complex (PIC) might not be complete yet (Imbalzano AN *et al.* 1994, Ohkuma Y 1997, Wilkins RC and Lis JT 1997, Esnault C *et al*. 2008). Upon DNA binding, RNAP II is phosphorylated at the serine 5 residue of its C-terminal tail by TFIIH, driving the formation of a transcription elongating complex (Akoulitchev S *et al.* 1995, Nechaev S and Adelman K 2011).

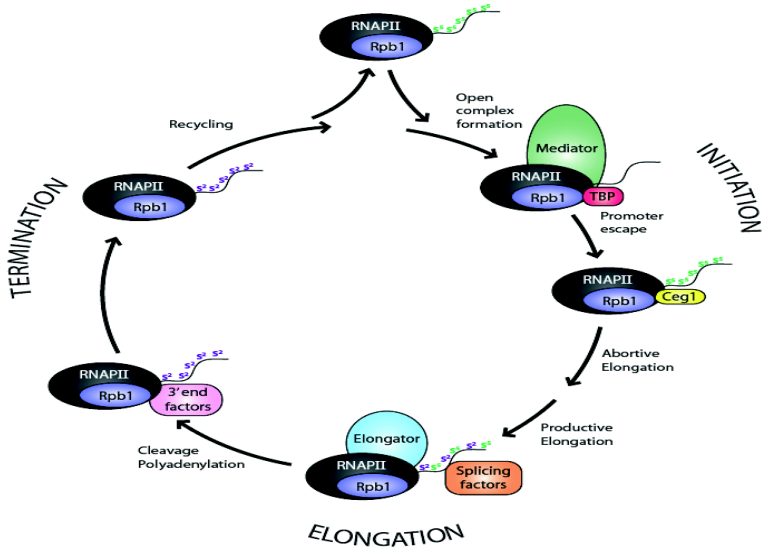

Figure 1.4: Transcription cycle

Pre-initiation/initiation

The earliest stages of transcription are marked by instability of the transcription complex and a pronounced tendency to release short pieces of RNA (2-5mers) in a phase, named “abortive initiation”. Synthesis of about 23 bases renders the complex maximally stable (Wu CH *et al.* 2003). RNAP II then proceeds into productive transcription elongation and completes transcription of the gene (Figure 1.4.). The mechanism involves tight connection with chromatin modulation and RNAP II CTD.

Promoter clearance and early elongation

The transition to elongation goes along with partial PIC disassembly. A subset of common TFII proteins, and the mediator complex, stays at the promoter, serving as a scaffold for the formation of the next transcription initiation complex (Pal M and Luse DS 2003, Yudkovsky N *et al.* 2000, Zawel L *et al.* 1995). Therefore, re-initiation of transcription is a much faster process compared to the initial round (Jiang Y and Gralla JD 1993, Orphanides G and Reinberg D 2000, Ranish JA *et al.* 1999). Of all the general components of the PIC, only TFIIF can be found associated to RNAP II during the elongation phase (Sims RJ 3rd *et al.* 2004).

Transcription elongation factors

Transcription elongation by RNAP II is regulated at different stages by auxiliary factors (Saunders A *et al.* 2006). There are three main categories of transcription elongation factors. A classic example of the first is TFIIS. It re-activates elongation complexes that have paused or stopped during elongation (Wind M and Reines D 2000). The second class, which includes the CTDK-I and the Bur1/2 kinase complexes, facilitates the escape of the elongation complex from the promoter (Cho EJ *et al.* 2001, Jona G *et al.* 2001, Keogh MC *et al.* 2003). Finally, in the third class, we find proteins like Spt4/Spt5 and the THO complex that have been shown to increase elongation efficiency (Hartzog GA *et al.* 1998, Jimeno S *et al*. 2002, Strasser K *et al.* 2002, Rondon AG *et al.* 2003).

Termination and mRNA processing

The choreography of termination and mRNA processing is intimately linked in eukaryotes. Before a gene transcript leaves the nucleus as mature mRNA, it has to undergo three major processing events:

- Capping, a GMP molecule is fused to the 5'-terminus of nascent RNA via an unusual 5'-5' triphosphate linkage and then methylated at position N7. This cap protects the nascent RNA from exonucleolytic 5'→3' degradation and is recognised during nuclear export of mature mRNA.
- Splicing removes non-coding sequences (introns), which are present in most mammalian genes and some yeast genes. This subject will be addressed as a result of the present work.
- Polyadenylation, the 3'-terminus of mRNAs comprises a poly(A) tail of about 200 nucleotides. This poly(A) tail is attached to the pre-mRNA following cleavage by a specific RNA nuclease at polyadenylation sites, followed by incorporation of the poly A tail by the polyadenylation complex or by an intrinsic ribozyme (Teixeira A *et al.* 2004).

All three processes are known to be interconnected and co-regulated with the transcriptional initiation and termination (Proudfoot N 2004, Proudfoot NJ *et al.*, 2002). However, control of eukaryotic termination is still not well understood. During termination, the transcript is released from the transcription site and RNAP II gets detached from the DNA template.

1.2.4. Noncoding RNAs

In the year 2000, sequencing of nearly the entire human genome revealed approximately 20 000 protein-coding genes (approximately 1.5% of the genome). The rest of the genome is made up of noncoding RNA molecules, regulatory DNA sequences, introns and sequences to which no function has been assigned. There is increasing evidence that expression of noncoding RNAs, such as microRNAs, small RNAs and large RNAs, plays a role in gene regulation at all levels, including those dependent on epigenetic modifications (Costa FF 2008, Chuang JC and Jones PA 2007). Noncoding RNAs can direct both cytosine methylation and histone modification to silence DNA repeats in the genome.

Since the discovery of the first small silencing RNA in 1993, a remarkable number of small RNA classes have been discovered, including microRNAs (miRNAs), small interfering RNAs (siRNAs), and Piwi-associated small RNAs (piRNAs), which have important roles in various biological processes. The discovery of new classes of small RNAs and new members of existing classes substantially expands our knowledge of small RNAs. For instance, a class of small RNAs originated from small nucleolar RNAs (snoRNAs) have been identified to function like miRNAs. Notably, a new type of siRNA, known as qiRNAs (QDE-2-interacting small RNAs), originates mostly from the rDNA locus and has roles in DNA damage response in the filamentous fungus *Neurospora crassa***.** Moreover, other novel classes of small RNA are being revealed, including ***cis*-**acting siRNA (casiRNA**), *trans*-**acting siRNA (tasiRNA), natural antisense transcript siRNA (natsiRNA), exogenous siRNA (exo-siRNA) and endogenous siRNA (endo-siRNA). Besides, there are also a number of small RNA classes, such as heterochromatic siRNA (hc-siRNA), stem bulge RNA (sbRNA), vault RNA (vtRNA), small scan RNA (scnRNA), Y RNA and DSB-induced small RNA (diRNA). Nevertheless, many small RNAs identified in high-throughput sequencing analysis do not belong to any of these classes, suggesting there are still more uncharacterized types of small RNAs.

2. Environmental adaptation

Living environments are dynamic rather than static. The ability of organisms to adapt to these environmental changes allows them to increase their survival potential and contribute to the evolution of the species. In single-cell eukaryotes, elaborate networks are in action to sense and respond to environmental changes. These principles of adaptive responses are conserved in multicellular organisms. Multiple regulatory inputs convert to implement the transcriptional program, i.e. the regulation and expression of new genes supporting specific cellular functions. An intimate connection between basic homeostatic pathways is necessary to ensure the coordinate control of cellular activities in response to environmental factors.

2.1. Signaling pathways regulating responses to metabolite availability

Transcriptional activity is modulated through several different classes of coregulators that do not bind to specific DNA sequences but are rather recruited to the PIC by classical transcription factors. Many of these co-regulators, commonly described as coactivators and corepressors, were initially identified following two hybrid approaches that aimed to identify interacting proteins of classical transcription factors (Glass CK and Rosenfeld MG 2000, McKenna NJ *et al.* 1999, Naar AM *et al*. 2001). Generally coregulators interact with members of the PIC to regulate transcription, and/or are responsible for epigenetic modifications elicited by themselves or by other factors recruited in a sequential or a combinatorial manner, generally forming large multiprotein complexes. Taking into account that each coregulator can interact with multiple transcription factors and vice versa, understanding the mechanisms that lead to specific protein complexes and the biological roles of these specific partnerships is fundamental. The large number of coactivators and coactivator complexes already identified show a large functional and mechanistic diversity, and integration of multiple signal clues in order to confer for example tissue and promoter-specific regulation of target genes. Two main types of coactivator complexes have been described based on their mechanism of action: ATP-dependent chromatin-remodeling complexes and histone-modifying complexes.

2.2. PGC-1 alpha family: inducible tissue specific coactivators

2.2.1. Structure features

Peroxisome Proliferator-Activated Receptor Gamma-Coactivator-1α (PGC-1α) is the founding member of the PGC-1 family of coactivators. They lack enzymatic activities and show several characteristic features (Figure 1.5).

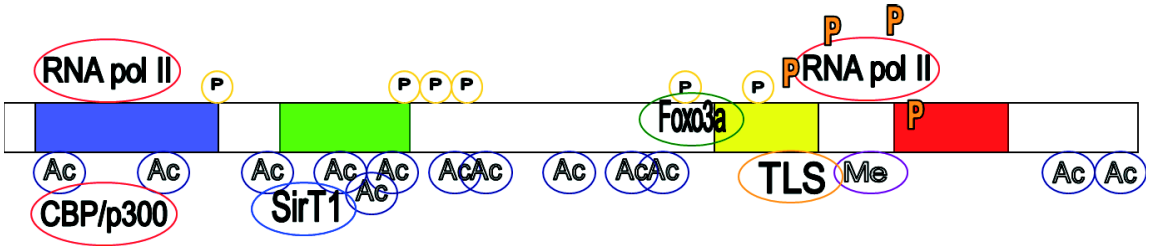

Figure 1.5: Peroxisome Proliferator-Activated Receptor Gamma-Coactivator-1α (PGC-1α)

The N-terminus of PGC-1α harbors a potent acidic transactivation domain and three leucine rich LXXLL motifs--L1, L2 and L3 that reside in predicted α-helices. These motifs are conserved among all the PGC-1α family members (Kressler D *et al.* 2002). Motif L2, in particular, serves as the major interaction surface for several transcription factors of the nuclear receptor superfamily, including GR ER, PPARs, RXR, LXR and probably others (Delerive P *et al.* 2002, Knutti D *et al.* 2001, Oberkofler H *et al.* 2003, Tcherepanova I *et al.* 2000, Vega RB *et al.* 2000). PGC-1α has additional interaction domains that have been proposed to bind PPARγ, NRF-1 and the muscle-specific transcription factor MEF2C (Michael LF *et al*. 2001, Puigserver P *et al.* 1998, Wu Z *et al.* 1999, Rodgers JT 2008). Two coactivators

(SRC-1 and CBP/p300) dock on the N-terminus activation domain with acetyl transferase activity. This interaction can promote chromatin opening thereby allowing initiation of the transcription through RNAP II binding (PIC-CTD; Monsalve M *et al.* 2000).

At the C terminus, PGC-1α harbors two atypical motifs a serine/arginine rich (RS) domain and a RNA recognition motif (RRM) (Knutti D *et al.* 2000). Strikingly, both RRM and RS domains are characteristic features of SR splicing factors, components and/or regulators of the spliceosome (Graveley BR 2000, Hastings ML and Krainer AR 2001, Reed R and Magni K 2001). The C-terminal PGC-1α is proposed to interact with the elongation form of polymerase II (RNAP II ph), and to regulate mRNA processing (Monsalve M *et al.* 2000). The RS domains are shown to be important for protein-protein interactions, especially transcription factors like FoxO3a. The RRM motif has been shown to be relevant for PGC-1α activity but so far it was unknown whether it actually bound RNA and the regulatory function of the ligand RNA. Since the ligated RNA would be expected to regulate PGC-1α activity, its identification as well as the determination of its regulatory activity might serve to modulate PGC-1α activity in vivo. The work presented has as one of its main aim to characterize the role of the RRM of PGC-1α.

Post-translational mechanisms regulating PGC-1α

PGC-1α undergoes several posttranslational modifications (PTMs) including phosphorylation, methylation, acetylation and ubiquitination. The phosphorylation by the MAPK, p38 at Thr262-Ser265-Thr298 correlates with a more active and stable protein (Puigserver P et al. 2001). AMP kinase (AMPK) targets residues Thr 177 and Ser 38 resulting in a more active protein. Moreover, Akt/PKB phosphorylation of Ser 570 in the SR domain leads to a more unstable protein (Figure 1.5.). GCN5 acetylates and inactivates PGC-1α while the deacetylated active status of PGC-1α is maintained by the class III NAD^+ dependent deacetylase SirT1.

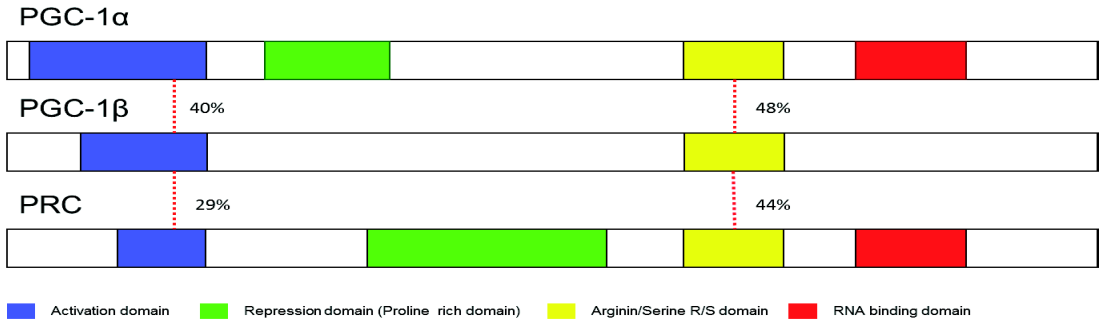

Figure 1.6: Peroxisome Proliferator-Activated Receptor Gamma-Coactivator-1α (PGC-1α) Family

PGC-1-related coactivator (**PRC**) was the first homologue of PGC-1α to be identified based on its N-terminus sequence homology (Andersson U and Scarpulla RC 2001, Figure 1.6). Even though the PRC overall sequence similarity with PGC-1α is fairly low, the domain pattern is highly similar. Both coactivators contain the N-terminal acidic transactivation domain, the nuclear receptor interaction (LXXLL) motif, the proline rich region, the RS domain and the RNA binding domain.

Later, a second, more closely related homologue was cloned, named PGC-1β (mouse) (Kressler D *et al.* 2002, Lin J *et al.* 2002). Sequences of PGCP 1α, β and PRC display around 45 to 46 % (over 450 amino acids) similarity in the C-terminus; whereas all three proteins contain an RNA recognition motif, PGC-1β does not contain an RS domain. PGC-1β displays a marked specificity in the interaction with nuclear receptors (Kressler D *et al.* 2002), showing a strong regulatory activity of ERα. PGC-1α and PGC-1β have been shown important additional functional differences, indicating that the two coactivators have overlapping but not identical functions (St-Pierre J *et al*. 2003).

2.2.2. Implications of PGC-1 alpha in environmental changes, regulation of PGC-1 alpha activity

Activation of PGC-1α

PGC-1α is a transcriptional coactivator identified as an upstream regulator of lipid catabolism, mitochondrial number and function. PGC-1α is expressed in a tissue-specific manner and induced by specific metabolic signals. Consistent with its emerging role as a central regulator of energy metabolism, PGC-1α is abundantly expressed in tissues with high metabolic rates that have a high density of active mitochondria, like heart, skeletal muscle, brown adipose tissue (BAT), kidney, liver and brain (Esterbauer H *et al.* 1999, Knutti D *et al.* 2000, Puigserver P *et al.* 1998). In addition, PGC-1α is induced in physiological states that have high energy demands, such as exposure to cold and physical exercise (Goto M *et al.* 2000, Herzig S *et al.* 2001, Lehman JJ *et al.* 2000, Puigserver P *et al.* 1998) PGC-1α is tightly regulated in a temporally and spatially defined manner since both increased and decreased levels could potentially contribute to diseases.

PGC-1α regulates mitochondrial biogenesis in response to specific signals

Mitochondria provide cellular energy in the form of ATP. The mitochondrial content and respiration efficiency vary greatly from cell type to cell type and reflect the energy demand defined by the physiological status of the cell (Moyes CD and Hood DA 2003). The modulation of mitochondrial functions is a complex process, which requires the coordinate expression of mitochondrial and nuclear encoded proteins. A number of studies have shown that PGC-1α works as a master regulator of mitochondrial biogenesis. Ectopic expression of PGC-1α in adipocytes, myocytes and cardiomyocytes induces the biosynthesis of mitochondria and increases cellular respiration (Goto M *et al.* 2000, Lehman JJ *et al.* 2000, Puigserver P *et al.* 1998, Wu Z *et al*. 1999). Significantly, PGC-1α up regulation is detected in the heart of mice directly after birth, shortly before a strong increase of mitochondrial biogenesis and oxidative metabolism (Lehman JJ *et al.* 2000) and PGC-1α levels are increased in muscle after exercise, a situation of high energetic demand (Goto M *et al.* 2000).

ROS (reactive oxygen species) are by-products of several metabolic reactions in the cell and primarily in mitochondria. An excess of ROS in mitochondria is able to cause oxidative stress. To prevent the oxidative damage of cellular machineries and in particular of the DNA, cells have developed a complex antioxidant defense system consisting of superoxide dismutases and glutathione

transferring enzymes among others (Figure 1.7.). PGC-1α, a potent regulator of mitochondrial biogenesis, has been involved in the cellular response to oxidative stress.

Oxidative stress

ROS (reactive oxygen species) are by-products of several metabolic reactions in the cell and a by-product of mitochondrial oxidative metabolism. An excess of mitochondrial ROS production results in cellular oxidative stress. To prevent the oxidative damage of cellular machineries and in particular of the DNA, cells have developed a complex antioxidant defense system consisting of superoxide dismutases and glutathione transferring enzymes. PGC-1α, a potent regulator of mitochondrial activity, has been shown to coordinately regulate the expression of antioxidant genes preventing oxidative stress upon mitochondrial activation through its interaction with the transcription factor FoxO3a.

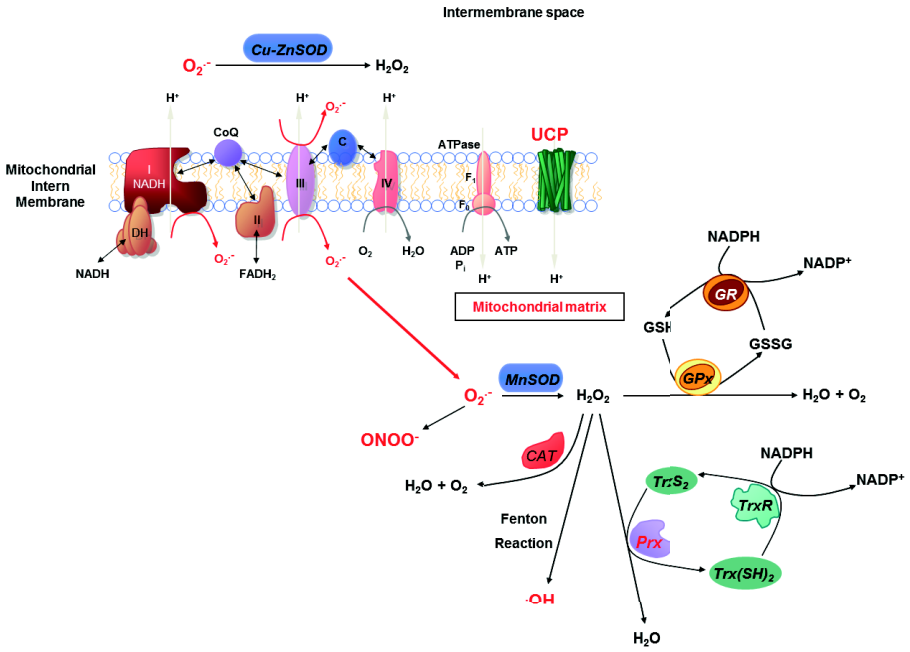

Figure 1.7: Antioxidant defense system

PGC-1α role in adaptive thermogenesis

Adaptive thermogenesis is a process closely associated with the function of mitochondria and energy expenditure. This program is switched on in response to exposure to cold and overfeeding, and leads to the production of heat instead of energy through the uncoupling of the respiratory chain (Puigserver P and Spiegelman BM 2003). PGC-1α is strongly induced in the brown fat and muscle (i.e. thermogenic tissues) of mice upon exposure of the animals to cold. Overexpression studies reveal that PGC-1α is capable of up regulating molecular components of the adaptive thermogenesis, e.g. the UCPs (uncoupling proteins), a process likely to depend on the interaction of PGC-1α with PPARα, PPARγ, RAR and TR (Puigserver P et al. 1998).

PGC-1α function in glucose metabolism

Fasting induces a strong upregulation of PGC-1α in the liver and the heart (Lehman JJ et *al.* 2000, Yoon JC *et al.* 2001). The main regulators of the fasting state are glucagon, which is acting through the cAMP pathway, and glucocorticoids. After cAMP levels rise, protein kinase A (PKA) exerts increased activity and activates the cAMP-response element binding protein (CREB). The treatment of hepatic cells with cAMP leads to an upregulation of PGC-1α (Yoon JC et al. 2001). The PGC-1α promoter harbors binding sites for CREB and seems to be regulated by this factor (Herzig S *et al.* 2001). In the fasting state, gluconeogenesis is increased in the liver to ensure glucose availability to tissues like the brain. Overexpression of PGC-1α induces the expression of PEPCK and glucose-6-phosphatase, two key enzymes of gluconeogenesis, through the coactivation of HNF4, GR and FOXO1 (Herzig S *et al.* 2001, Puigserver P and Spiegelman BM 2003, Yoon JC *et al.* 2001).

2.3. Implication of Sirtuins in environmental changes

2.3.1. Sirtuins and caloric restriction

SirT1 belongs to a NAD+ dependent histone deacetylase family of enzymes known as sirtuins, first described in yeast (Frye RA 1999, Howitz KT *et al.* 2003, Denu JM 2005). In C. elegans, overexpression of the homolog Sir2 increases lifespan, which requires DAF-16, the homolog of mammalian FOXO and the induction of antioxidant genes like *sod2* (Tissenbaum HA and Guarente L 2001).

In humans and rodents, seven genes share the Sir2 conserved domain (sirtuin (SIRT) 1 to 7). SirT1 is the major effector of increased NAD^+, making it a key sensor of the cellular redox status. It is located in the nucleus and is involved in chromatin remodeling, inducing gene silencing and genomic stability and also in the regulation by deacetylation of transcription factors like p53 (Kang J *et al.* 2005). SirT1 promotes cell survival by negatively regulating the pro-apoptotic activity of the tumor suppressor p53 (Vaziri H *et al.* 2001).

Caloric restriction induces SirT1 expression and activity in a wide array of tissues, which shifts the balance away from cell death towards cell survival. SirT1 regulates the gluconeogenic/glycolytic pathways in the liver in response to fasting signals through the transcriptional co-activator PGC-1α. Once SirT1 is induced, it interacts with and deacetylates PGC-1α at specific lysine residues in an NAD^+ dependent manner (Rodgers JT *et al.* 2005). SirT1 has also been shown to coregulate PGC-1α in the induction of oxphos genes, increasing oxygen consumption in response to fasting and exercise in the muscle.

SirT1 also regulates cell fate in response to oxidative stress by regulating FOXO transcription factors. FOXO are a family of transcription factors that in response to changes in the insulin signalling pathway regulates cell metabolism and stress response, being as already mentioned key mediators of increased organism longevity in response to CR. In mammalian cells, in response to oxidative stress, SirT1 deacetylase forms a protein complex with the Forkhead transcription factor FoxO3a and

deacetylates it. SirT1 differentially affects the function of FoxO3a, increasing FOXO3a's effect on cell cycle arrest and DNA repair target genes, but attenuating FoxO3a-dependent apoptosis in the presence of stress stimuli (Brunet A *et al.* 2004). Furthermore, under non-restricted nutrient availability conditions, p53 represses SirT1 expression. In contrast, under starvation conditions, the ability of activated FoxO3a to stimulate SirT1 expression requires p53. This suggests that in the absence of p53, the basal expression level of SirT1 might marginally respond to FoxO3a, while the starvation-induced increase would be more pronounced (Nemoto S *et al.* 2004). Our group has further demonstrated that PGC-1α, SirT1 and FoxO3a form a complex involved in the regulation of antioxidant gene expression.

2.3.2. Sirtuins enzymatic properties

The sirtuin family of enzymes is characterized by a highly conserved core domain which carries a catalytic activity and is flanked by N- and C-terminal regions of variable length. The flaked regions are particularly prevalent in the more recent additions of the evolutionary time-scale. Two enzymatic activities have been associated with sirtuins, ADP-ribosyltransferase and NAD^+ dependent protein deacetylase. Using computer-based homology searches, Frye provided the first comprehensive description of the sirtuin family, discovering the first five human orthologues. He provided experimental evidence that some bacterial, yeast and human sirtuin members harbor ADP-ribosyltransferase activity (Frye RA 1999). Interestingly, this activity seems to depend on nicotinamide adenine dinucleotide (NAD^+). Mammalians SirT6 was shown to be an ADP-ribosyltransferase (Liszt G *et al.* 2005). Further studies have confirmed the same enzymatic activity for other sirtuins in yeast, *Drosophila* and mammals.

2.3.3. Nicotinamide and NAD^+ biosynthesis pathway

Biochemical studies, along with structural data, have provided sound evidence that two naturally occurring metabolites, NAD^+ and nicotinamide, may regulate SirT1 activity.

In both prokaryotic and eukaryotic cells two pathways participate in NAD^+ biosynthesis, the *de novo* pathway and the salvage pathway. Both pathways share, as a common intermediate, the nicotinic acid mononucleotide (NaMN). NAD^+ is involved in many metabolic, primarily catabolic, processes such as glycolysis and the tricarboxylic acid (TCA) cycle, where it participates as a proton acceptor leading to its reduction to $NADH^+$. It is also very important in DNA metabolism since enzymes like DNA ligase and poly(ADP) ribose polymerase (PARP) depend on NAD^+ for their activity.

The ratio of NAD^+ to $NADH^+$ mirrors the redox state of the cell and fluctuates in response to metabolic changes. As a result, it modulates the activity of enzymes like glyceraldehyde 3-phosphate dehydrogenase (GAPDH) of the glycolysis pathway and pyruvate dehydrogenase (PDH), which converts pyruvate to acetyl-CoA, driving the oxidative catabolism of glucose. Thus, homeostatic mechanisms exist ensuring constant re-oxidation of NADH to NAD^+, of which the most important is

the mitochondrial respiratory chain. Therefore, when mitochondrial activity is not enough to replenish the $NADH^+$ pool, elevated NAD^+ activate SirT1, that in turn enhances PGC-1α activity on mitochondrial genes.

2.4. Involvement of forkhead transcription factors in environmental changes

2.4.1. Forkhead transcription factors and caloric restriction

The insulin receptor (IR) pathway has been described as a phylogenetically conserved signaling module that determines life-span in *Drosophila* and *C. elegans*. The forkhead transcription factor *daf-16*, which is negatively regulated by the insulin pathway, is a key mediator of increased longevity in the absence of IR or its downstream effectors, PI3K and AKT (Giannakou ME and Partridge L 2004). In mammals, the functional orthologues of *daf-16* are represented by the "O" class of the forkhead or winged helix family of transcription factors (FoxOs), with four members, FoxO1 (or FKHR), FoxO3a (or FKHRL1), FoxO4 (or AFX) and FoxO6. AKT dependent phosphorylation of these factors leads to their exclusion from the nucleus under conditions of growth factor availability. FoxO1 binds PGC-1α to induce gluconeogenesis, while FoxO3a binds PGC-1α to induce antioxidant genes.

The acetyltransferase CBP/p300 enhances acetylation of FoxO1, FoxO3a and FOXO4. PCAF has the same effect on FoxO3a. These acetyltransferases have also been shown to acetylate PGC-1α. SirT1, as already mentioned, deacetylates FoxO1, FoxO3 and FoxO4 factors as well as PGC-1α.

Regulation of cell cycle arrest genes by FoxO factors in response to oxidative stress depends on SIRT1 activity (Brunet A *et al.* 2004). In response to oxidative stress FoxO factors becomes first acetylated by the acetylase p300 and then deacetylated by SirT1 (van der Horst A *et al.* 2004, Kobayashi Y *et al.* 2005). Acetylation impairs the capacity of FoxOs to regulate cell cycle arrest but keeps intact or enhances its capacity to induce pro-apoptotic genes. That implies that in response to oxidative stress FoxO will induce apoptosis unless it becomes deacetylated.

Importantly, acetylation of FoxO factors in response to oxidative stress increases their sensitivity to phosphorylation by the phosphatidylinositol 3-kinase (PI3K)/AKT pathway (Jing E et *al.* 2007, Matsuzaki H *et al.* 2005) which in turn promotes their ubiquitination and degradation (Plas DR and Thompson CB 2003) while deacetylation by SirT1 promotes protein stabilization (Olmos Y *et al*. 2013). Intriguingly, deacetylation has also been shown to drive FoxO3 degradation (Wang F *et al.* 2012) and resveratrol, an activator of SirT1, has been proposed to be able to regulate FoxO in a SirT1 and AKT independent manner (Qiang L et *al.* 2010).

The first antioxidant gene that was demonstrated to be regulated be regulated by FoxO in a SirT1 dependent manner was *sod2*, coding for the mitochondrial Mn^{2+} superoxide dismutase (MnSOD) (van der Horst A *et al.* 2004). The relevance of this regulation was later demonstrated in mouse models of oxidative stress induced heart failure (Tanno M *et al.* 2010, Alcendor RR *et al.* 2007). The report by Alcendor RR *et al.* (2007) also showed that SirT1 regulated the expression of another antioxidant

gene previously characterised as a FoxO target gene, catalase. A later study demonstrated the relevant of catalase regulation by the FoxO/Sirt1 complex in, renal tubular cells (Hasegawa K *et al.* 2008). More recently, it was shown that SirT1 acts as a coactivator of FoxO in the regulation of the ROS detoxification enzymes, peroxiredoxins 3 and 5 (Prx3, Prx5), thioredoxin 2 (Trx2), thioredoxin reductase 2 (TR2), and also uncoupling protein 2 (UCP-2), a protein that protects mitochondria from excessive O_2^- generation in the electron transport chain (ETC, Olmos Y *et al.* 2013). All these results stress the crucial interplay between SirT1 activity and FoxOs in the response to oxidative stress. Importantly, it has been recently shown that FoxOs are indispensable for SIRT1-dependent cell survival against oxidative stress (Hori YS et *al*. 2013).

2.4.2. Forkhead transcription factors: structure and cellular expression

The FoxO class has been shown to recognize two distinct types of DNA binding elements (DBE) the insulin response element (IRE), and the Daf-16 binding element. The DBE was defined as TTGTTTAC, which overlaps with the IRE: CACTAGCAAAACAAACTTATTTTGAACAC. The consensus sequence is generally regarded to be (G/A)(T/C)(C/A)AA(C/T)A. FoxOs can also regulate target gene expression in a DNA-binding independent manner through their interaction with other transcription factors such as CCAAT/enhancer binding protein β (CEBPB), and Creb/binding protein (CBP), several nuclear receptors (NRs) and Smads.

FoxO3a

FoxO3a protein is encoded by *foxO3* gene, which is located in chromosome 6q21 and is 124.7kb. The transcription factor FoxO3a is a downstream target of several signalling pathways. FoxO3a can shuttle between the cytoplasm and the nucleus and many PTMs impact its subcellular location. FoxO3a target genes are involved in the cellular stress responses. FoxO3a can induce either cell survival or cell death genes depending on the activity of other TF, coactivators, or PTMS. Target genes include genes that play a role in DNA repair, cell cycle arrest, cell death, tumor suppression, cellular differentiation and proliferation, ROS detoxification and metabolism. FoxO3a works as a tumor suppressor inducing apoptosis of terminally damaged cells. Other oncogenic kinases have also been related to FoxO3a inactivation in tumors, including SGK and ERK. However, FoxO3a can also promote tumorogenesis, enhancing chemoresistance of cancer cells.

Objectives

Objectivos

Identificar los mecanismos transcripcionales implicados en la regulación de la expresión de los genes antioxidantes, esencialmente:

1) Valorar la contribución del factor SirT1 a la regulación génica e identificar los mecanismos implicados

- Determinar si la histone desacetilasa SirT1 actúa como regulador de la expresión de genes clave en la defensa antioxidante, especialmente a nivel mitocondrial, tales como MnSOD, CAT, Prx3, Prx5, Trx2, TR2, UCP-2 así que los cofactores FoxO3a y PGC-1α.
- Analizar el efecto de SirT1 sobre la formación de un complejo FoxO3a/PGC-1α.
- Determinar los sitios de reclutamiento de SirT1 en las regiones reguladoras de los genes diana.
- Determinar el entorno de estas regiones al nivel de acetilación.
- Analizar la secuencia del proceso de activación de la transcripción por estos genes diana en situación de estrés oxidativo.

2) Analizar la función del dominio RRM de PGC-1α a la actividad de este factor y los mecanismos implicados

2.1) Caracterización funcional del dominio RRM

- Identificar los genes afectados en ausencia de PGC-1α en los hepatocitos usando análisis a nivel genómico (WGE).
- Analizar el efecto funcional de la ausencia del dominio RRM en los hepatocitos usando nivel genómico (WGE).
- Determinar el efecto regulador del RRM sobre la maturación de los RNAs.

2.2) Identificación de los posible RNAs ligados

- Estudiar si PGC-1α es capaz de interaccionar con ácidos nucleicos y determinar de qué tipo.
- Identificar los ácidos nucleicos que se unen a PGC-1α en los hepatocitos utilizando la técnica de HITS-CLIP.

Objectives

Identify transcriptional mechanisms involved in regualtion of antioxidant gene expression, essentially:

1) Assess the SirT1 contribution in gene regulation and identify the implied mechanisms

- Determine if the histone deacetylase SirT1 regulates expression of key antioxidant genes, essentially at mitocondrial level, as MnSOD, CAT, Prx3, Prx5, Trx2, TR2, UCP-2 and the cofactors: FoxO3a y PGC-1α.
- Analize SirT1 implication on the establishment of a complex FoxO3a/PGC-1α.
- Determine SirT1 recruitment sites within the regulatory regions of the target genes.
- Determine the acetylation level of the regulatory regions of the target genes.
- Analize the transcription activation sequence of the target genes when submitted to oxidative stress.

2) Analize PGC-1α RRM domain fonction , its activity and the regulatory mechanisms involved

2.1) Characterize the RRM fonctional domain

- Identify genes affected in absence of PGC-1α in hepatocytes when performing whole gene expression analysis (WGE).
- Analize the functional effect when the PGC-1α RRM domain is missing in hepatocytes when performing whole gene expression analysis (WGE).
- Determine the RRM regulatory effect on RNAs maturation.

2.2) Identification of possible bound RNAs

- Investigate if PGC-1α is able to interact with nucleic acids and determine the specific type.
- Identify the nucleic acid bound to PGC-1α in hepatocytes applying the HITS-CLIP technique.

Materials and Methods

Materials and Methods

1. Mice

C57BL6 PGC-1$\alpha^{-/-}$ mice were part of a colony established within the CNIC and IIB animal facilities by embryonic transfer. The funder PGC-1$\alpha^{-/-}$ mice were originally provided by Dr. Bruce Siegelman (DFCI, USA), head of the lab were the animals were initially generated (Lin J et *al*. 2004).

C57BL6 SirT1$^{+/-}$ mice used were part of a colony established within the CNIC and IIB animal facilities. The funder Sirt1$^{+/-}$ mice were originally provided by Dr. Manuel Serrano (CNIO, Spain), who established a colony from mice donated by the laboratory of Dr. David Sinclair (HMS, USA), where they were initially generated (Pfluger PT et *al*. 2008).

Animal care protocols are in accordance with Spanish legislation on care of experimental animals (Real Decreto 1201/2005 and Law. Law 6/2013 of the 11th of July, 2013 that modifies the previous Law 32/2007 of the 7th of November, 2007 for animal care for animal exploitation, transport, experimentation and sacrifice. And it also conforms to European Council Directive 86/609/EEC on the protection of Animals used for Experimental and other scientific purposes. Housing and handling procedures are in accordance with the recommendations of the European Commission of the 18th of June, 2007 that provides guidelines on housing and care of experimental animals.

Animals were maintained free of disease and specific parasites and under controlled conditions of light, pressure and temperature with access ad libitum to water and food. Colonies were maintained with a standard CHOW diet from Harlam.

The animal experimental protocols were approved by the Institutional Animal Care and Use Committee of the CNIC and the CISC. All protocols used conform to the Declaration of Helsinki and to the Guide for the Care and Use of Laboratory Animals published by the US National Institute of Health (NIH publication No. 85-23).

2. Cell culture

2.1. Primary Cells

Bovine aortic endothelial cells (BAEC) were isolated and cultured as previously described (Lamas S et *al*. 1991, Lopez-Ongil S et *al*. 1996). In brief, aorta sections from under one-year-old cows were donated for scientific use by an authorized slaughter house, “El Matadero” (Colmenar Viejo, Madrid). The aortic sections were washed with PBS and endothelial cells were recovered following incubation with 0.1% collagenase A in PBS for 20 min at 37ºC. Recovered endothelial cells were collected in Hank’s solution, decanted by centrifugation and resuspended in culture medium [RPMI supplemented with 10% FBS (Gibco), and antibiotics (100 μg/ml pen/strept (Biowhittaker)]. Cells

were grown in gelatin coated plates in a humidified cell incubator at 5% $C0_2$. BAEC were used from passages 3-6.

Mouse Embryonic Fibroblasts (MEFs) were prepared from day 13.5 embryos derived from crosses between $Sirt1^{+/-}$ mice and cultured as described (Serrano M *et al.* 1997). The $SirT1^{+/-}$ mice used were part of a colony established within the CNIC animal facility. In brief, embryos were extracted from the placenta and washed with PBS. The head and the internal organs were removed and the remaining tissues where fractionated and incubated in a trypsin solution (0.25% 1mM EDTA, Gibco) at 37ºC during 45 minutes. The mixture was repeatedly passed through a 1ml micropipette every 15 min to facilitate tissue rupture. Dispersed MEFs were grown DMEM tissue culture media (Sigma) supplemented with 10% FBS (Gibco), 2 mM L-glutamine, 1% non-essential amino acids and antibiotics (100 μg/ml penicillin/streptomycin (Biowhittaker). 24 h post seeding, media was renewed to remove cellular debris. Cells were in a humidified cell incubator at 5% $C0_2$. MEF were used from passages 2-5.

Mouse Primary Hepatocytes were isolated by hepatic perfusion and digestion with collagenase as described (Bahjat FR et *al.* 2000, Rana B et *al*. 1994). In brief, anesthetized mice were subjected to laparotomy and prefunded through the caudal cava vein with a constant flux of 7 ml/ml generated by a perfusion pump Masterflex L/S modelo 7518-00 (Cole-Parmer instrument Company). Mice were first perfused with a wash solution for 10 min containing NaCl 150 mM; KCl 5.5 mM; HEPES 10 mM, pH 7.5; $NaHCO_3$ 25 mM and EGTA 0.5 mM. Then the mise were prefunded with a digestion solution containing NaCl 150 mM; KCl 5.5 mM; HEPES 10 mM, pH 7.5; $NaHCO_3$ 25 mM; $CaCl_2$ 0.5 mM and collagenase (150 Units/ml, Roche) at 0.05% (p/v). Following digestion the liver is deposited in a ceramic bowl and mechanically disaggregated with a pestle. The resulting preparation is passed through a 70 μm filter (Becton Dickinson) and centrifuged at a 50 g during 5 minutes at 4ºC to remove the digestion solution. The cells are then resuspended in Williams E (Gibco) cell culture media supplemented with 10% FBS, and filtered again. The ratio of viable hepatocytes in the preparation is estimated by trypan blue staining followed by manual counting in a Neubauer chamber. The hepatocytes are seeded in tissue culture dishes on a gelatin and collagen matrix (0.2% gelatin, 1% collagen) and grown in Williams E media supplemented with 10% FBS, 2 mM de L-glutamine, 100 nM dexametasone (Sigma), 100 nM insulin (ROCHE) and 100 μg/ml penicillin/streptomycin (Biowhittaker)**.** Fresh medium was added 4 h after plating to remove cellular debris. Cells were in a humidified cell incubator at 5% $C0_2$.

2.2. Cell lines

The rat hepatoma cell line FAO was grown in RPMI (Sigma) cell culture medium supplemented with 10% FBS, 2 mM L-glutamine and 100 μg/ml penicillin/streptomycin. Cells were in a humidified cell incubator at 5% $C0_2$.

The human embryonic kidney cell line *HEK-293A* (Invitrogen) were grown in DMEM cell culture medium supplemented with 10% FBS and 100 μg/ml penicillin/streptomycin. Cells were in a humidified cell incubator at 5% $C0_2$.

3. Plasmid constructs

The pShuttle-HA-PGC-1α shuttle vector has been described (Valle et *al*. 2005). Versions containing the PGC-1α mutants PGC-1α-ΔSR (Δ564-634), PGC-1α-ΔRRM/SR (Δ564-710), PGC-1α-ΔCTD (Δ564-797) and PGC-1α-ΔRRM (Δ677-710) (Monsalve M et *al.* 2000) were generated using the same cloning strategy. The shuttle vectors were used to generate pAdEasy-1 (Quantum) derivatives by recombination. Adenoviruses (Ad) were amplified as previously described (Valle I et *al*. 2005). Plasmids pcDNA3.1-Flag-PGC-1α and pcDNA3.1-Flag-PGC-1α-ΔCTD have been described (Monsalve M et *al.* 2000), and plasmids pcDNA3.1-Flag-PGC-1α-ΔSR, PGC-1α-ΔRM/SR and PGC-1α-ΔRRM were generated using the same cloning strategy.

TLS cDNA was cloned in the KpnI-XhoI sites of pShuttle-CMV to generate pS-TLS. The following plasmids are as described: pSG5-FL-TLS (Yang et *al.* 2000), pShuttle-TLS, pcDNA3.1-TLS (Sanchez-Ramos C et *al*. 2011, Table 1).

To create pDR-1-luc, three copies of the UCP-1 DR-1 element and a TATA box were subcloned into the BamH1 and Hind III sites of pGL3 (Promega). Plasmid p3k consisted of the rat fibronectine genomic fragment comprising the alternative IIIB exon and the two flanking exons 7b and 8a inserted in-frame into the BstB1 site of pDR-1-luc. pSV-RXRα and pSV-PPARγ_2 have been described (Mangelsdorf DJ et *al*. 1990, Tontononoz P et *al*. 1994).

3.1. Adenoviral vectors

3.1.1. Generation

Recombinant adenoviruses Ad-PGC-1α, Ad-SirT1, Ad-FoxO3a, Ad-shFoxO3a and corresponding control adenoviruses have been previously described (Olmos Y et *al*. 2009, Rodgers JT et *al*. 2005, Skurk C et *al*. 2004, Valle I et *al*. 2005, Ueki N et *al*. 1998). Versions containing TLS and the PGC-1α mutants PGC-1α-ΔSR (Δ564-634), PGC-1α-ΔRRM/SR (Δ564-710), PGC-1α-ΔCTD (Δ564-797) and PGC-1α-ΔRRM (Δ677-710) (Monsalve M et *al.* 2000) were generated using the same strategy and amplified as previously described (Valle I et *al*. 2005).

Plasmids	Characteristics	References
pShuttle-CMV	-	Quantum
Shuttle pS-HA-PGC-1α	HA tag 5' (SalI-EcoRV)	Valle I et *al*. 2005
pS-HA-PGC-1α -ΔSR	HA tag 5' (SalI-EcoRV) Δ 564-634 sequence PGC-1α	Monsalve M et *al*. 2000 Sanchez-Ramos C et *al*. 2011
pS-HA-PGC-1α-ΔRRM/SR	HA tag 5' (SalI-EcoRV) Δ 564-710 sequence PGC-1α	Monsalve M et *al*. 2000 Sanchez-Ramos C et *al*. 2011
pS-HA-PGC-1α-ΔCTD	HA tag 5' (SalI-EcoRV) Δ 564-797 sequence PGC-1α	Monsalve M et *al*. 2000 Sanchez-Ramos C et *al*. 2011
pS-HA-PGC-1α-ΔRRM	HA tag 5' (SalI-EcoRV) Δ 677-710 sequence PGC-1α	Monsalve M et *al*. 2000 Sanchez-Ramos C et *al*. 2011
pShuttle-TLS	cDNA TLS KpnI-XhoI	Sanchez-Ramos C et *al.* 2011
pcDNA3.1	-	Invitogen
pcDNA3.1-Flag-PGC-1α	-	Monsalve M et *al*. 2000
pcDNA 3.1-Flag-PGC-1α-ΔCTD	-	Monsalve M et *al.* 2000
pcDNA3.1-Flag-PGC-1α-ΔSR	Flag tag 5' (AgeI-EcoRV) Δ 564-634 sequence PGC-1α	Sanchez-Ramos C et *al*. 2011
pcDNA 3.1-Flag PGC-1α-ΔRRM/SR	Flag tag 5' (AgeI-EcoRV) Δ 564-710 sequence PGC-1α	Sanchez-Ramos C et *al*. 2011
pcDNA 3.1-Flag PGC-1α-ΔRRM	Flag tag 5' (AgeI-EcoRV) Δ 677-710 sequence PGC-1α	Sanchez-Ramos C et *al*. 2011
pcDNA3.1V5-TLS	-	Sanchez-Ramos C et *al*. 2011
pAdEasy-1	-	Quantum
pAd- Shuttle	Recombination pAdEasy-1 and pShuttle-CMV	Valle I et *al*. 2005
pAd- PGC-1α	-	Olmos Y et *al*. 2009
pAd-PGC-1α-ΔRRM/SR	-	Sanchez-Ramos C et *al*. 2011
pAd-SirT1	Dr. P. Puigserver	Olmos Y et *al*. 2013
pAd-FoxO3a	Dr. K. Walsh	Olmos Y et *al*. 2009
pAd-TLS	-	Sanchez-Ramos C et *al*. 2011
p-Shuttle silencer 1.0-CMV	-	Ambion
pAd-shPGC-1α	-	Sanchez-Ramos C et *al*. 2011
pAd-shFoxO3a	-	Olmos Y et *al*. 2009
pAd-shSirT1	-	Olmos Y et *al*. 2013
p-Ad-shControl	-	Sanchez-Ramos C et *al*. 2011
p-Adenoviral LacZBackbone	-	Ambion
pGEX-6P-2	-	GE Healthcare
pGEX-PGC-1α-CTD	CTD domain aa558-797 (XhoI-NotI)	Sanchez-Ramos C et *al*. 2011
pSG5-FL-TLS	Dr. D. Hickstein	Chen Y et *al.* 2011

Table 1: Vector summary

Silencing adenoviruses Ad-shPGC1α, and Ad-shSirt1 were constructed using the pSilencer™ Adeno 1.0 Cytomegalovirus Promoter System from Ambion. In brief, ssDNA oligonucleotides were designed that contained specific direct and reverse sequences for a specific shRNA targeting the gene of interest (Table 2). The oligonucleotides were hybridized and ligated to the linearized vector Shuttle 1.0 CMV. The ligation products were used to transform competent *Escherichia coli (E.coli)* DH5α. Transformed bacteria were selected by growth on agar plates supplemented with ampicillin. Selected clones were grown to obtain plasmid preparations. Inserts were verified by DNA sequencing. Silencing efficiency was tested by transfection of the plasmid into relevant cell lines and ratio of decreased mRNA and protein levels was monitored by RT-qPCR and western blot respectively. Finally viral particles were generated by co-transfection of the Shuttle 1.0 CMV-shRNA and Adenoviral LacZ Backbone vectors in HEK-293A.

shPGC-1α	5'-TCGAGTTCATGGAGCAATAAAGCGTTCAAGAGACGCTTTATTGCTCCATGAATTA-3'	forward
	5'-CTAGTAATTCATGGAGCAATAAAGCGTCTCTTGAACGCTTTATTGCTCCATGAAC-3'	reverse
shSirT1	5'-TCGAGCATGAAGTATGACAAAGATTTCAAGAGAATCTTTGTCATACTTCATGGCA-3'	forward
	5'-CTAGTGCCATGAAGTATGACAAAGATTCTCTTGAAATCTTTGTCATACTTCATGC-3'	reverse

Table 2: Adenoviral silencing oligonucleotides

Cells were infected with the adenoviral vectors at a multiplicity of infection of 10-25 for 12-16 hours. The viruses were washed off 3 times with PBS, and the cells were harvested 24 or 48 h post-infection. mRNA and protein were analysed by real time PCR of reverse transcribed cDNA (qRT-PCR) and Western blot.

3.1.2. Viral amplification, preparation of adenoviral stocks and titration

Viruses were generated and amplified in the cell line HEK-293A, that provides in trans the constitutively expressed E1 viral elements, absent from the replicative deficient adenoviral vectors. Expansion is carried out by the consecutive infection of continuously large amounts of HEK-293A and generation of consecutively higher titre preparations. When infected HEK-293A cells show cytopathic effects, they are harvested by scraping, centrifuged, and resuspended in PBS. Viral particles are then released by repeated cycles of freezing (in dry ice) and thawing (at 37ºC) followed by intense vortexing. Finally, the preparation is centrifuged for 5 min at 4.000 rpm to remove cellular debris.

Determination of viral titre followed the terminal dilution method. In short, HEK-293A cells were seeded at confluence in 96 well plates. Each well in a given row was incubated with 1 μl of a dilution of the virus preparation. Dilutions rates increased 10 times for each consecutive row. Cells were maintained in culture for two weeks and then the number of wells showing lysis halos was determined. Titres were in the 10^{11}PFU/ml range.

3.1.3. Adenoviral Infections

FAO cells, MEF and hepatocytes were infected overnight with adenoviral vectors at a multiplicity of infection (moi) of 1-50. Viruses were washed off and cells were harvested 48h post-infection. In all cases we compared the effect of an adenovirus driving the expression or knock down of a particular gene with the effect of a control, non-targeting adenovirus.

Ad-Shuttle was used as control for Ad-PGC1α, its mutant derivatives and Ad-SIRT1; Ad-shControl was used as control for Ad-shSIRT, Ad-shFoxO3a and shPGC-1α.

mRNA and protein were analysed by qRT-PCR of retro-transcribed cDNA (qRT-PCR) and western blot (WB). The primers and antibodies used were as described (Valle I et *al*. 2005, Borniquel S et *al*. 2006, Olmos Y et *al*. 2009, Sanchez-Ramos C et *al*. 2011).

3.2. Cell transfections

70-80% confluent cells were transfected with Lipofectamine 2000 (Invitrogen). DNA and Lipofectamine 2000 were diluted in Opti-MEM 1 medium in the absence of serum. Following 5 min incubation at RT the two preparations were mixed and incubated for another 20 min at RT. Complexes DNA-Lipofectamine were formed at a ratio 1 μg DNA -2 μl Lipofectemine. The mixture was added to the cells wells containing cell culture media without antibiotics. The transfection was allowed to proceed for 4-6 h at 37ºC in a cell culture incubator. The cells were washed with PBS and fresh media was added to the cell culture. Cells were harvested 24-48 h later.

4. RNA and protein assays

4.1. Determination of luciferase activity

Luciferase activity was determined using the Dual-luciferase Reporter Assay System from Promega, following the manufacturer instructions. Signals were monitored in Orion Microplate luminometer (Berthold Detection Systems).

4.2. RNA extraction and quantitative RT-PCR

Total RNA was isolated using TRIzol® reagent (Invitrogen) according to the manufacturer's protocol. Cells were washed twice with cold PBS and lysed with TRIzol®. Following chloroform (MERCK) addition and centrifugation, RNA was recovered from the aqueous phase by precipitation with isopropyl alcohol (Sigma-Aldrich). The precipitated material was washed with 70% ethanol (MERCK) and resuspended in RNAse free water. Purity and concentration of the recovered material was analysed using a spectophotometer (Nanodrop). The RNA was also analysed in ethidium bromide (EtBr) stained agarose gel to confirm the preservation of the integrity of the material. RNAs that were being prepared for microchip hybridization were also analysed in a Bio-analyser (Agilent).

Complementary DNA (cDNA) was generated by Moloney Murine Leucemia Reverse Transcriptase (MMLV-RT, Invitrogen) using 1 μg of total mRNA previously heated 2 min at 72ºC. Random hexamers (GE Healthcare) were used to prime the reaction that was allowed to proceed for 45 min.

4.3. Determination of relative mRNA levels, real time PCR (qRT-PCR)

The resulting cDNA was analysed by quantitative RT-PCR using Power SYBR Green and Taqman PCR Mixes from Applied Biosystems in Sequence Detection Systems (SDS) 7900 and 7000FAST from Applied Biosystems. Amplification conditions were: 2 min at 50ºC, 10 min. at 95ºC, and 40 cycles of 15 s at 95ºC, 30 s at 55-60ºC and 30 s at 72ºC.

Data were analysed using the software *Sequence Detection System* (Applied Bioystems) using the relative quantification system of C_T (*threshold cycle*) comparison. All data were normalized to 18S expression (18S rRNA VIC-MGB, Applied Biosystems). Primers were as previously described (Valle I et *al*. 2005, Borniquel S et *al*. 2006, Olmos Y et *al*. 2009, Sanchez-Ramos C et *al*. 2011).

The primers were designed in the laboratory and tested in a gradient temperature PCR for optimal amplification temperature and absence of double peaks. Before we run our assays, we run a test qPCR with serially diluted DNA to make sure we have no secondary amplifications and the amplification curve follows the predicted exponential. We analyse the data using the ΔΔCt method. We run triplicates for each DNA sample. For each one of the triplicates, we first we correct for loading using the 18S signal as reference for each one of the samples, then we choose a reference sample and calculate the ΔΔCt and then calculate the 2ΔΔCt. Finally, we calculate mean and standard deviation for the triplicates. This procedure is followed for every experiment; all experiments were carried out at least twice. A final analysis of all the experiments included determination of statistical significance.

4.4. RNA pull-down from cell extracts

70% confluent FAO cells in 10 cm Ø plates were infected at an moi of 5 with recombinant Adenovirus. Cells were harvested 48 h posttransfection, and whole cell extract (WCE, DNase I treated) were diluted to 1 μg/μl. 250μl of WCE were then incubated for 20 min at RT with 2 ng of ^{32}P labeled *in vitro* transcribed RNA and 50 μg or tRNA that was added as non-specific competitor. Finally 1 μg of heparine was added and the samples were placed on ice. PGC-1α was immunoprecipitated with HA-agarose beads (Babco), RNA was extracted from the immunoprecipitates, and loaded on an 8% polyacrylamide gel containing 8 M urea.

4.5. RNA Immunoprecipitation and RT-PCR amplification

70% confluent 293T cells (two 15 cm Ø plates per lane) were transfected with 3.1-Flag-PGC-1α, 3.1-Flag-PGC-1α-ΔRRM, or the corresponding empty vector. Whole cell extract (DNase I treated) and immunoprecipitation reactions were carried out as in (Monsalve M et *al.* 2000). RNA was isolated

from the immunoprecipitate with Trizol (Invitrogen). RT was performed using primer Round A as template, followed by 20 cycles of PCR amplification with primer Round B (Table 3).

5'-GTTTCCCAGTCACGATCNNNNNNNNNN-3'	Round A
5´-GTTTCCCAGTCACGATC-3´	Round B

Table 3: RNA Immunoprecipitation oligonucleotides

4.6. GST-pull down assays

The fusion protein GST-PGC-1α-CTD (GST, Glutation S-transferase) was generated by cloning of the PCR amplified CTD domain (aa 558-797) of PGC-1α between XhoI and NotI sites of the expression vector pGEX-6P-2 (GE Healthcare). The recombinant GST-PGC-1α-CTD protein was expressed in *E.coli* Bl21DE3 following IPTG induction and purified by affinity chromatography using glutathione-agarose beads (GE Healthcare). 0.8 μg of purified GST-CTD immobilized on glutation beads were incubated in binding buffer (20 M Tris-HCl (pH 8.0), 10% glycerol, 400 mM KCl, 5 mM $MgCl_2$, 0.5 mM EDTA, 0.5 mM EGTA, 2 mM DTT, 0.4% NP-40, 0.2 units RNasin). The following RNA: processed mRNA of LR-1 (coding region only, 1.2 kb, RNA1) or the 3' 1.7 kb of the pre-mRNA (RNA2) were the 2 ng of ^{32}P-labeled probe used for the test. This fragment was selected because it contained the E2 coding intron together with putative regulatory mRNA processing sequences. The binding of the 2 ng of ^{32}P-labeled probe was competed with 0, 1 or 10 μg or tRNA, used as non-specific competitor. Incubation was for 1h at room temperature in binding buffer, 200 μl final volume. Beads were washed three times with 1 ml binding buffer. ^{32}P labelled polynucleotides were extracted with phenol-chloroform, ethanol precipitated, and detected by autoradiography following separation on 1% agarose gels.

4.7. *In vivo* RNA crosslinking assay

In vivo cross-linking of PGC-1α to polynucleotides was performed basically as described (Kelley RL and Kuroda MI 2000) except that whole cell extracts (WCE) were prepared essentially as in (Monsalve M et *al.* 2000), with two modifications, the lysis buffer contained 1% NP-40 and the freezing-thawing step was omitted.

4.8. Preparation of cellular extracts and immunodetection (Western Blot)

Whole-cell lysates were obtained as described (Monsalve M et *al.* 2000). Cells were washed twice with cold PBS, centrifuged and resuspended in lysis buffer containing 20 mM HEPES pH 7.9, 125 mM NaCl, 1% NP-40, 1 mM EDTA, 5 mM β-glycerol phosphate, 0.2 mM NaV, 0.2 mM NaF, 10 mM NaP and protease inhibitors (Protease Inhibitor Cocktail, Sigma). The suspension was vortexed vigorously and centrifuged at 13.000 rpm in a minifuge to remove insoluble materials. Protein concentration in the extract was determined by a modified Lowry method (Bio-Rad DC Protein Assay). 20-25 μg of whole-cell protein extracts were denatured resolved on 8-15% sodium dodecyl sulfatepolyacrylamide gel

electrophoresis (SDS-PAGE), transferred onto PVDF Hybond-P membranes (Amersham Biosciences) using a semi-dry transfer system from Bio-Rad and incubated with specific antibodies.

PGC-1α	Cayman Chemical (WB)
	Santa Cruz H-300 (IP)
FoxO3a	Cell Signalling
	Santa Cruz
SirT1	Santa Cruz (WB-IP)
	Bethyl laboratories (ChIP)
Prx5	Santa Cruz
Prx3	LabFrontier
Trx2	LabFrontier
TR2	LabFrontier
Catalase	Chemicon International
MnSOD	Stressgen
UCP-2	Santa Cruz
	Biolegend
Acetylated-Lysine	Cell Signaling
β-actin	Sigma
HA	Hybridoma 12CA5
TLS	BD biosciences (IP)
	Novus Biologicals (WB)
normal immunoglobulin G (mouse or rabbit)	Santa Cruz
PGC-1α	Santa Cruz H-300
HA-tagged FoxO3a	Hybridoma 12CA5
Sirt1	Santa Cruz
SirT1	Bethyl laboratories
H4K16Ac	Millipore
RNAP II	monoclonal antibody 8WG15: COVANCE
CTD-S2P-RNAP II	monoclonal antibody H5: COVANCE

Table 4: Antibodies summary

Membranes were incubated for 1h in blocking solution (5% w/v fat-free dry milk in saline tris buffer (TBS) and 0.1% Tween 20 (TBS-T) to prevent non-specific antibody interactions with the membrane. Then, membranes were incubated with specific antibodies diluted in TBS-T against specific primary antibodies for 2h at room temperature or overnight at 4ºC. β-actin was used as a loading control.

Membranes were then washed twice with TBS-T with shaking for 10 min, incubated with corresponding secondary antibodies conjugated with horseradish peroxidase (HRP, Table 4) for 45 min at room temperature, washed again twice with TBS-T for 10 min and signal developed following exposure to the chemodetection system ECL (Amersham Biosciences), that was captured by exposure to an autoradiography film (AGFA).

4.9. Protein immunoprecipitation (IP)

Protein-protein interactions were analysed by co-immunoprecipitation experiments essentially as previously described (Monsalve *et al.*, 2000). Cells were scraped from the dish, washed twice with cold PBS and resuspended in lysis solution (20 mM HEPES pH 7.9, 125 mM NaCl, 0.1% NP-40, 1 mM EDTA, 5 mM β-glicerolfosfato, 0.2 mM NaV, 0.2 mM NaF, 10 mM NaP and proteinase inhibitors. Following a fast freezing-thawing cycle (freezing in liquid nitrogen and thawing at 37ºC), samples were vortexed vigorously, and centrifuged at 13.000 rpm for 10 min in a microfuge to remove non-soluble material. Following protein quantitation as indicated for whole cell extract preparations, 1mg of protein in 1ml of buffer was incubated with the corresponding immunoprecipitated antibody overnight at 4ºC in an orbital rotator. Then, 40 µl of 50:50 A/G-agarose slurry was added to the

sample and following 2 h incubation, the immune-complexes were collected by centrifugation (1 min at 1.000 rpm), washed twice with cold PBS and finally resuspended in denaturing buffer, heat denatured and loaded on SDS-PAGE gels, for western blot analysis. Control immunoprecipitation samples were analysed in parallel that used normal immunoglobulin G (mouse or rabbit) instead of a specific antibody (Table 4).

5. Genomic analysis

5.1. Chromatin Immunoprecipitation (ChIP)

ChIP experiments were carried out essentially as previously described (Valle I et *al*. 2005) with some modifications. In brief, cells were first cross-linked with 1% formaldehyde, and lysed (lysis buffer: 50 mM Tris HCl pH8.0, 150 mM NaCl, 5 mM EDTA, 1 %, Triton-X 100, 0.5 % NP-40). The resulting chromatin preparation was sheared by sonication and incubated overnight at 4ºC with antibodies against specific proteins, and then with Dynabeads® A/G for 2h. The magnetic beads were collected, and washed extensively. To isolate the immunoprecipitated DNA, the crosslinks were reversed (6h 65ºC), the protein was digested with proteinase K, and the RNA degraded with RNAse A. The nucleic acid fraction was extracted with phenol:chlorophorm and ethanol precipitated using glycogen as carrier. The resulting co-precipitated DNA preparations were analysed by qPCR with specific primers. Oligonucleotides designed against the coding sequence of β-actin were used as negative control (Table 5).

5.2. Genome-wide microarray analysis

For each experiment three independently-isolated cultures of primary hepatocytes from PGC-1$\alpha^{+/+}$ and PGC-1$\alpha^{-/-}$ mice were infected with the indicated adenovirus. RNA was extracted by TRIzol® extraction, re-purified with RNAeasy (Invitrogen), and checked for integrity and quantity with the Agilent Bio-Analyser QC. RNA was amplified and labelled with the One-Color Microarray-Based Gene Expression Analysis Protocol (Agilent Technologies, Palo Alto, CA, USA). Briefly, 800 ng total RNA were reverse transcribed using T7 promoter primer and the Moloney murine leukemia virus (MMLV) reverse transcriptase (RT). cDNA was then converted to anti-sense RNA (aRNA) with T7 RNA polymerase, which amplifies target material and simultaneously incorporates cyanine 3 (Cy3)-labeled CTP. Samples were hybridized to a G4122F 4x44K whole mouse genome microarray (Agilent Technologies). Cy3-labeled aRNA (1.65 µg), in a final concentration of 1x GEx HIRPM hybridization buffer (Agilent Technologies), was hybridized for 17 h at 65ºC in an G2545A hybridization oven (Agilent Technologies) set to 10 rpm.

β actin (*Mm, Rn, Bt*)	5'-GTTCCTCTTCGCCTGACTGTT-3'	forward
	5'-CTGAACCGTTTCCGTTGCTT-3'	reverse
MnSOD (-200)	5'-GAGCCGTACCATCTCTTTCG-3'	forward
	5'-CTCGGCACTGTGGTCGG-3'	reverse
MnSOD (ATG)	5'-AGTTGGAAGCGGCGCGCGCA-3'	forward
	5'-GCCGCGCTGACCTGAGACGA-3'	reverse
catalase (-300)	5'-AGAGCTGAAAGCATGTTAACAG-3'	forward
	5'-CTGCAAACGCCCGATTAACTA-3'	reverse
catalase (ATG)	5'-GAAGTCGCCTATTTCAGCTG-3'	forward
	5'-GCTCCTTCCAGTGTTTCATC-3'	reverse
prx3 (-1400)	5'-TCCCACATGCCGTAACTAAGAGT-3'	forward
	5'-ACTGGGTTGGTGGGTGTGGA-3'	reverse
prx3 (-1100)	5'-CAAAGTACCGTGCTCACCAC-3'	forward
	5'-CACCAATAAGCCAAGTGGGTC-3'	reverse
prx3 (-800)	5'-GACCCACTTGGCTTATTGGT-3'	forward
	5'-CAACTAAGACTTGGTGCAATC-3'	reverse
prx3 (-148)	5'-TCTTGCCACCCTGGATTGGA-3'	forward
	5'-ACG TGG AAG AGC TAC GAC CT-3'	reverse
prx3 (ATG)	5'-AGGTCGTAGCTCTTCCACGT-3'	forward
	5'-ACCGAAGCCCGAAACAACCT-3'	reverse
prx3 (+ 250)	5'-GGGCAGCGTCTAAGGCAGGC-3'	forward
	5'-AACCGGGACCAGGGGACAGG-3'	reverse
prx3 (+ 500)	5'-GGGTTTCCGTGAGCATCCCCT-3'	forward
	5'-GTTTGCTCAATTTCAGGGTTCTGC-3'	reverse
prx3 (+ 1700)	5'-AGGAACAAGGCCAGCGGAGG-3'	forward
	5'-AGA AGC AGC AGG CCT AAG GGC-3'	reverse
prx5 (-300)	5'-TGGCTGAGCTAAACCTCAG-3'	forward
	5'-CGAGTTGCCGCTGTTTCGA-3'	reverse
prx5 (ATG)	5'-TCTTCCGCAGGATTGCGTC-3'	forward
	5'-TGTCGTTGACGCACCCTCA-3'	reverse
ucp-2 (-2800)	5'-CTGAAAGAGCAATGTGTGATAC-3'	forward
	5'-CATTAGCGTATTCAGTCCTTG-3'	reverse
ucp-2 (-2500)	5'-GCTCTACAGGACACATAGTATG-3'	forward
	5'-CTCCTTTAGACTGGACTCTTAC-3'	reverse
ucp-2 (-2200)	5'-AGGCCCCAATGGGACAGTGA-3'	forward
	5'-TCGCAGTCTCAGGGACAGTCC-3'	reverse
ucp-2 (-500)	5'-TGGGCTGGTGAGCTCTGAGA-3'	forward
	5'-AGAGGGCAGGCAGATGAGGG-3'	reverse
ucp-2 (ATG)	5'-GTTCGGCTGCTGATGGACCT-3'	forward
	5'-GTAGGGGGCACATCTGTGGC-3'	reverse
ucp-2 (+ 250)	5'-CAAGGAGAAAGGCAGGGGCC-3'	forward
	5'-CGGAGGCGAAGCTCATCTGG-3'	reverse
ucp-2 (+ 700)	5'-AGCAGGAGAGGCTGAGGCTT-3'	forward
	5'-GGGTGAACGTGGCATGCTGA-3'	reverse
pgc-1α (-300)	5'-TCATTCAGGAGCTGG ATGGC-3'	forward
	5'-TCACCCAAACCCAAGCCCT-3'	reverse
pgc-1α (ATG)	5'-AGCGTTACTTCACTGAGGCA-3'	forward
	5'-ACAGTCCCCAGTCACATGA-3'	reverse
FoxO3a promoter	5'-ACCTAGCCCAGGAGAGACCT-3'	forward
	5'-AGCAGGCAGACCTGGAGAC-3'	reverse

Table 5: ChIP oligonucleotides summary

Arrays were washed and dried by centrifugation as indicated in the manufacturer's protocol. Arrays were scanned at 5 mm resolution with a G2565BA DNA microarray scanner (Agilent Technologies) at the default settings for 4x44k format one-color arrays. Images were analysed using Feature Extraction software v10.1.1.1 (Agilent Technologies). Raw signals were thresholded to 1 and normalization by quantile (Bolstad BM et *al.* 2003) was performed using GeneSpring software. Data were considered in the log2 scale. Default flags were considered as absent, except saturated spots that were flagged as marginal. From the initial 41081 probes present in the Agilent 4x44K chip, 25280 remained if (i) they exhibit a signal within the higher 80th percentile in at least 50% of the replicates in one condition; (ii) at least 50% of the replicates in one condition were flagged as present or marginal (iii) are not control probes and (iv) have a standard deviation across samples larger than 0.25. Quality Control checks based on the bioconductor package Array Quality Metrics (www.bioconductor.org) did not detect any sample as statistical outlier. All samples were hence used for statistical analysis using the limma bioconductor package (Smyth et *al*. 2004). The data were adjusted to a paired two factorial lineal model, considering as fixed factors the genotype (PGC-1$\alpha^{+/+}$ and PGC-1$\alpha^{-/-}$) and the adenovirus, and the animal as random factor. For each contrast of interest genes with a Benjamini-Hochberg corrected p-value smaller than 0.05 were considered as differentially expressed (Smitten AL *et al.* 2008). To identify relevant functions regulated by PGC-1α and their dependency on PGC-1α-RRM we carried out gene functional analysis of regulated genes using the Ingenuity software (Table 6).

Inpp5j 1 F	5'-GGGATGATGTTCCTCTGGTG-3'	forward
Inpp5j 1 R	5'-ATCCACTTCCTCATGCTTGG-3'	reverse
Inpp5j 2 F	5'-CCCCAAACTCAGTCCTGGTA-3'	forward
Inpp5j 2 R	5'-ATGGATGACCTCCAAGATGG-3'	reverse
Cxcl1 1 F	5'-TGTTGTGCGAAAAGAAGTGC-3'	forward
Cxcl1 1 R	5'-ACAAAATGTCCAAGGGAAGC-3'	reverse
Slc17a3 a F	5'-TCCAAGGTATGCCAGCTTTC-3'	forward
Slc17a3 a R	5'-GCTTTCCCAAACACGAGGTA-3'	reverse
Slc17a3 b F	5'-GGAAGCTCACTCGTTTGTGA-3'	forward
Slc17a3 c F	5'-CAGTGAAGTAGGGCTCATAGCA-3'	forward
Slc17a3 c R	5'-TTTCCCACCCCTCTTCTCTT-3'	reverse
CamK2b a F	5'-CTCTCCCACCCACCTTGTTA-3'	forward
CamK2b a R	5'-TGCGAACACCTAGCCAGTTA-3'	reverse
CamK2b b F	5'-TGGCCAGTGCTGTAGTGTGT-3'	forward
CamK2b b R	5'-GCAGTTTCCCGAGACAGAAC-3'	reverse
CamK2b c F	5'-ACTTTGAGGCCTATGCGAAA-3'	forward
CamK2b c R	5'-TTCAGGATGGTGGTGTGGAT-3'	reverse
Cyp24a1 a F	5'-AGTCACAGCTTCGAGGGATG-3'	forward
Cyp24a1 a R	5'-GGCTCAAGCCCCACTATACA-3'	reverse
Cxcr7 a F	5'-AGCACCAGGACAGGCTCTTA-3'	forward
Cxcr7 a R	5'-CAGCCTTACACCTCCCATACA-3'	reverse

Table 6: Array target oligonucleotides

5.3. Crosslinking Immunoprecipitation (CLIP)

The rat hepatoma cell line FAO and mouse primary hepatocytes (PGC-1$\alpha^{-/-}$) expressing HA-tagged PGC-1α, PGC-1-ΔRRM were prepared in 20 cm Ø dishes as described under cell culture. Living cells were irradiated with 365 nm UV light for 2 min after removal of the medium and replacement with a thin layer of PBS. Cells were harvested and lysed in lysis buffer (as decribed in ChIP and Monsalve M et *al*. 2000). The cleared cell lysates were treated with RNase T1. HA-tagged proteins were immunoprecipitated with anti-HA antibodies bound to Protein A/G Dynabeads. RNase T1 was added to the immunoprecipitate. Beads were washed and resuspended in dephosphorylation buffer. Calf intestinal alkaline phosphatase was added to dephosphorylate the RNA. Beads were washed and incubated with polynucleotide kinase and radioactive ATP to label the crosslinked RNA. The protein-RNA complexes were separated by SDS-PAGE. The specific protein/RNA band was cut from the SDS-PAGE gel and electroeluted. The electroeluate was proteinase K digested. The RNA was recovered by acidic phenol/chloroform extraction and ethanol precipitation. Importantly, use siliconised tubes for all manipulations of the small RNAs. The minute amounts of small RNAs to be recovered after gel purification will readily adsorb to the walls of standard tubes.

The protocol from Tushl was first applied as follows.

The specific RNA was prepared to form a library labelled by distinct oligonucleotides on 3’ and 5’ end named barcode. These steps were applied to PGC-1α bound RNA and control oligomers 19 mer and 24 mer (Table 7).

Collect the small RNA pellet after ethanol precipitation in a tabletop centrifuge for 15 min at maximum speed (~14,000×g) at 4°C. Remove the supernatant and collect the residual liquid at the bottom of the tube by an additional 5 s centrifuge spin. Remove the residual liquid completely using a small pipette tip without perturbing the pellet. The additional spin is needed to collect all residual liquid. If necessary air-dry the RNA pellet to evaporate residual ethanol. Be sure that the ethanol has been evaporated as it may inhibit the subsequent enzymatic steps. All subsequent RNA precipitations are performed similarly.

19-nt	5'-CGUACGCGG***GUUUAAAC***GA-3'
24-nt	5'-CGUACGCGGAAUA***GUUUAAAC***UGU-3'
Adapter set 3'	5'-AppTCGTATGCCGTCTTCTGCTTG-L-3'
Adapter set 5'	5'-rGrUrUrCrArGrArGrUrUrCrUrArCrArGrUrCrCrGrArCrGrArUrC-3'
A,C,G,T, DNA residues; rA, rU, rC, rG, RNA residues; L, 3'OH blocking group	

Table 7: CLIP oligonucleotides

Adapters need to be joined to the small RNA pool to allow for Reverse transcription PCR amplification (RT-PCR). The adapters used to introduce the constant regions and their corresponding PCR primers vary, depending on the sequencing method that is being used. The adapter and the

primer sets for Solexa high-throughput sequencing-by-nucleotide are different because this method did not yet allow for reads similar in size to 454. Therefore, the sequencing primer-binding site has to be already present in the 5' adapter.

The 3' adapter ligation is performed using chemically pre-adenylated oligodeoxynucleotides.

Dissolve the RNA pellet in 10.5 µl water. Prepare a reaction mixture for ligation of the 3' adenylated adapter by combining the following components: 2 µl of 10× RNA ligase buffer without ATP (0.5 M Tris-HCl, pH 7.6; 0.1 M $MgCl_2$; 0.1 M 2-mercaptoethanol; 1 mg/ml acetylated BSA (Sigma, B-8894), 6µl 50% aqueous DMSO, 0.5 µl 100 µM adenylated 3' adapter oligodeoxynucleotide. Add the 8.5 µl of the mixture to the sample.

Denature the RNA by incubating the tube for 30 s at 90°C. Place the tube immediately on ice for 20 s.

Add 1 µl of Rnl2 (1–249) (1 µg/µl), mix gently, and incubate overnight at 0°C. Rnl2(1–249) is commercially available from New England Biolabs.

Add 20 µl of gel loading solution [formamide loading solution (50 mM EDTA, 0.05 % (w/v) bromophenol blue in formamide)] and load the samples in two adjacent wells of a 20-well 15% acrylamide gel (15 cm×17 cm×0.8 mm; 30 ml gel volume). Make sure to space different samples appropriately, typically at a two-well distance, to avoid cross contamination. Run the gel for 1 h at 30 W using 0.5× TBE buffer until the bromophenol blue dye is close to the bottom of the gel. Image the gel by exposure to a phosphorimaging screen for at least 45 min depending on the amount of RNA ligated. Excise the ligation product. Elute the ligation product from the gel slices overnight at 4°C with constant agitation with at least 3 to 4 volumes of 0.4 M NaCl. Ethanol-precipitate and collect the RNA.

Dissolve the pellet in 9 µl water. Prepare the following reaction mixture by combining 1 µl of 100 µM 5' adapter oligonucleotide, 2 µl of 10× RNA ligase buffer with ATP (0.5 M Tris-HCl, pH 7.6; 0.1 M $MgCl_2$; 0.1 M 2-mercaptoethanol; 1 mg/ml acetylated BSA (Sigma, B-8894); 2 mM ATP) and 6 µl 50% aqueous DMSO. Add the 9 µl of this mixture to the sample. Denature the RNA by incubation for 30 s at 90°C. Place the tube immediately on ice for 20 s. Add 2 µl of T4 RNA ligase 1 (Rnl1) (Fermentas), mix gently, and incubate for 1 h at 37°C.

Add 20 µl of gel loading solution (see above) and load the samples in two adjacent wells of a 20-well 15% acrylamide gel (15 cm×17 cm×0.8 mm; 30 ml gel volume). Run the gel for 1 h at 30 W using 0.5× TBE buffer until the bromophenol blue dye is close to the bottom of the gel. Image the gel and excise the new ligation product. Elute the ligation product from the gel slices overnight at 4°C with constant agitation using at least 3 to 4 volumes of 0.4 M NaCl. Add 1 µl of 100 µM 3' primer during the elution as carrier to facilitate the recovery of the ligation product. Ethanol-precipitate and collect the RNA (Hafner M et *al*. 2008).

As this approach was not successful, we ligate the recovered RNA applying the TruSeq™ Small RNA kit from Illumina. 3' Adapter and 5' Adapter ligation was performed as described, followed by a RT-PCR amplification and gel purification of the fragment. The obtained library was validated on gel and Bioanalyser. High-throughput sequencing was performed with an Illumina Genome Analyser.

For each of the datasets mentioned above, the Illumina-Solexa small RNA sequencing data was filtered by eliminating low quality reads, adaptor sequences and adaptor contaminants in order to generate clean reads using Cutadapt 1.0.

In order to identify clusters of sequences, the ClustalW software was used. The identified sequences (Table 8) were aligned to the mouse reference genome (NCBI v37, mm9) using Integrative Genomics Viewer (IGV).

CLIP17/6 a F	5'-CGGAACTGAGGCCATGATTA-3'	forward
CLIP17/6 a R	5'-GCCGGTCCAAGAATTTCAC-3'	reverse
CLIP17/6/10 b F	5'-CGAAAGCATTTGCCAAGAAT-3'	forward
CLIP17 b R	5'-AGTCGGCATCGTTTATGGTT-3'	reverse
CLIP17 c F	5'-AGTCGGAGTTTCGAAGACGA-3'	forward
CLIP17/6/10 c R	5'-CCCTTCCGTCAATTCCTTTA-3'	reverse
CLIP6/17 a F	5'-GTTGGTTTTCGGAACTGAGG-3'	forward
CLIP6/17 b R	5'-CAAATGCTTTCGCTCTGGTC-3'	reverse
CLIP10 a F	5'-ACCCACAGAAGCGAGAAAGA-3'	forward
CLIP10 aR	5'-TGGAGCCTGTGGCTTAATTT-3'	reverse
CLIP10 b F	5'-AACCATACTCTCCCCGGAAC-3'	forward
CLIP10 b R	5'-ACCATAAACGAAGCCGACTG-3'	reverse
CLIP2/1/5 a F	5'-CACGCCCTCTTGAACTCTCT-3'	forward
CLIP2 a R	5'-TTCAACAAGTACCGTAAGGGAAA-3'	reverse
CLIP1/2/5 a F	5'-GAGAGTTCAAGAGGGCGTGA-3'	forward
CLIP1 a R	5'-ATCGACAATTTCCAGCCTTG-3'	reverse
CLIP1/2/5 a F	5'-GAGAGTTCAAGAGGGCGTGA-3'	forward
CLIP5 a R	5'-ACAGGGTGCGGGAAAGAT-3'	reverse
CLIP15 a F	5'-TCCTGTCAGCTGGAAAAACTG-3'	forward
CLIP15 a R	5'-GCCATGGTAAGGAGGTGAGA-3'	reverse

Table 8: CLIP target oligonucleotides

5.4. Statistical analysis

Statistical differences were determined by t-test or analysis of variance (ANOVA) as appropriate. Data are expressed as means ± SD. *p* values were considered significant at <0.05 (#). n≥3 for all experiments.

Results

Results

1. Promoter regulation of antioxidant genes

To investigate PGC-1α transcriptional activity the focus was given to the posttranslational modification. In particular, the role played by the type III deacetylase protein SirT1 and its interaction with the transcription factor FoxO3a and the coactivator PGC-1α was analysed. The collaboration was studied on the promoter region of the detoxification genes where PGC-1α has a key role.

1.1. SirT1 over-expression induces the antioxidant genes

PGC-1α and FoxO3a are two known key transcriptional regulators of antioxidant gene expression Introduction section 2.2. and 2.4.). In this chapter, to develop knowledge on PGC-1α and the upstream transcriptional regulation, the focus is given to SirT1 mechanism of action. SirT1 was identified as a potential key player in transcription regulations due to its main characteristic as histone deacetylase (Introduction section 1.1.3.1.).

Moreover, at the time this study was initiated SirT1 has been shown to control the activity of both PGC-1α and FoxO3a by deacetylation (Rodgers JT *et al.* 2005, van der Horst A *et al.* 2004, Kobayashi Y *et al.* 2005). Importantly, SirT1 activity on PGC-1α and FoxO3a has also been found to be functionally relevant in the control of endothelial activity during angiogenesis and liver, a process where ROS levels are known to be highly relevant (Introduction section 2.3.). In this light, the role played by SirT1 in the control of antioxidant gene expression was investigated and specifically if this regulation was dependent on PGC-1α and FoxO3a, since these two factors have previously shown direct implication in the coordinated regulation of antioxidant gene expression.

Previous results, from our laboratory, showed that SirT1 over-expression induced the expression of several antioxidant genes (*sod2-MnSOD, catalase, prx5 and tr2*) in bovine aortic endothelial cells (BAEC), as well as the levels of PGC-1α and FoxO3a. This result suggested that SirT1 may be in fact a regulator of at least some antioxidant genes in endothelial cells. Importantly, SirT1 also up-regulated the mRNA and protein levels of both PGC-1α and FoxO3a. These results indicate that SirT1 activity on antioxidant genes could be at least partially dependent on PGC-1α and FoxO3a transcriptional regulation (Figure 2.1).

The induction of the antioxidant genes by SirT1 is related to the levels of PGC-1α and Fox3a. The SirT1 induction of antioxidant gene expression occurs in a PGC-1α and FoxO3a dependent manner.

These results also support the idea that SirT1 is required to regulate PGC-1α and FoxO3a expression levels; SirT1 is likely to be relevant in the process maintaining the basal expression levels of a whole set of oxidative stress protection genes in endothelial cells.

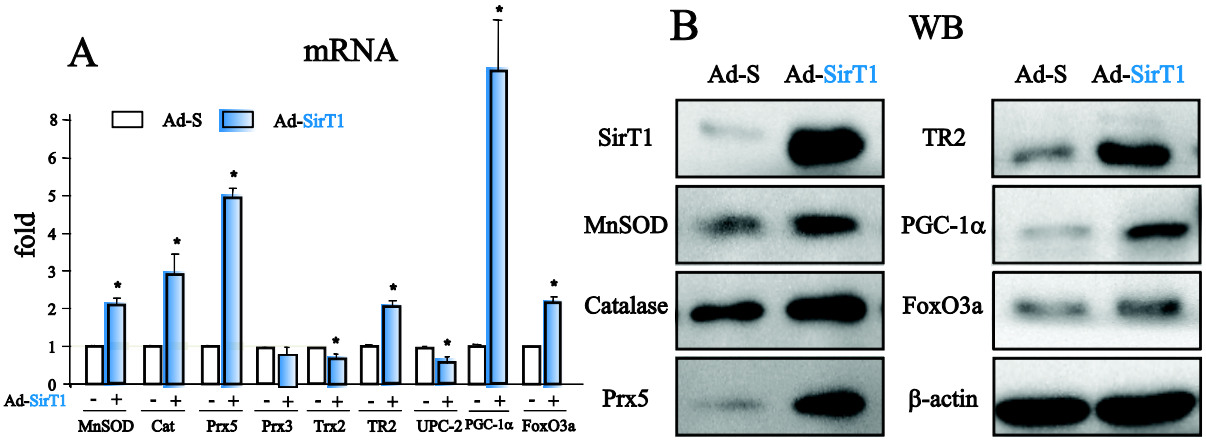

***Figure 2.1**: SirT1 induction of PGC-1a, FoxO3a and antioxidant genes at mRNA and protein level. Analysis of oxidative stress protection genes in BAEC that were infected o/n with recombinant adenovirus as indicated and harvested 24 h post-infection. A) qRT-PCR mRNA expression analysis. B) Protein analysis by WB. Data are from ≥3 independent experiments.*

Furthermore, as SirT1 is a deacetylase, not only of histones but also of proteins, the acetylation levels of the PGC-1α and FoxO3a were investigated.

It is shown that SirT1 over-expression in BAEC reduced both PGC-1α and FoxO3a acetylation in oxidative stress conditions (Figure 2.2). Since acetylation had been previously shown to reduce both PGC-1α and Foxo3a activity and stability, deacetylation could contribute to the observed induction of antioxidant gene expression by SirT1 in a PGC-1α and FoxO3a dependent manner.

Control of key transcriptional regulators and antioxidant genes by SirT1

In order to further dissect the mechanisms that mediated SirT1 regulation of antioxidant gene expression, SirT1 was silenced in BAEC using a recombinant adenovirus that drives the expression of a SirT1 specific shRNA (shSirT1). Observation that Ad-shSirT1 decreased the mRNA and protein levels of MnSOD, catalase, Prx5, TR2, Prx3, Trx2, UCP-2, PGC-1α and FoxO3a, suggests that they are all targets of SirT1 (Figure 2.3).

To determine if this regulation was cell type specific or could be observed in other cell types, we determined the expression levels of the antioxidant genes under study in $SirT1^{+/+}$, and $SirT1^{-/-}$ MEFs. Analysis by qRT-PCR and Western Blot showed that the expression levels of the oxidative stress protection genes studied as well as PGC-1α and FoxO3a are lower in $SirT1^{-/-}$ MEFs than in $SirT1^{+/+}$ MEFs, supporting the notion that SirT1 is a general regulator of antioxidant genes and is required to maintain the basal expression levels of the antioxidant system.

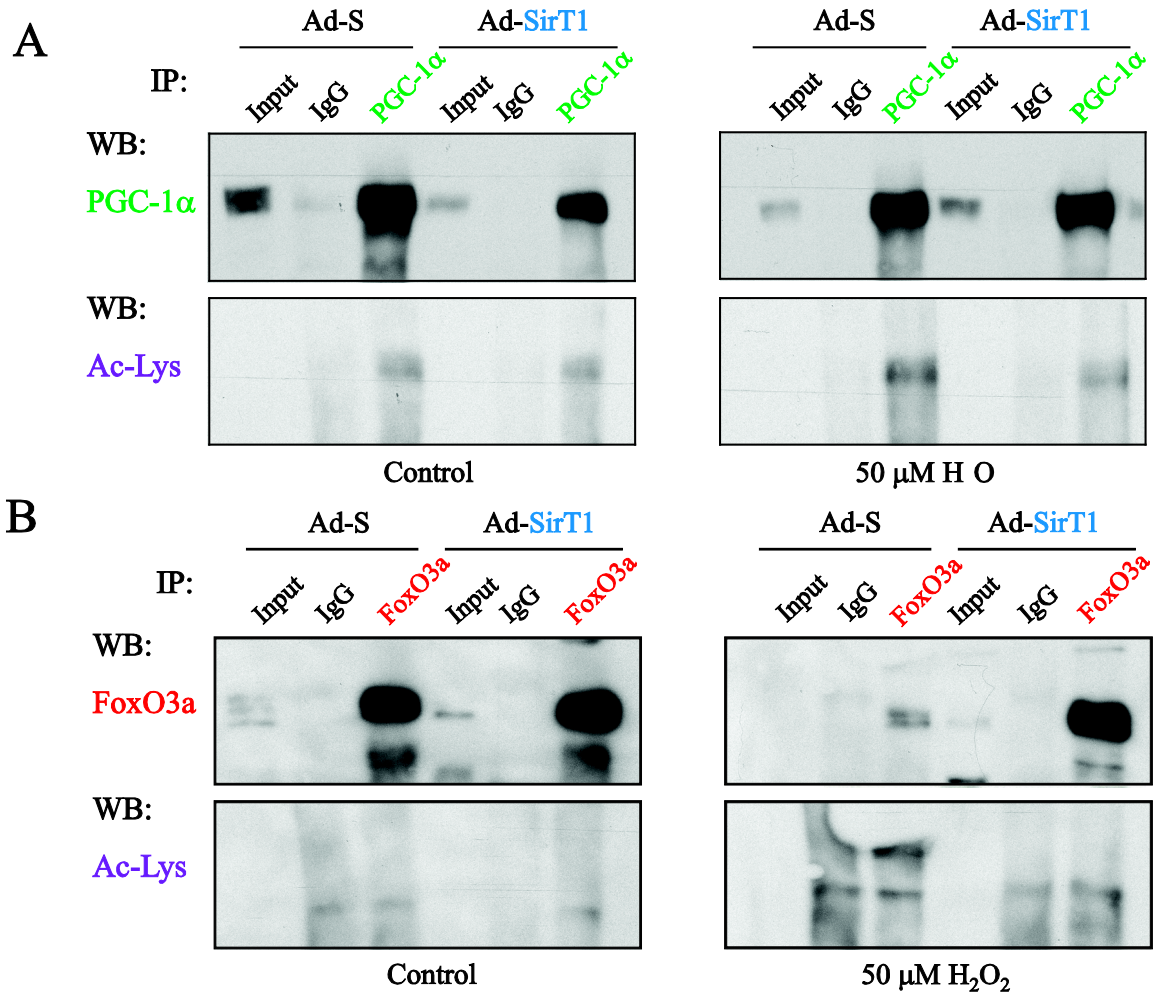

***Figure 2.2**: SirT1 deacetylaton of PGC-1α and FoxO3a in oxidative stress conditions. BAEC were co-infected o/n with Ad-SirT1 and Ad-PGC-1α (A) or Ad-FoxO3a (B), or the respective control adenoviruses. 24h post-infection cells were deprived of serum o/n and then treated with 50 µM H_2O_2 or vehicle for 4h. Whole cell extracts were subjected to immunoprecipitation (IP) with specific PGC-1α, FoxO3a or SirT1 antibodies or normal IgG, as a control, and analysed by western blot as indicated. Data are from ≥3 independent experiments. Data are means +SD (*) p ≤ 0.05 vs. control. The blots presented correspond to a representative experiment.*

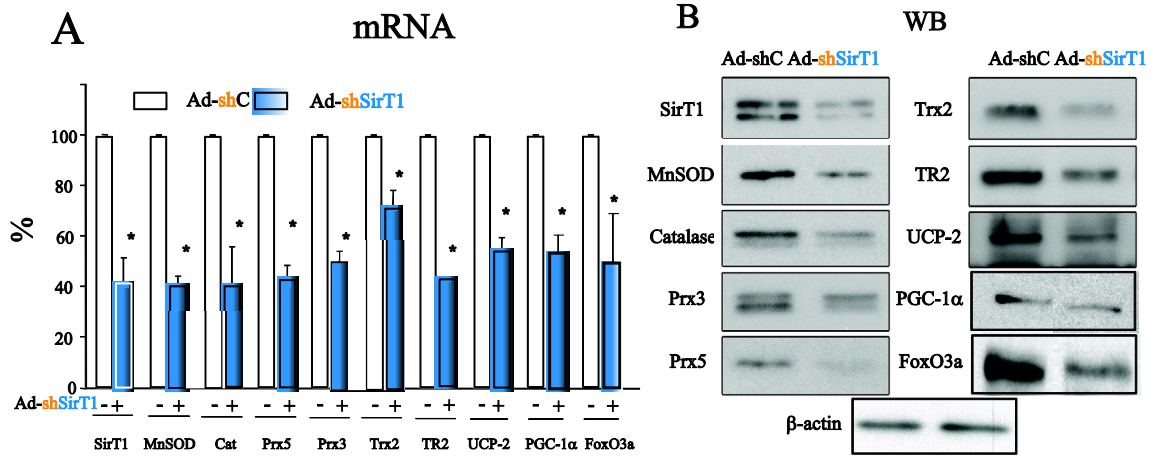

***Figure 2.3**: Silencing of SirT1 down regulates PGC-1a, FoxO3a and antioxidant genes at mRNA and protein level. Analysis of antioxidant genes in BAEC that were infected o/n with recombinant adenovirus as indicated and harvested 24 h post-infection. A) qRT-PCR mRNA expression analysis. B) Protein analysis by WB. Data are from ≥3 independent experiments. Data are means +SD (*) p ≤ 0.05 vs. control. The blots presented correspond to a representative experiment.*

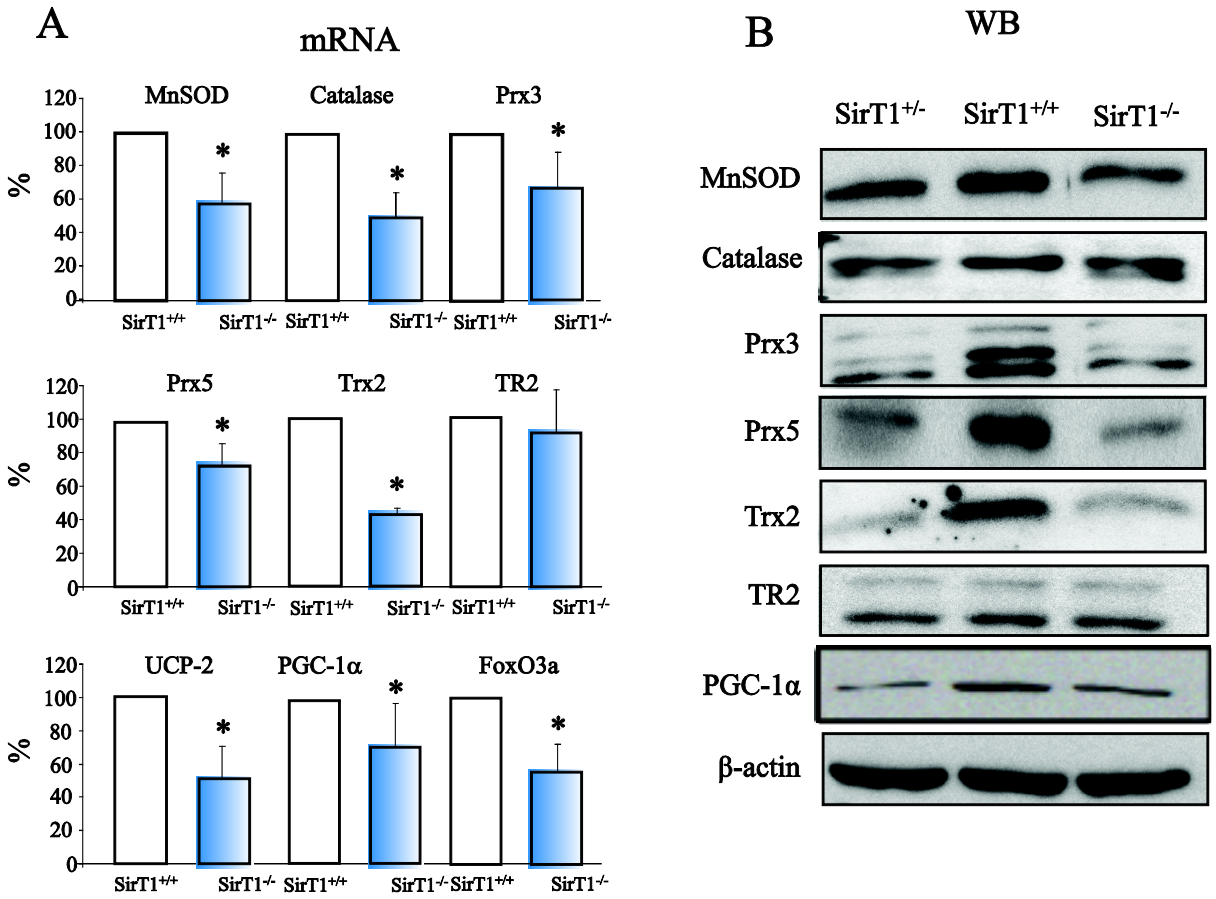

***Figure 2.4**: Analysis of oxidative stress protection genes in serum deprived SirT1$^{+/+}$ and SirT1$^{-/-}$ MEFs. A) qRT-PCR. B) Western Blot. Data are from ≥3 independent experiments. Data are means +SD (*) $p \leq 0.05$ vs. control. The blots presented correspond to a representative experiment.*

1.2. SirT1 regulation of PGC-1α/FoxO3a complex

To investigate the mechanisms involved in SirT1 regulation of PGC-1α and SirT1 activity, it was investigated whether SirT1 regulated the formation of the PGC-1α/FoxO3a complex.

First, the effect of SirT1 over-expression (Ad-SirT1) on the level of co-immunoprecipitated PGC-1α/FoxO3a complex was tested.

It was found that SirT1 increased the levels of FoxO3a associated with PGC-1α in these conditions (Fig. 2.5). Conversely, silencing of SirT1 (Ad-shSirT1) had the opposite effect (Fig. 2.6.).

The results show that SirT1 decrease the levels of FoxO3a associated with PGC-1α in these conditions. Therefore SirT1 positively regulates the formation of a PGC-1α/FoxO3a complex.

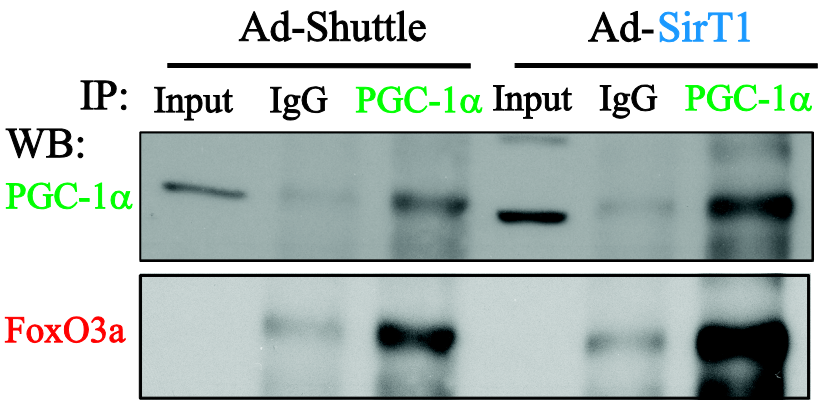

***Figure 2.5**: SirT1 overexpression promotes the formation of a PGC-1α/FoxO3a complex. BAEC were co-infected o/n with Ad-PGC-1α and the indicated adenoviruses. 12 h post-infection, cells were deprived of serum o/n and then treated for 4 h with 50 μM H_2O_2. Whole cell extracts were subjected to immunoprecipitation (IP) with a specific PGC-1α antibody or normal IgG, as a control, and analysed by Western Blot as indicated. Input indicates a 1/10 of whole cell extract not subjected to immunoprecipitation. The blots presented correspond to a representative experiment from ≥3 independent experiments.*

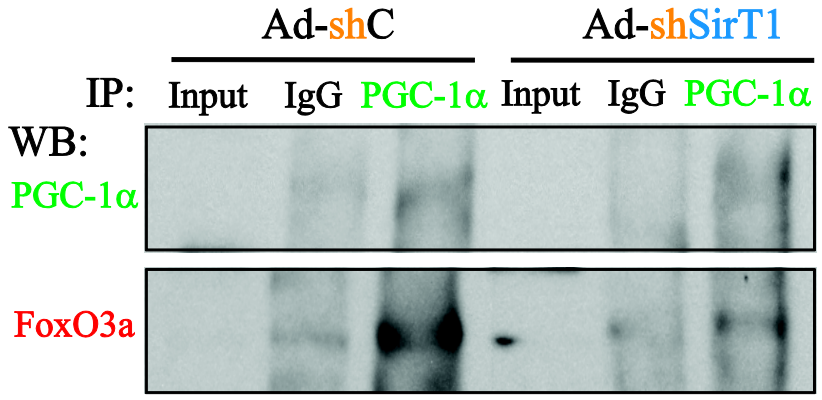

***Figure 2.6**: SirT1 knockdown downregulates the formation of a PGC-1α/FoxO3a complex. A) BAEC were co-infected o/n with Ad-PGC-1α and the indicated adenoviruses. 12 h post-infection, cells were deprived of serum o/n and then treated for 4 h with 50 μM H_2O_2. Whole cell extracts were subjected to immunoprecipitation (IP) with a specific PGC-1α antibody or normal IgG, as a control, and analysed by Western Blot as indicated. Input indicates a 1/10 of whole cell extract not subjected to immunoprecipitation. The blots presented correspond to a representative experiment from ≥3 independent experiments.*

As previously shown (Figure 2.1-2.4), SirT1 is a general regulator of antioxidant genes in bovine aortic endothelial cells and in mouse embryonic fibroblasts. To further investigate the role of SirT1 in the regulation of the PGC-1α/FOXO3a complex formation, $SIRT1^{+/+}$ and $SIRT1^{-/-}$ MEFs that over-expressed PGC-1α (Ad-PGC-1α) were used and the amount of FoxO3a that co-immunoprecipitate (co-IP) with PGC-1α was monitored.

The result show that FoxO3a amount found in PGC-1α immunoprecipitation was lower in $SirT1^{-/-}$ MEFs than in $SirT1^{+/+}$ MEFs. Previous observation and the mentioned results are supporting the evidence that SirT1 is a positive regulator of FoxO3a/PGC-1α complex formation (Fig. 2.7).

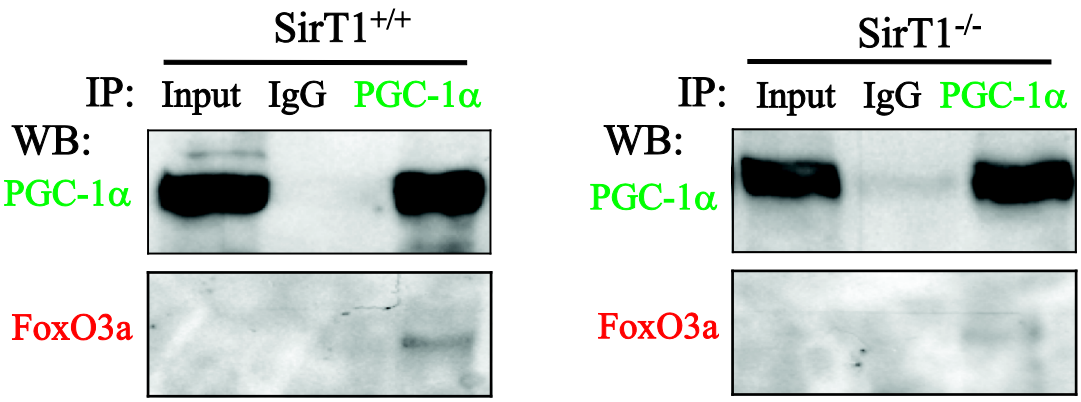

***Figure 2.7**: SirT1 deficient MEFs show reduced levels of the PGC-1α/FoxO3a complex SIRT1$^{+/+}$ and SIRT1$^{-/-}$ MEFs were infected o/n with Ad-PGC1α and 12 h post-infection cells were deprived of serum o/n. Cell extracts were immunoprecipitated with an specific anti-PGC1α antibody (PGC-1α) or rabbit IgG as control (IgG) and analysed by western blot. The blots presented correspond to a representative experiment from ≥3 independent experiments.*

Next it was investigated how Sirt1 could regulate the PGC-1α/FoxO3a complex formation.

Two alternative mechanisms could explain SirT1 activity on the PGC-1α/FoxO3a complex, SirT1 could act either on PGC-1α and FoxO3a individually or on a pre-formed complex (Figure 2.8). As already introduced (Introduction and Figure 2.2), posttranslational modifications play an important role in the localisation, stability and specificity of interaction for both FoxO3a and PGC-1α.

In order to determine whether the acetylation status of either PGC-1α or FoxO3a could be influenced by the formation of a PGC-1α/FoxO3a complex, FoxO3a acetylation levels in PGC-1α silenced BAEC and PGC-1α acetylation levels in FoxO3a silenced BAEC were tested.

Suppression of PGC-1α expression resulted in a dramatic increase in FoxO3a acetylation (Figure 2.8). Similarly, shRNA-mediated silencing of FoxO3a induced an increase in acetylated PGC-1α (Figure 2.9).

This result might suggest that SirT1 is likely to be active on the PGC-1α/FoxO3a complex, since in the absence of one of these factors, the other might not be deacetylated.

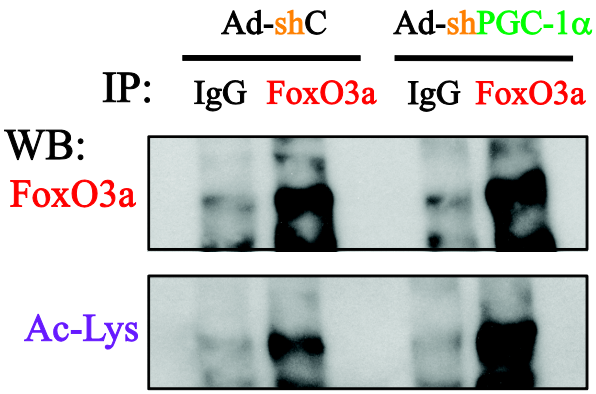

***Figure 2.8**: FoxO3a and PGC-1α influence each other level of acetylation: Silencing of PGC-1α. BAEC were infected o/n with Ad-shPGC-1α or the corresponding control adenoviruses, 12 h post-infection, cells were deprived of serum o/n and harvested. Whole cell extracts were subjected to immunoprecipitation (IP) with FoxO3a specific antibodies, or normal IgG, as a control. Acetylation levels were analysed by western blot. Data are from ≥3 independent experiments. Data are means +SD (*) p ≤ 0.05 vs. control.*

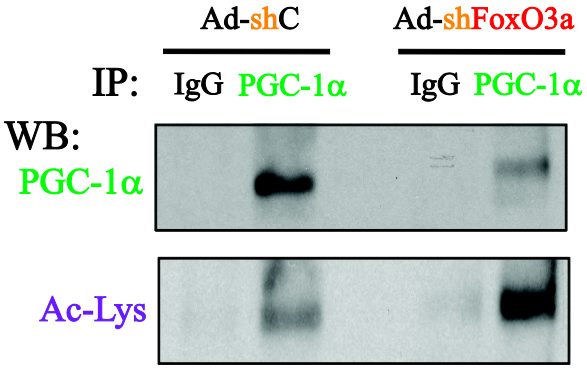

***Figure 2.9**: FoxO3a and PGC-1α influence each other level of acetylation: Silencing of FoxO3a. BAEC were infected o/n with Ad-shFoxO3a or the corresponding control adenoviruses, 12 h post-infection, cells were deprived of serum o/n and harvested. Whole cell extracts were subjected to immunoprecipitation (IP) with PGC-1α specific antibodies, or normal IgG, as a control. Acetylation levels were analysed by western blot. Data are from ≥3 independent experiments. Data are means +SD (*) p ≤ 0.05 vs. control.*

Generally speaking, modifying enzymes tend to work on a hit and go mechanism where they recognize the unmodified moiety of the target protein and the affinity drops following modification. Since the deacetylase activity of SirT1 is expected to work on two different proteins forming a complex while they are still in a complex. This results not only argues on the enhanced stability of a PGC-1α/Foxo3a complex when both are deacetylated, it further suggests that SirT1 may not leave the complex once the target protein is deacetylated but may actually stay associated with it and able to modify a different but nearby protein. This evidence would argue for two different interaction surfaces one for docking and one for modification within the SirT1 protein. Furthermore it may indicate that SirT1 can have different docking surfaces for PGC-1α and FoxO3a different from the acetyl binding domain.

1.3. SirT1 is recruited to the promoter regions of PGC-1α, FoxO3a and several antioxidant genes

Taking into account the previous results, suggesting that SirT1 was part of a ternary complex with PGC-1α and FoxO3a together with evidence showing that PGC-1α and FoxO3a formed a complex that bound to regulatory elements of target antioxidant genes and data indicating that SirT1 was also important for this regulation, the question raised whether SirT1 could also be recruited to regulatory promoter regions in these genes together with PGC-1α.

In order to elucidate the regulation mechanisms involving SirT1, SirT1 association with the promoter regions of the genes under survey, was questioned. To provide an answer, chromatin immunoprecipitation (ChIP) was the technique chosen.

SirT1 recruitment to promoter regions where PGC-1α/FoxO3a complex have previously shown to associate was tested. An attempt to identify putative SirT1 binding sites in PGC-1α and FoxO3a promoters was made.

Advantage was taken from the knowledge that SirT1 activity in cultured cells is dramatically modified by serum levels (Brunet A *et al.* 2004). Interestingly, one of the mildest conditions to

induce the detoxification system is serum starvation. Therefore 10% fetal bovine serum (FBS) and 0.5% FBS conditions were used as a simple strategy to modulate SirT1 activity (Brunet A. *et al.* 2004).

SirT1 did associate with the promoter regions of *sod2* (*MnSOD*), *catalase*, *prx3, prx5, ucp-2, pgc-1α, and foxO3a* (*trx2, tr2* were not analysed). Until now, Sirt1 was not mapped to a specific site in the promoter region of FoxO3a nor the antioxidant genes. Serum starvation generally increased SirT1 recruitment with the remarkable exception of the *prx5* gene, where it had the opposite effect (Figure 2.10.). These data suggested that SirT1 is likely to be directly involved in the regulation of mitochondrial antioxidant genes, including *pgc-1α* and *foxo3a*, while forming a ternary complex with PGC-1α and FoxO3a recruited to the promoter regulatory sites (Olmos Y *et al.* 2013).

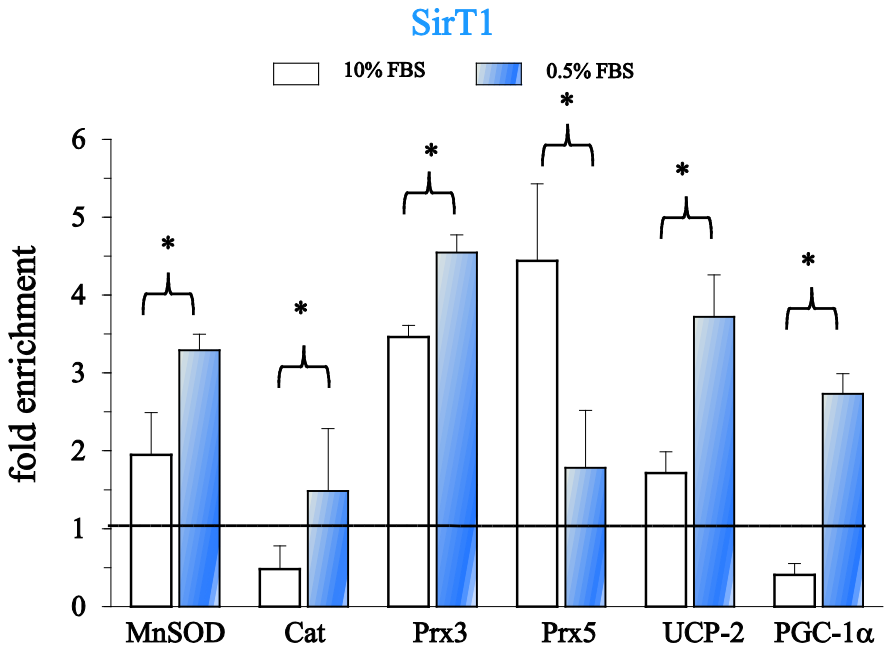

***Figure 2.10**: SirT1 is recruited to promoter regions of ROS detoxification genes upon serum starvation. ChIP assays to identify SirT1 binding sites of promoter regions corresponding to the indicated ROS detoxification genes. Cross linked chromatin Promoter occupancy was analysed by qPCR using specific primers. ß-actin CDS was used to control for non-specific enrichment. Data are from ≥3 independent experiments. Data are means +SD (*) p ≤ 0.05 vs. control.*

1.4. Promoter environment: Acetylation levels

SirT1 is a deacetylase whose role in histone deacetylation is well characterized (Introduction 1.1.3.1). From the above results, SirT1 seemed to be recruited to specific target sites in the regulatory regions of the promoters of antioxidant genes (Figure 2.10.).

This leads to the question of SirT1 recruitment to antioxidant genes and if upon recruitment to this specific sites, SirT1 would target nearby histone deacetylation. So far SirT1 histone deacetylase activity was presumed to work over large targeted chromatin domains rather than discrete specific binding sites.

Therefore, testing of whether SirT1 recruitment to antioxidant genes would be associated with a reduction in histone acetylation was carried out. H4 on lysine 16 (H4K16Ac) has been described as a position highly sensitive to SirT1 activity (Skurk C *et al.* 2004). To evaluate the deacetylation activity of SirT1, ChIP assays against the promoter regions of antioxidant genes were performed. Specific antibodies against the H4K16Ac epigenetic mark were used on SirT1 specific promoter binding regions.

The result show that at the sites where SirT1 binding could be detected (*catalase*, *prx3*, *prx5*, *ucp-2*), changes in H4K16 acetylation levels in response to serum deprivation mirrored changes in SirT1 recruitment (Figure 2.11.). In other words, more SirT1 binding correlated with reduced histone acetylation at the binding sites, and the opposite would also hold true. In general, increased SirT1 binding correlated with decreased acetylation levels and vice versa. This observation suggested that upon recruitment of SirT1 to FoxO3a/PGC-1α binding sites, it deacetylated nearby H4K16 residues.

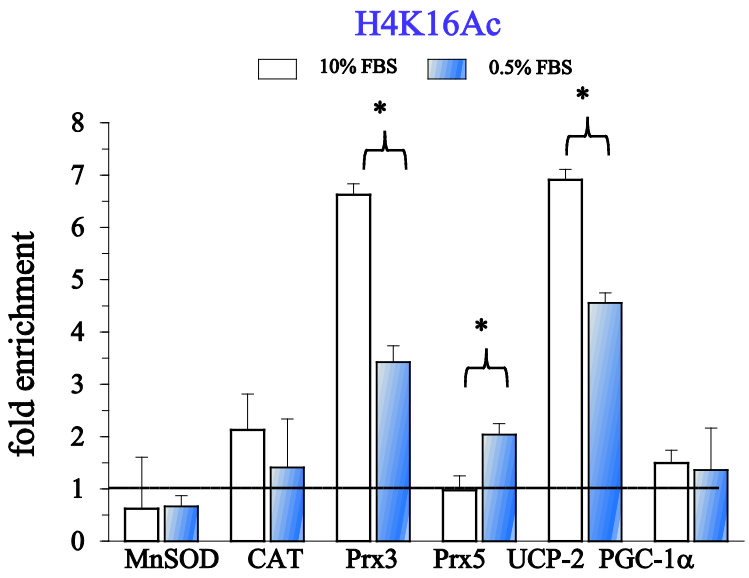

***Figure 2.11**: Acetylation level correlates with SirT1 localization at promoter sites. H4K16Ac ChIP assays of promoter regions corresponding to the indicated ROS detoxification genes. Cross linked chromatin Promoter occupancy was analysed by qPCR using specific primers. β-actin CDS was used to control for non specific enrichment. H4K16 acetylation levels at SirT1 sites. The position of the analysed fragments is indicated, using as reference (+1), the position of the ATG. Data are from ≥3 independent experiments. Data are means +SD (*) p ≤ 0.05 vs. control.*

1.5. Transcription activation: a sequential process

The results from the former section 1.4., where somehow puzzling, since histone deacetylation is normally associated with gene silencing and reduced recruitment of RNAP II to promoter sites. The results identified SirT1 as a positive and specific regulator of antioxidant gene expression. In order to elucidate how SirT1 regulates antioxidant gene expression while deacetylating histones at the targeted binding sites, ChIP assays was used to monitor RNAP II recruitment to antioxidant genes. A scanning from the SirT1 binding sites to the initiation of the CDS sequences was performed. RNAP II is generally recruited close to the ATG, the transcription start site. As bona fide transcription start sites

where unknown, ATG sites were used as an approximate reference for RNAP II localization. To target RNAP II by ChIP, these sequences were investigated and specific oligonucleotides were designed.

It was found that at positions proximal to the transcription start site (ATG primers for all genes except for *ucp-2*/-2500 since in this case the ATG is in exon 3) serum deprivation resulted in a dramatic decrease in RNAP II recruitment, suggesting that SirT1 dependent histone deacetylation negatively impacts on RNAP II recruitment at transcription start sites (Figure 2.12.).

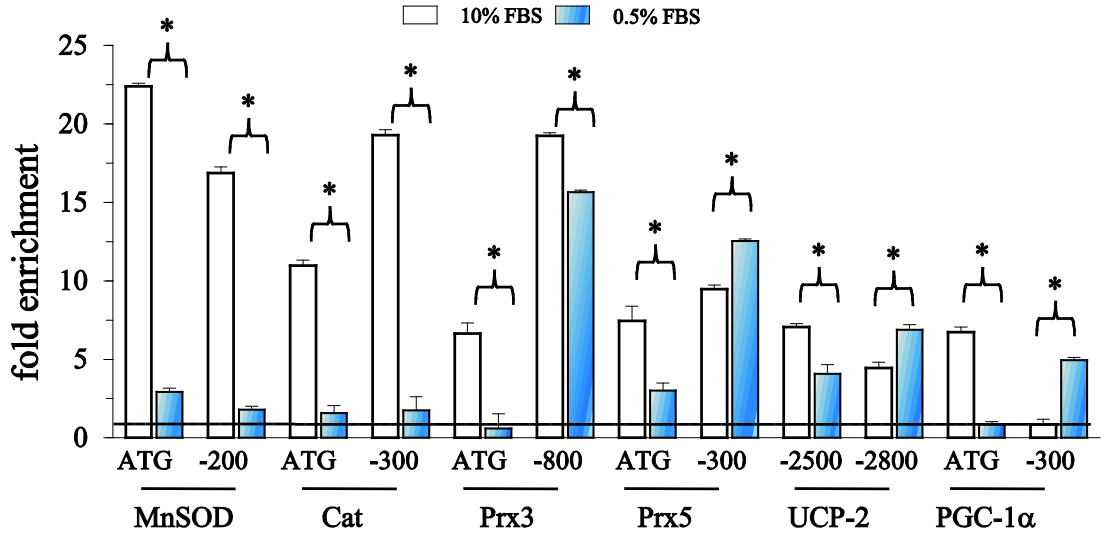

***Figure 2.12**: RNA polymerase chromatin immunoprecipitation on promoter region of antioxidant defense system ChIP assays of promoter regions corresponding to the indicated ROS detoxification genes. RNA P II recruitment. The position of the analysed fragments is indicated, using as reference (+1), the position of the ATG. The position of the analysed fragments is indicated, using as reference (+1), the position of the ATG. Data are from ≥3 independent experiments. Data are means +SD (*) p ≤ 0.05 vs. control.*

To monitor RNAP II recruitment to antioxidant genes, a scanning of the upstream sequences (from SirT1 binding to the ATG) of the genes under survey was made.

It was found that the upstream sites where SirT1 binding had been identified showed two distinct patterns for RNAP II binding. On one hand at *MnSOD*, *catalase* and *prx3*, RNAP II binding was also reduced in starvation conditions, but only very moderately at the *prx3* promoter (Figure 2.12.). Nevertheless, RNAP II recruitment was actually increased by serum deprivation at the *prx5*, *ucp-2* and *pgc-1α* promoters, suggesting that SirT1 recruitment could, at least in some cases, be associated to increased RNAP II recruitment at alternative start sites, despite of reduced acetylation on the site itself (Figure 2.12.).

In order to elucidate how, regardless of a reduced RNAP II recruitment, SirT1 could enhance transcriptional levels of these target genes, two genes were selected with the two apparently disparate recruitment patters for further analysis, *prx3* and *ucp-2*.

SirT1 binding, RNAP II recruitment, and levels of elongating RNA Polymerase II (RNAP II; CTD serine-2 phosphorylated: CTDS2P) versus initiation RNAP II (CTD serine-5 phosphorylated: CTDS5P) along each of the selected genes (*prx3* and *ucp-2*) were monitored.

In positions proximal to the transcription start site, serum deprivation resulted in a reduction in RNAP II recruitment, but downstream of the sites where SirT1 binding had been identified, it resulted in an increase in RNAP II levels. Reduced recruitment at the start site and increased levels downstream could be indicative of increased transcription rates.

The levels of elongating RNAP II by ChIP were performed using antibodies against the phosphorylated form of the C-terminal domain of RNAP II (CTD2P). Dramatic increases in "elongating RNAP II" in serum starvation conditions in both *prx3* and *ucp-2* genes were found, suggesting that reduced RNAP II recruitment at the start site was compensated by increased promoter clearance.

These results might explain how SirT1 recruitment can be associated with a sustained or increased gene expression despite of a general reduction in RNAP II recruitment induced by serum deprivation (Figure 2.13.).

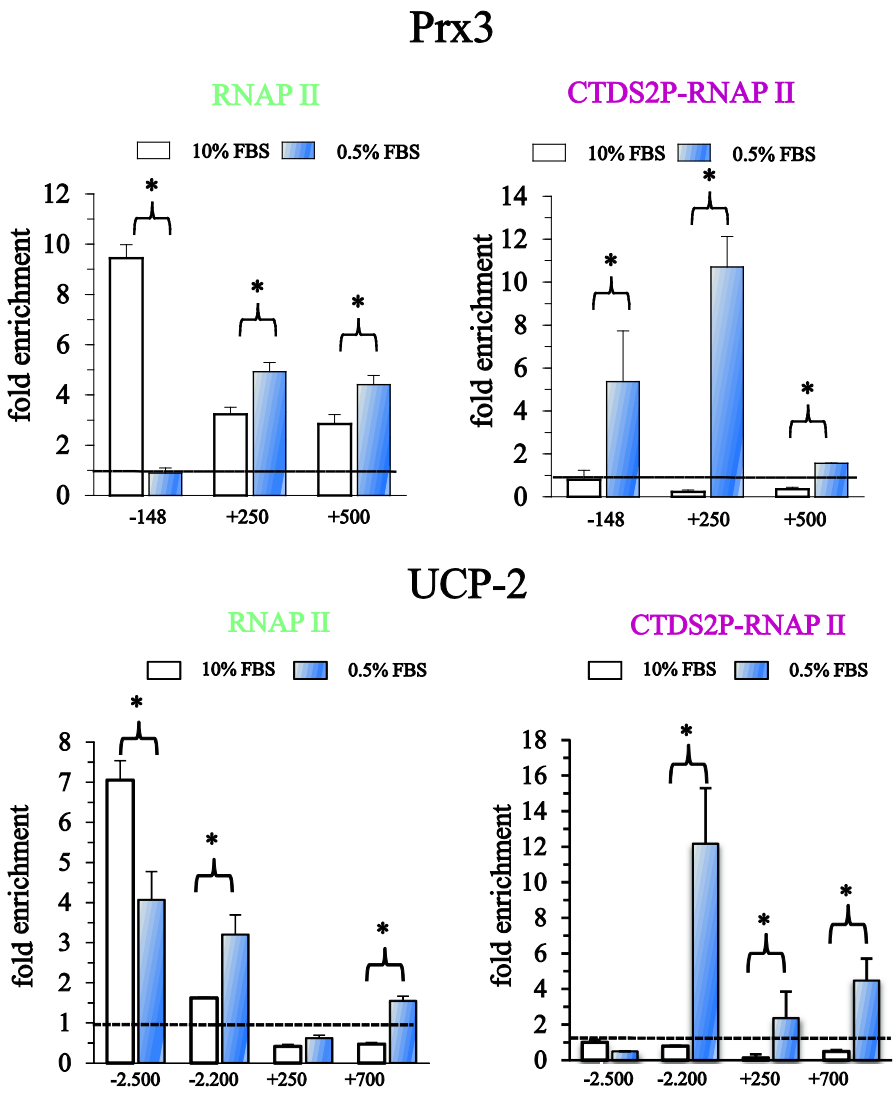

***Figure 2.13**: Increased levels of elongating RNAP II are associated with SirT1 recruitment. ChIP assays of promoter regions corresponding to the indicated ROS detoxification genes (Prx3 and UCP-2). Cross linked chromatin Promoter occupancy was analysed by qPCR using specific primers. β-actin CDS was used to control for non-specific enrichment. The position of the analysed fragments is indicated, using as reference (+1), the position of the ATG. Prx3 and ucp-2 were analysed. Left panels analysis of RNA P II at the transcriptional start region and along the genes. Right panel, analysis of "elongating" RNA P II levels (RNA P II phosphorylated in the Ser2 positions of the CTD repeats of the RNA P II largest subunit) at the transcriptional start region and downstream of the ATG. Data are from ≥3 independent experiments. Data are means +SD (*) $p \leq 0.05$ vs. control.*

In order to correlate histone deacetylation, SirT1 localisation on the target promoter region and gene transcription, SirT1 ChIP along the promoter and the coding sequence was performed.

Importantly, the results showed that SirT1 binding could only be detected at promoter sites in the *prx3* gene. In the *ucp-2* sequence, binding to SirT1 was detected in the promoter region and, some extent, within the transcribed region but downstream of the ATG, suggesting that SirT1 at these selected promoters binds to specific sites mainly at the promoter region. The absence of SirT1, where elongating RNAP II is located, makes it unlikely to be associated with the elongating RNAP II complex. Therefore SirT1 is not directly involved in the epigenetic modification of the CDSs regions (Figure 2.14.).

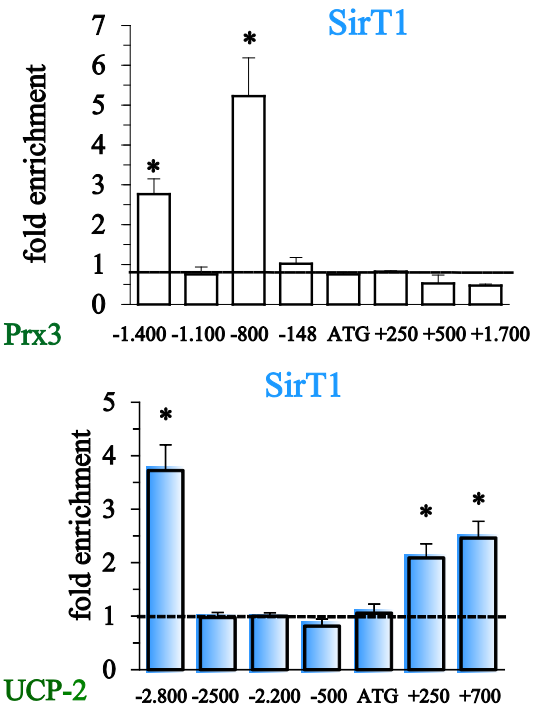

***Figure 2.14**: SirT1 is recruited to promoter regions (Prx3 and UCP-2). ChIP assays of promoter regions corresponding to the indicated ROS detoxification genes. Cross linked chromatin Promoter occupancy was analysed by qPCR using specific primers. β-actin CDS was used to control for non-specific enrichment. SirT1 recruitment along the genes, upstream and downstream of the ATG. Data are from ≥3 independent experiments. Data are means +SD (*) p ≤ 0.05 vs. control.*

Observation that serum starvation of BAEC resulted in a significant induction in the mRNA of SirT1, MnSOD, UCP-2, and PGC-1α suggesting that some genes are positively induced under this conditions (Figure 2.15). Catalase, Peroxiredoxin 3 and 5 did show a great variability in the measurements, however a tendency towards increase is observed.

These results might explain how SirT1 recruitment can be associated with a sustained or increased gene expression despite of the genome wide general reduction in RNAP II recruitment induced by serum deprivation (Figure 2.15.).

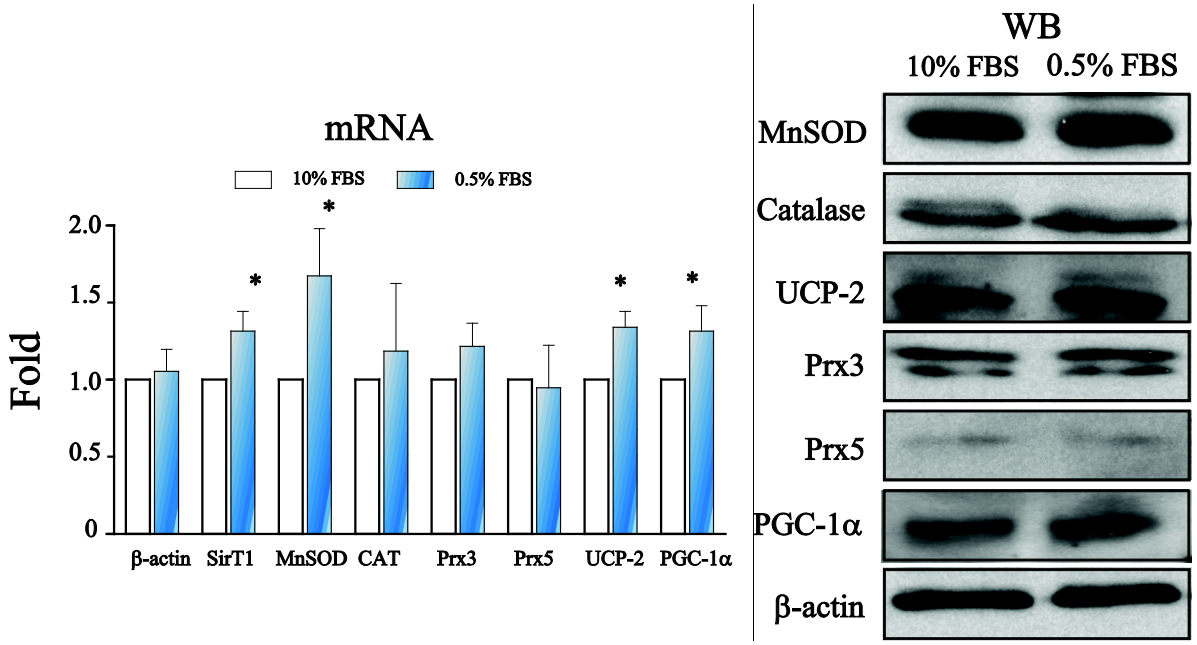

***Figure 2.15**: Antioxidant gene expression is sustained upon serum starvation. mRNA and protein levels of SirT1 target genes in confluent BAEC cells in 10 % FBS or serum deprived (0.5% FBS) o/n were analysed by qRT-PCR and western blot respectively. Data are from ≥3 independent experiments. Data are means +SD (*) $p \leq 0.05$ vs. control. The blots presented correspond to a representative experiment.*

The first aim of the work presented in this thesis was to determine if SirT1 collaborates with PGC-1α in regulating antioxidant genes and to find out through which mechanisms this regulation is mediated. The results demonstrate not only that SirT1 deacetylates PGC-1α and FoxO3a, but also that all three proteins together form an efficient ternary transcription elongation complex recruited to the regulating regions of the target antioxidant genes. After recruitment to the regulating regions, SirT1 deacetylates the nearby histones; this specific deacetylation does not lead to a gene silencing. However the exact mechanism of regulation is still not clear and remains to be elucidated. These results show for the first time that SirT1 can not only lead to a general silencing of chromatin, but can also induce specific gene expression when involved in a specific transcription complex.

2. Functional characterisation of PGC-1α RRM

The transcriptional co-activator PGC-1α has been shown to be a key regulator of mitochondrial biogenesis, adaptive thermogenesis, glucose metabolism and oxidative stress in response to specific signals (Introduction section 2.2.). The PGC-1α carboxyl terminal domain has specific domains with roles in transducing cellular metabolic signals. To elucidate the function of the RNA recognition motif (RRM) and the Arginine/Serine (RS) domain, several DNA constructs were generated by molecular biology engineering. Some constructs generated lack both the RRM and RS domains (ΔRRM/ΔRS PGC-1α), other constructs lack either the RRM (ΔRRM PGC-1α) or RS (ΔRS PGC-1α) domain (Figure 2.16.). These constructs were used to clarify the role of the domains in PGC-1α activity. In this section ΔRRM PGC-1α was studied.

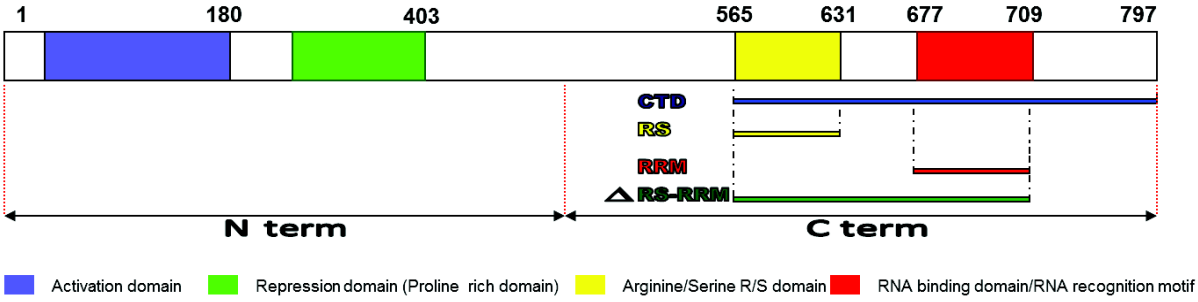

***Figure 2.16**: PGC-1α C-terminal constructs: lacking the C-terminal region, lacking both the RRM and RS domains (ΔRRM/ΔRS PGC-1α), either the RRM (ΔRRM PGC-1α) or RS (ΔRS PGC-1α) domain.*

Previous studies from the group (Sanchez-Ramos C *et al.* 2013) have shown that deletion of the RRM of PGC-1α reduces its capacity to trans-activate several genes involved in mitochondrial biogenesis. In order to investigate the mechanisms involved and the target specificity the activity of mutants of PGC-1α carboxyl that harbour a specific deletion of the RRM was tested and its capacity to regulate antioxidant gene expression was analysed. It was found that a mutant lacking the RRM was less efficient than the wild type protein in the induction of all antioxidant genes tested (*sod2-MnSOD, catalase, prx3, prx5, trx2, ucp-2*) with the possible exception of *tr2* in MEFs (Figure 2.17.).

***Figure 2.17**: PGC-1α adenovirus can restore the antioxidant gene induction but not Ad-PGC-1α-ΔSR/ΔRRM. MEFs were infected with the indicated adenoviruses (Ad, Ad-PGC-1α Ad-PGC-1α-ΔSR/ΔRRM). mRNA expression is shown as the fold induction above the level in cells infected with control adenovirus (Ad). Control samples were assigned the value of 1. Mn superoxide dismutase (MnSOD), uncoupling protein 2 (UCP-2), peroxiredoxins 3 and 5 (Prx3 and Prx5), thioredoxin 2 (Trx2), thioredoxin reductase 2 (TrxR2) and catalase (Cat). Data are means +SD. (*) P ≤0.05.*

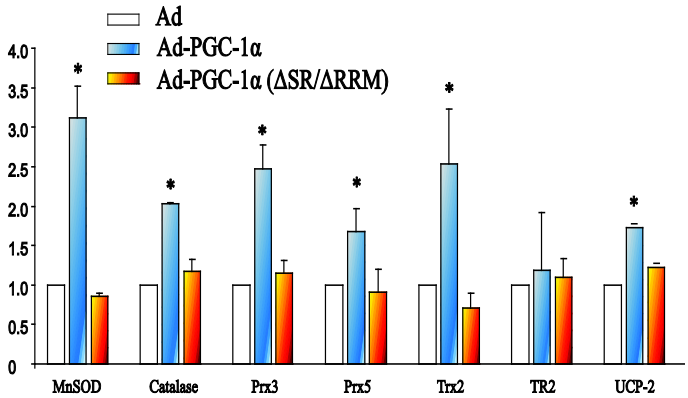

Translocated in liposarcoma (TLS) is a transcriptional cofactor of PGC-1α that interacts with its CTD. TLS regulates PGC-1α activity on antioxidant genes (Sanchez-Ramos C *et al.* 2013). When the coactivation activity of TLS on a PGC-1α mutant lacking the RRM was tested, it was found that even though TLS could still interact with PGC-1α-ΔRRM, TLS could not coactivate the PGC-1α-ΔRRM mutant to induce *catalase, prx5, trx2 and ucp-2.* However, it was still able to coactivate *sod2, prx3 and tr2* gene (Figure 2.18.).

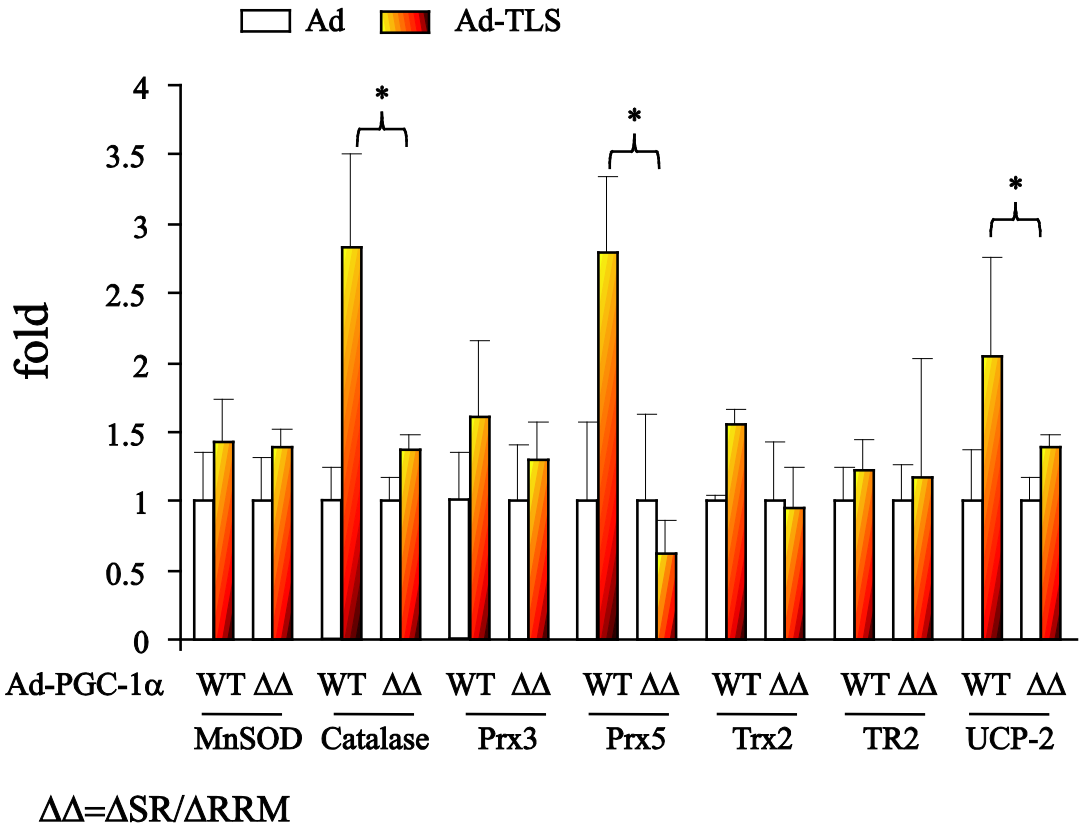

***Figure 2.18**: TLS activation of PGC-1α and PGC-1α-ΔΔ, consequences on the induction of the antioxidant genes. MEFs were infected with the indicated adenoviruses (Ad, Ad-TLS, Ad-PGC-1α Ad-PGC-1α-ΔΔ). mRNA expression is shown as the fold induction above the level in cells infected with control adenovirus (Ad). Control samples were assigned the value of 1. Mn superoxide dismutase (MnSOD), uncoupling protein 2 (UCP-2), peroxiredoxins 3 and 5 (Prx3 and Prx5), thioredoxin 2 (Trx2), thioredoxin reductase 2 (TrxR2) and catalase (Cat). Data are means +SD. (*) p ≤0.05.*

In order to investigate the coactivation mechanisms involved, the capacity of the coactivator TLS to coactivate PGC-1α wt or a mutant lacking the RRM on the proximal UCP2 promoter using a luciferase reporter assay was tested.

It was found that the WT but not the ΔRRM was able to coactivate TLS on the proximal UCP-2 promoter (Figure 2.19.). These results suggest that the RRM is necessary for the regulation of some but not all PGC-1α target genes and it may be required for functional interaction with some coactivators in a promoter specific manner. Importantly, promoter sequences are sufficient for RRM dependent regulation of target gene expression.

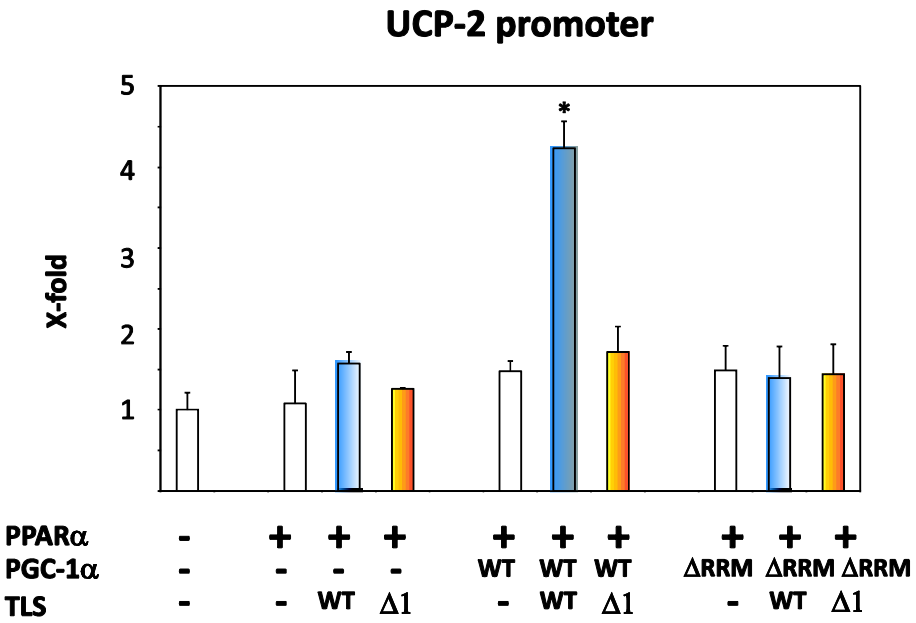

***Figure 2.19**: TLS can coactivate PGC-1α WT but not PGC-1α-ΔRRM at the UCP-2 promoter. 30% confluent FAO cells were transfected with 0.25 μg of pUCP2-luc, 0.25μg of S-HA-PGC-1α, or S-HA-PGC-1α-ΔRRM, 1 μg pSG5-FL-TLS or the corresponding empty vectors. Luciferase activity was determined 24 h post-transfection.*

2.1. Analysis of PGC-1α activity in hepatocytes

To further characterise the gene specificity of the RRM motif whole genome analysis of PGC-1α activity was carried out. Primary hepatocytes were selected as a relevant cell type, since the liver is the central metabolic organ of the organism and PGC-1α is essentially a metabolic regulator playing a key role in liver function. Primary hepatocytes isolated from PGC-1$\alpha^{+/+}$ and PGC-1$\alpha^{-/-}$ mice were chosen as a cellular model for this study.

First as a control analysis, total RNA was isolated from primary hepatocytes from wild-type (WT) and KO PGC-1α animals and analysed by qRT-PCR to determine the expression levels of several antioxidant genes. In the absence of PGC-1α in KO hepatocytes the levels of *prx3, prx5, ucp-2* and *catalase* were significantly lower than in the WT hepatocytes (Fig.2.20.).

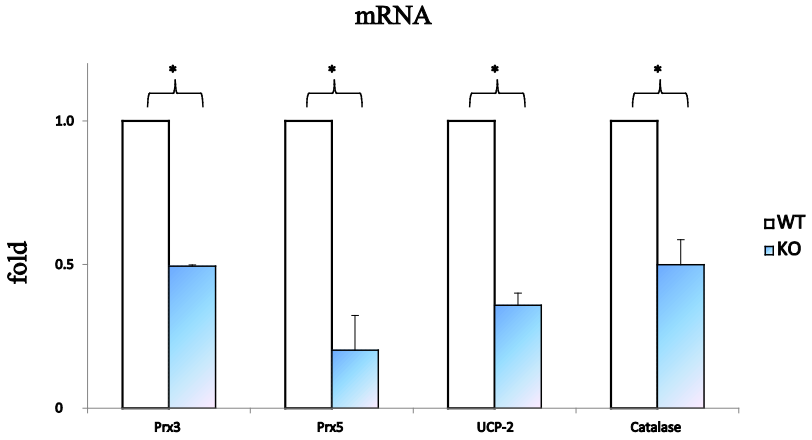

***Figure 2.20**: PGC-1α regulation of oxidative stress protection genes. qRT-PCR analysis oxidative stress protection genes in PGC-1α+/+ and PGC-1α-/- hepatocytes. 18S RNA was used as a loading control. Control samples were assigned the value of 1. Data are means +SD. (*) P ≤0.05.*

2.2. Whole genome expression analysis of PGC-1α$^{+/+}$ and PGC-1α$^{-/-}$ primary hepatocytes

To get further insight into the regulatory activity of PGC-1α in hepatocytes, it was considered to be informative to carry out a whole genome expression analysis of PGC-1α using a microarray based palteform. Microarrays (i.e Affymetrix Exon Arrays) and RNA-Seq (i.e. Illumina sequencing system) are currently the two most common experimental platforms for the whole genome expression analysis. The selected platform, Affymetrix GeneChip microarrays makes use of 60nt long probes corresponding to transcript sequences.

The probes are synthesized in situ on the slide using a photolithographic method. Labeled cDNA prepared from mRNA isolated from PGC-1α$^{+/+}$ and PGC-1α$^{-/-}$ primary hepatocytes was hybridized on the slides. Two independent array analysis were carried out, each used samples from 3 different WT and 3 different KO mice (total 6 WT and 6 KO mice), and for each of the samples three technical replicates were processed. Following slide scanning, a relative quantification analysis of transcript levels was performed as implemented (Dalma-Weiszhausz DD *et al*. 2002). Data outcomes after background correction and inter-chip, extra-chip normalization, showed that the up-regulated and down-regulated genes were consistently replicated in the two experiments. Considering that the primary cells are used after extraction from living animals, and that the preparation requires technical skill to perform the liver transfusion, the results obtained show a very low inter-assay variability. The array data from the two experiments shows reproducibility and consistency when analyzing the inter-assay and the intra-assay results.

In this experiment, a gene is considered to be up-regulated by PGC-1α when the log2 ratio signal (WT/KO) is greater than 2. Similarly, a gene is considered to be down-regulated when the log2 ratio signal (WT/KO) is less than -2.

Of the 421 genes identified as being positively regulated by PGC-1α in the first experiment, 288 of them were also found to show significantly higher levels in the WT than in the KO hepatocytes in the second experiment (Figure 2.21.). Similarly, of the 238 genes identified as negatively regulated by PGC-1α in the first experiment, 145 of them were also found to have lower expression level in the second experiment. The remaining 133 differentially expressed genes identified in the first experiment, in the second experiment these genes either did not reach the threshold of log value of 2 (eg.: Olfr1450), did not share a common identifying tag, or were not present in the second set of arrays (Figure 2.21.).

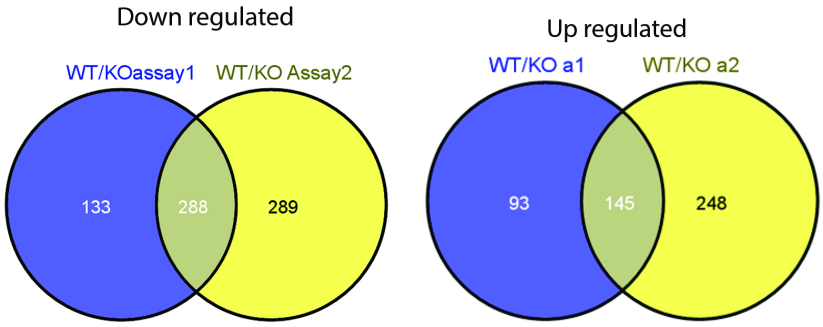

***Figure 2.21**: Genome wide analysis of PGC-1α WT and KO hepatocytes. Whole genome expression arrays were used to evaluate the gene expression changes between PGC-1α$^{+/+}$ and PGC-1α$^{-/-}$ hepatocytes. The diagram illustrates the total number of genes differentially down or up regulated by PGC-1α in hepatocytes, comparing the first and the second experiment.*

The following tables summarize twenty representative genes up-regulated and twenty down-regulated within the two assays (Tables 9 and 10).

Protein	Gene Symbol	Reference sequence	log (WT shuttle / KO shuttle)	p. value
WD repeat domain 72	Wdr72	AK142559	-4,482	0,0005
			-4,001	0,0003
chemokine (C-X-C motif) ligand 13	Cxcl13	NM_018866	-4,042	0,0515
			-3,946	0,0164
	6030487A22Rik	AK031681	-3,455	0,0020
			-3,105	0,0026
integrin, alpha X (complement component 3 receptor 4 subunit)	Itgax	NM_021334	-3,442	0,0037
			3,260	0,0017
solute carrier family 46, member 2	Slc46a2	NM_021053	-3,366	0,0338
			-3,316	0,0121
phospholipase A2, group VII (platelet-activating factor acetylhydrolase, plasma)	Pla2g7	NM_013737	-3,067	0,0205
			-2,841	0,0010
src kinase associated phosphoprotein 1	Skap1	NM_001033186	-3,046	0,0121
			-3,148	0,0014
CD5 molecule-like	Cd5l	NM_009690	-3,046	0,0501
			-2,985	0,0062
Src-like-adaptor	Sla	NM_001029841	-2,957	0,0262
			-2,747	0,0013
macrophage scavenger receptor 1		NM_031195	-2,939	0,0580
			-2,793	0,0278
	Msr1		-2,836	0,0613
			-2,891	0,0268
			-2,769	0,0748
			-2,849	0,0356
chemokine (C-C motif) ligand 12	Ccl12	NM_011331	-2,930	0,0593
			-2,931	0,0226
V-set and immunoglobulin domain containing 4	Vsig4	NM_177789	-2,896	0,1036
			-2,795	0,0229
alpha-1,4-N-acetylglucosaminyl transferase	A4gnt	NM_001077424	-2,896	0,0136
			-2,588	0,0125
interleukin 1, beta	Il1b	NM_008361	-2,881	0,2031
			-2,508	0,0928
complement component 1, q subcomponent, A chain	C1qa	NM_007572	-2,875	0,0934
			-2,787	0,0242
olfactory receptor 533	Olfr533	NM_001011815	-2,854	0,0266
			-2,909	0,0135
lymphoid-restricted membrane protein	Lrmp	NM_008511	-2,846	0,0009
			-2,625	0,0010
sulfatase 1	Sulf1	NM_172294	-2,819	0,0041
			-2,579	0,0002
membrane-spanning 4-domains, subfamily A, member 8A	Ms4a8a	NM_022430	-2,802	0,1176
			-2,475	0,0146
allograft inflammatory factor 1	Aif1	NM_019467	-2,780	0,1019
			-2,042	0,0265
solute carrier family 17 (organic anion transporter), member 3	Slc17a3	NM_134069	-1,911	0,0623
			-1,784	0,0386
chemokine (C-X-C motif) ligand 1	Cxcl1	NM_008176	-2,019	0,0917
			-1,978	0,0073

***Table 9**: List of the 20 top genes down regulated by PGC-1α in hepatocytes. The fold change in PGC-1α+/+ and PGC-1α-/- hepatocytes, and the corrected p values are indicated.*

Protein	Reference sequence	Gene Symbol	log (WT shuttle / KO shuttle)	p. value
cytochrome P450, family 2, subfamily b, polypeptide 13	NM_007813	Cyp2b13	4,355	0,0018
			4,450	0,0005
cytochrome P450, family 2, subfamily b, polypeptide 10	NM_009999	Cyp2b10	4,271	0,0018
			4,355	0,0005
			4,012	0,0016
			4,083	0,0004
cytochrome P450, family 2, subfamily b, polypeptide 9	NM_010000	Cyp2b9	3,973	0,0015
			4,145	0,0003
			3,869	0,0015
			3,899	0,0004
X-prolyl aminopeptidase (aminopeptidase P) 2	NM_133213	Xpnpep2	3,794	0,0016
			3,864	0,0002
Transducin-like enhancer protein 3	X73360	Tle3	3,711	0,0817
			3,997	0,0686
	NM_138654	5033411D12Rik	3,778	0,0042
			3,752	0,0004
			3,438	0,0677
			3,384	0,0202
solute carrier family 30, member 10	NM_001033286	Slc30a10	3,381	0,0010
			3,496	0,0002
	NM_029198	4930538K18Rik	3,093	0,0014
			3,231	0,0005
			4,580	0,0004
			4,565	0,0003
teneurin-4 or tenascin-M4	NM_011858	Odz4	3,159	0,0349
			3,280	0,0183
			3,093	0,0389
			3,196	0,0210
potassium channel tetramerization domain containing 16	XM_993798	Kctd16	3,078	0,0522
			3,227	0,0067
retinitis pigmentosa GTPase regulator interacting protein 1	NM_023879	Rpgrip1	3,153	0,0089
			3,212	0,0033
			3,075	0,0092
			3,132	0,0035
interleukin 3	NM_010556	Il3	3,006	0,0085
			2,983	0,0037
	AK054265	LOC620079	2,999	0,0056
			3,079	0,0011
cytochrome P450, family 2, subfamily S, polypeptide 1	NM_028775	Cyp2s1	2,988	0,0221
			3,116	0,0002
	BC089626	2310046A06Rik	2,963	0,0029
			2,988	0,0003
peptidoglycan recognition protein 1	NM_009402	Pglyrp1	2,879	0,2474
			3,068	0,0655
crystallin, beta B3	NM_021352	Crybb3	2,856	0,0180
			2,951	0,0053
kelch repeat and BTB (POZ) domain containing 11	BC080858	Kbtbd11	3,886	0,0009
			3,842	0,0009
			3,905	0,0004
			2,801	0,0237
			2,907	0,0040
liver expressed antimicrobial peptide 2	NM_153069	Leap2	2,762	0,1728
			2,765	0,0710
mucin 2	BC034197	Muc2	2,694	0,0442
			2,857	0,0032
calcium/calmodulin-dependent protein kinase II beta	NM_007595	Camk2b	2,569	0,0024
			2,650	0,0004
C-X-C chemokine receptor type 7	NM_007722	Cxcr7	1,644	0,0335
			1,739	0,0089

Table 10: List of the 20 top genes up regulated by PGC-1α in hepatocytes. The fold change in PGC-1α+/+ and PGC-1α-/- hepatocytes, and the corrected p values are indicated.

Novel putative PGC-1α regulated gene families

Gene cluster analysis identified new gene families of PGC-1α regulated genes, in particular, the cytochrome P450, family2. This gene family includes a group of xenobiotic metabolizing enzymes regulated in response to fasting, known to be transcriptionally regulated by the nuclear receptors constituve active/androstane receptor (CAR) and pregnane X receptor (PXR). PGC-1α has been previously shown to coactivate PXR and CAR and to be directly involved in the regulation of Cyp2A5 (Konno Y *et al.* 2008). Now it is observed that PGC-1α can also positively regulate two other family members, *Cyp2b13/Cyp2b9*, whose protein products work in a coordinated manner and are known to be responsive to a common set of regulatory signals. Both have been shown to be induced by fasting, in response to glucagon and cAMP, by CREB, a transcription factor that induces PGC-1α expression and, is also coactivated by PGC-1α (Hawkins GA *et al.* 2002). These proteins are involved in oxidation-reduction reactions that produce as a by-product, H_2O_2, so their activity increases cellular oxidative stress unless there is a coordinated induction of antioxidant proteins. By-product, H_2O_2, xenobiotic activity has also been shown to play a relevant role in drug resistance in cancer. Importantly these genes have also been shown to be co-transcriptionally regulated with solute carrier transporters that also play a role in drug resistance by decreasing the cellular concentration of the chemotherapeutic drug, in the liver and in other tissues (Horvath HC *et al.* 2010). Consistently, several solute carrier proteins where found to be regulated by PGC-1α in hepatocytes.

One interesting member of the solute carrier proteins that was found to be positively regulated by PGC-1α is Solute carrier family 30, member 10, Slc30a10 (NM_001033286). Slc30a10 is highly expressed in the liver and is inducible by manganese (Mn). Its protein product appears to be critical in maintaining manganese levels, and has higher specificity for Mn than zinc (Zn). Mn is a key co-factor of several enzymes, including MnSOD. Loss of function mutations appear to result in a pleomorphic phenotype, including dystonia and adult-onset Parkinsonism in humans, both alterations may be the result of deficient mitochondrial function. Two different RNA probes for this gene were present in the Affymetrix GeneChip microarray. Interestingly, only one seems to be positively regulated by PGC-1α (A_52_P883557) while the other probe was not (A_51_P173445). Both sequences are present in the 3'UTR. The differentially regulated probe (A_52_P883557) is at the far end of the sequence, whereas the probe (A_51_P173445) is found close to the fourth exon. This observation may suggest that mRNAs with alterative 3'UTRs RNAs may be differentially regulated by PGC-1α.

A part from the families described above, the *Itgax gene* (NM_021334) is also significantly higher in WT than in PGC-1α KO hepatocytes. This gene encodes the integrin alpha X chain protein. This protein is involved in the interaction of circulating neutrophils and monocytes with the activated

vascular endothelium to promote their extravasation. This protein combines with the beta 2 chain (ITGB2) to form a leukocyte-specific integrin referred to as inactivated-C3b (iC3b) receptor 4 (CR4). The alpha X beta 2 complex seems to overlap the properties of the alpha M beta 2 integrin in the adherence of neutrophils and monocytes to stimulate endothelium cells, and in the phagocytosis of complement coated particles. Two transcript variants encoding different isoforms have been found for this gene (Ensembl). Its role in hepatocytes is currently uncharacterized.

2.3. The RNA recognition motif (RRM) of PGC-1α regulates the transcription of antioxidant genes

To elucidate the genome wide functional contribution of the RNA recognition motif (RRM) to the regulation of liver target genes of PGC-1α, adenoviral vectors coding WT PGC-1α or a construct where the RRM was deleted (PGC-1α-ΔRRM) was used. Primary hepatocytes from PGC-1α WT and KO mice were transfected with Ad-PGC-1α, Ad-PGC-1α-ΔRRM or a control adenovirus (Ad-S). 48h after infection, mRNA was isolated and analysed. As a control, qRT-PCR analysis of antioxidant genes was used to test whether Ad-PGC-1α recovered target gene expression in PGC-1α KO hepatocytes. The results indicate that when transfecting the KO PGC-1α hepatocytes with full length PGC-1α gene, full length PGC-1α is expressed and the functionality of PGC-1α in the KO hepatocytes, on the antioxidant genes is restored. Consistently Ad-PGC-1α infection resulted in a general induction of antioxidant genes (Figure 2.22.). It is possible to suggest that the functionality of PGC-1α in other pathways is also restored.

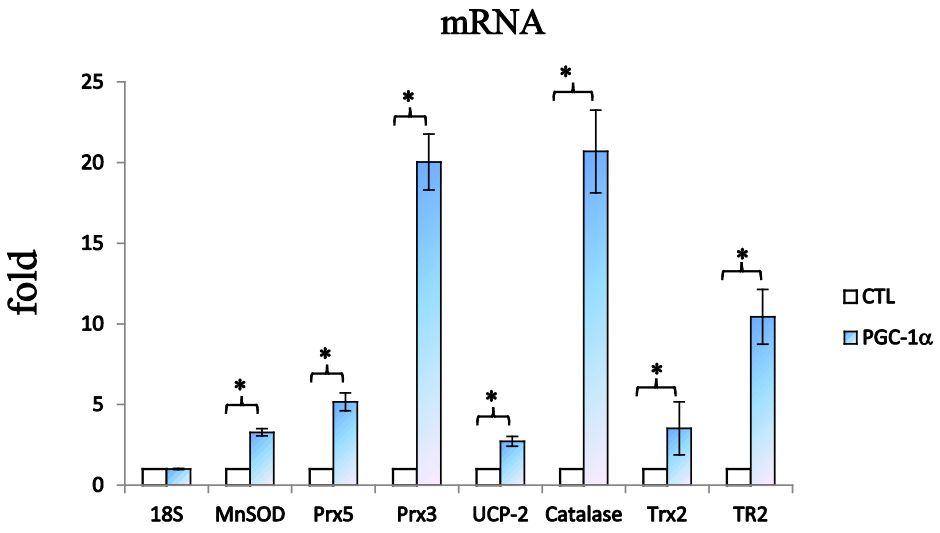

***Figure 2.22**: PGC-1α restores oxidative stress expression in PGC-1α$^{-/-}$ hepatocytes. qRT-PCR analysis of the induction of oxidative stress protection genes in PGC-1α$^{-/-}$ hepatocytes that were infected with PGC-1α or the corresponding control. mRNA expression is shown as the fold induction above the level in cells infected with control adenovirus. Control samples were assigned the value of 1. 18S was used as a loading control. Data are means +SD. *P< 0.05.*

When infecting the KO PGC-1α cells with the adenovirus driven wild type PGC-1α or PGC-1α mutant lacking the RRM motif (ΔRRM PGC-1α), expressing the PGC-1α protein without the RRM domain, two distinct patterns of gene regulation were observed.

For some antioxidant genes, mRNA levels were restored to the same level after infection with the full length PGC-1α protein or with the ΔRRM deletion mutant (*sod-2* (*MnSOD*) and *prx3*). This indicates that transcription regulation of these specific genes is independent from the RRM.

For other antioxidant genes, mRNA levels were significantly decreased, less induced by PGC-1α-ΔRRM than by the WT protein (*prx5, catalase and ucp-2*). This gene profile suggests that the transcriptional regulation of these genes requires at least partially the RRM of PGC-1α. In particular, UCP-2 levels were not significantly induced by the ΔRRM mutant, suggesting that tis gene is strongly dependent on the RRM.

This experiment therefore supports the relevance of the RRM domain in PGC-1α mediated regulation of transcription for specific genes (Figure 2.23.). These results support a gene and context specific dependency on RRM related function.

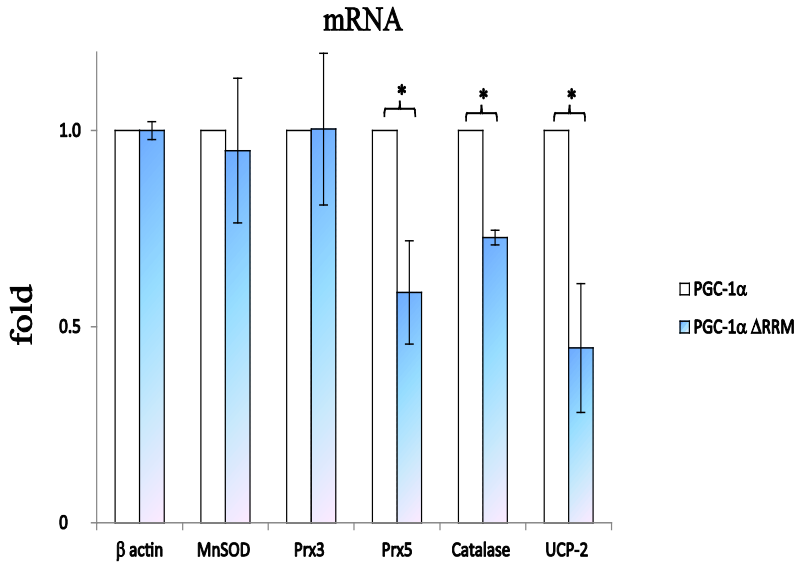

***Figure 2.23**: PGC-1α and PGC-1α-ΔRRM in the regulation of oxidative stress protection genes in hepatocytes. qRT-PCR analysis of the induction of oxidative stress protection genes in PGC-1α$^{-/-}$ hepatocytes that were infected with PGC-1α or PGC-1α-ΔRRM. mRNA expression is shown as the fold induction above the level in cells infected with control adenovirus. Control samples were assigned the value of 1. The CDS of β-actin was used as a negative enrichment control. Data are means +SD. *P< 0.05.*

2.4. Expression of ΔRRM PGC-1α in PGC-1α KO hepatocytes effect on the cell expression profile

In order to gain further insight into the functional relevance of PGC-1α RRM, mRNA from PGC-1α$^{-/-}$ primary hepatocytes transfected with adenovirus with either full-length PGC-1α or PGC-1α-ΔRRM was hybridized on GeneChip arrays. Three independent experiments were analysed using three replicates. Raw data was analysed following background correction and inter-chip, extra-chip normalization as indicated above (Materials and Methods).

The top twenty differentially regulated genes showing lower levels of expression in the PGC-1α-ΔRRM samples than in the WT PGC-1α samples are shown in the table below (Table 11).

GeneSymbol	ID	logFC	P.Value
Nrxn2	A_55_P1954067	3,465	0,0000
Hnrnpul1	A_55_P2025855	3,244	0,0549
0610033M10Rik	A_55_P2335933	3,102	0,0000
Pgm5	A_51_P451052	2,785	0,0001
Ptgds	A_55_P2100928	2,664	0,0000
Cyp24a1	A_52_P88648	2,633	0,0004
Pcp4l1	A_55_P1983754	2,380	0,0002
C2cd4b	A_51_P415395	2,375	0,0003
Nnt	A_55_P2008956	2,300	0,0034
Ptgfr	A_52_P153019	2,261	0,0003
Hpca	A_55_P2161595	2,227	0,0061
Lcn13	A_55_P2135153	2,147	0,0064
Adipoq	A_51_P458451	2,129	0,0020
Fam40a	A_55_P2035559	2,088	0,0166
Spdyb	A_52_P406242	2,077	0,0007
Grm6	A_55_P1990623	2,061	0,0005
Fam71a	A_55_P2147956	2,026	0,0003
Ifnab	A_55_P2030076	2,009	0,0005
Cxcr7	A_52_P675395	1,936	0,0685
Camk2b	A_55_P2109377	1,827	0,0008

***Table 11**: List of the 20 top genes showing significantly reduced expression in PGC-1α$^{-/-}$ hepatocytes infected with PGC-1α-ΔRRM than in PGC-1α$^{-/-}$ hepatocytes. The fold change and the corrected p values are indicated.*

Interestingly, it was also found that for some previously identified PGC-1α target genes, induction by PGC-1α-ΔRRM was actually higher than that observed with WT protein. The 20 top examples are listed in the table below (Table 12).

GeneSymbol	ID	logFC	P.Value
Syn2	A_51_P346491	-3,627	0,0000
Kcnc2	A_51_P507333	-3,226	0,0090
Gm3807	A_55_P2129363	-3,038	0,4146
Sox3	A_55_P2163353	-3,017	0,2973
Cxcl1	A_51_P363187	-2,631	0,0002
Col22a1	A_55_P2031781	-2,567	0,0053
LOC641136	A_55_P2093519	-2,454	0,0207
Pax9	A_55_P1955756	-2,440	0,0001
Spin4	A_51_P362661	-2,371	0,0074
2010109I03Rik	A_51_P272066	-2,330	0,0065
Inpp5j	A_55_P2115871	-2,235	0,0065
Chst9	A_55_P2054082	-2,191	0,0001
Pls1	A_55_P2160128	-2,149	0,0020
Krt74	A_55_P1973950	-2,145	0,0005
Slc17a3	A_55_P2008933	-2,142	0,0001
Slc22a29	A_51_P144531	-2,118	0,0070
Gys2	A_55_P2175545	-2,104	0,0060
Tinag	A_51_P283004	-2,094	0,0023
Gys2	A_55_P1992555	-2,088	0,0078
Stra6	A_55_P1973451	-2,078	0,0088

***Table 12**: List of the 20 top genes showing significantly higher expression in PGC-1α$^{-/-}$ hepatocytes infected with PGC-1α-ΔRRM than in PGC-1α$^{-/-}$ hepatocytes. The fold change and the corrected p values are indicated.*

2.5. PGC-1α-ΔRRM qRT-PCR functional validation

qRT-PCR analysis was used to validate the micro array analysis. Three genes that were significantly more induced by PGC-1α-ΔRRM than by PGC-1α and three that were significantly less induced by PGC-1α-ΔRRM than by PGC-1α were selected for further investigation.

These genes are, *Cyp24a1, Cxcr7, Camk2b* from the more induced and*, Inpp5j, Cxcl1, Slc17a3* from the less induced (Figure 2.24. and 2.25.).

An example provided by cytochrome P450, family 24 subfamily a polypeptide 1 (*Cyp24a1)* is encoding a gene member of the cytochrome P450 superfamily of enzymes. The cytochrome P450 proteins are monooxygenases which catalyse many reactions involved in drug catabolism and the synthesis of cholesterol, vitamin D_3, steroids and other lipids. As noted above, PGC-1α has been shown to regulate several members of the P450 superfamily. It was found that PGC-1α-ΔRRM induced the expression of the 3'UTR more than the WT protein (PGC-1α) (Fig. 2.24.).

To validate the results, qRT-PCR is applied to the hepatocyte isolated RNA. qRT-PCR data was generally found to be consistent with the expression changes previously identified in the arrays, further supporting the gene specific activity of the PGC-1α RRM. The results are shown in Figure 2.24. However, within the six selected genes, some did not show the previously identified changes (*Camk2b* and *Inpp5j*).

In general, the results confirmed the observation in the array described in the upper section (2.4.). PGC-1α has an RNA recognition motif that has been shown to be functionally relevant in mediating PGC-1α transcriptional regulatory activities for specific genes. It can be concluded that the RRM is regulating the activity of the genes studied in this section (Figure 2.24. and 2.25.).

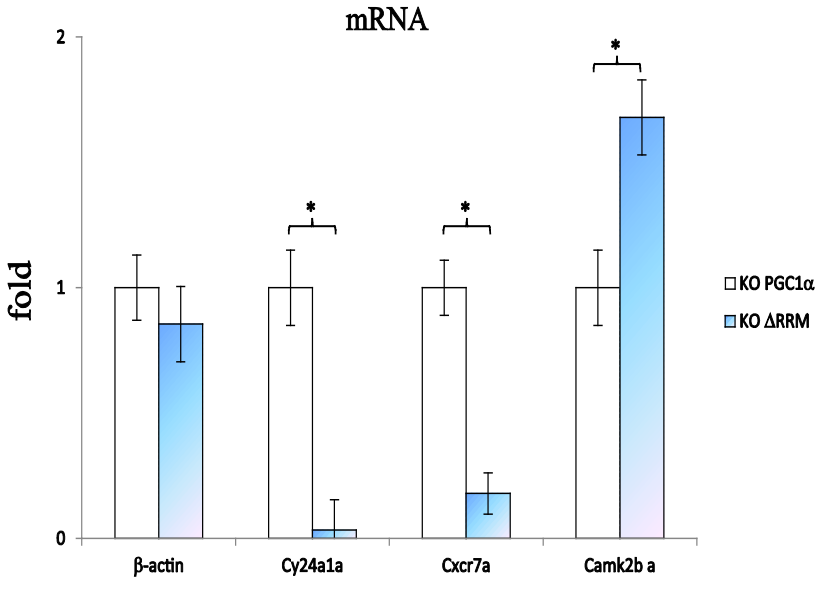

***Figure 2.24**: PGC-1α and PGC-1α-ΔRRM differentially regulate gene expression in hepatocytes: more induced in PGC-1α. qRT-PCR analysis of the induction of selected genes (Cyp24a1, Cxcr7, Camk2b) in PGC-1α$^{-/-}$ hepatocytes that were infected with PGC-1α or PGC-1α-ΔRRM. mRNA expression is shown as the fold induction above the level in cells transfected with control adenovirus. Control samples were assigned the value of 1. The CDS of ß-actin was used as a negative enrichment control Data are means +SD. *P< 0.05.*

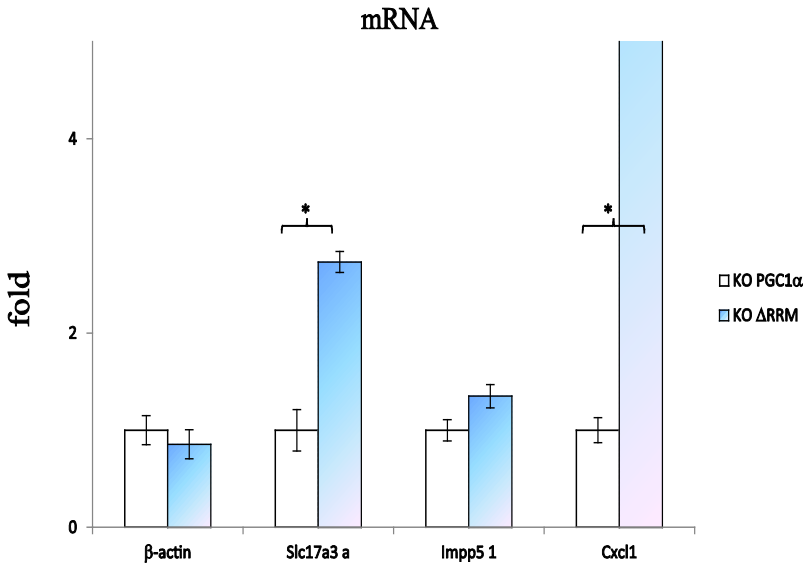

***Figure 2.25**: PGC-1α and PGC-1α-ΔRRM differentially regulate gene expression in hepatocytes: less induced in PGC-1α. qRT-PCR analysis of the induction of selected genes (Inpp5j, Cxcl1, Slc17a3) in PGC-1α$^{-/-}$ hepatocytes that were infected with PGC-1α or PGC-1α-ΔRRM. mRNA expression is shown as the fold induction above the level in cells transfected with control adenovirus. Control samples were assigned the value of 1. The CDS of ß-actin was used as a negative enrichment control. Data are means +SD. *P< 0.05.*

Alternative expression pattern: PGC-1α / ΔRRM PGC-1α

Gene expression microarrays include specific tags for several sequences within a single gene, allowing the identification of splicing variants. This feature was used to further investigate if PGC-1α-ΔRRM could play a role in differential regulation of splicing variants. Some tag specific differences were noticed between the PGC-1α and PGC-1α-ΔRRM. This variation prompted a careful examination of selected target genes, in particular *Camk2b* and *Slc17a3.* These two genes seemed to present possible differential expression patterns within the gene dependent on the presence of the RRM. It was noted that within a gene, some sequences were significantly and differentially expressed in a RRM dependent manner (Table 13).

The results from the former chapter showed a ternary complex formation (SirT1-PGC-1α-FoxO3a) involved in gene regulation. Interestingly, the database renders accessible results from array experiments where wild type hepatocytes were compared to siSirT1 hepatocytes. The comparison is included table 4 for the genes previously selected. Strikingly, some genes showed the same tendency.

qRT-PCR analysis was also performed on *Slc17a3* (NM_134069) (Figure 2.26.). The *slc17a3* gene has 4 splicing variants. The expression levels of the region between exons 9 and 11 is higher in PGC-1α KO cells transfected with PGC-1α-ΔRRM than with WT PGC-1α, but the expression levels of the 3' UTR are not affected by the presence or the absence of the RRM, again suggesting a role of the RRM in 3'UTR selection.

Protein	GeneSymbol	Array	ID	logFC	P.Value	Oligonucleotide	Sequence type
solute carrier family 17 (organic anion transporter), member 3	Slc17a3	WT/KO assay 1	A_51_P402267	-1,78	0,039	Slc17a3 a	exon 9-10/exon 11
		WT/KO assay 2	A_51_P402267	-1,91	0,062	Slc17a3 a	exon 9-10/exon 11
			A_52_P554720	0,06	0,902	Slc17a3 b	3´UTR
		KO PGC1a/KO DRRM	A_55_P2008933	-2,14	0,000	Slc17a3 c	3´UTR
		WT/KOSiSirT1	A_51_P402267	-1,93	0,089	Slc17a3 a	exon 9-10/exon 11
			A_52_P554720	-0,63	0,104	Slc17a3 b	3´UTR
inositol polyphosphate 5-phosphatase J	Inpp5j	WT/KO assay 1	not present				
		WT/KO assay 2	A_52_P339912	-1,20	0,056	Inpp5j a	exon 10/exon 11
		KO PGC1a/KO DRRM	A_55_P2115871	-2,23	0,006	Inpp5j b	exon 13
		WT/KOSiSirT1	A_52_P339912	1,64	0,129	Inpp5j a	exon 10/exon 11
chemokine (C-X-C motif) ligand 1	Cxcl1	WT/KO assay 1	A_51_P363187	1,98	0,007	Cxcl1 a	3'UTR....non coding...near 5S_rRNA.26-201
		WT/KO assay 2	A_51_P363187	-2,02	0,092	Cxcl1 a	
		KO PGC1a/KO DRRM	A_51_P363187	-2,63	0,000	Cxcl1 a	
		WT/KOSiSirT1	A_51_P363187	-1,57	0,239	Cxcl1 a	
calcium/calmodulin-dependent protein kinase II beta	Camk2b	WT/KO assay 1	A_51_P318933	2,65	0,000	CamK2b a	3'UTR
		WT/KO assay 2	A_51_P376776	1,74	0,008	-	
			A_51_P318933	2,57	0,002	CamK2b a	3'UTR
		KO PGC1a/KO DRRM	A_55_P2150578	0,72	0,393	CamK2b c	exon 19-21/exon 21
			A_55_P2109377	1,83	0,264	CamK2b b	3'UTR
		WT/KOSiSirT1	A_51_P318933	0,86	0,394	CamK2b a	3'UTR
cytochrome P450, family 24, subfamily a, polypeptide 1	Cyp24a1	WT/KO assay 1	not present				
		WT/KO assay 2	A_52_P88648	1,92	0,170	Cyp24a1 a	3'UTR
		KO PGC1a/KO DRRM	A_52_P88648	2,63	0,000	Cyp24a1 a	3'UTR
		WT/KOSiSirT1	not present				
C-X-C chemokine receptor type 7	Cxcr7	WT/KO assay 1	A_52_P675395	1,74	0,009	Cxcr7 a	3'UTR
		WT/KO assay 2	A_52_P675395	1,64	0,034	Cxcr7 a	3'UTR
		KO PGC1a/KO DRRM	A_52_P675395	1,94	0,069	Cxcr7 a	3'UTR
		WT/KOSiSirT1	A_52_P675395	1,24	0,143	Cxcr7 a	3'UTR

***Table 13**: Gene-tag specific changes for the contrast PGC-1α-ΔRRM/PGC-1α WT as identified in the microarray analysis.*

The Calcium/Calmodulin dependent protein kinase II beta (*Camk2b*) gene has several splicing variants as well as alternative 5' and 3' UTRs. The gene codes for a calcium sensitive kinase that has been proposed to regulate PGC-1α expression through the formation of a complex with PGC-1α itself that binds to the promoter region of the *pgc-1α* gene (Czubryt et al., 2003, Handschin et al., 2003). Three sets of qRT-PCR oligonucleotides were designed targeting two of the 3'UTR and one the region between exons 19-21 of Camk2b. The qRT-PCR analysis shows that the two 3'UTR sequences were up-regulated more strongly by PGC-1α-ΔRRM than by WT PGC-1α while no variation was observed in the CDS region. This result shows a specific role of RRM in the identification of transcriptional termination sites that has to be confirmed by further functional assays (Figure 2.26.).

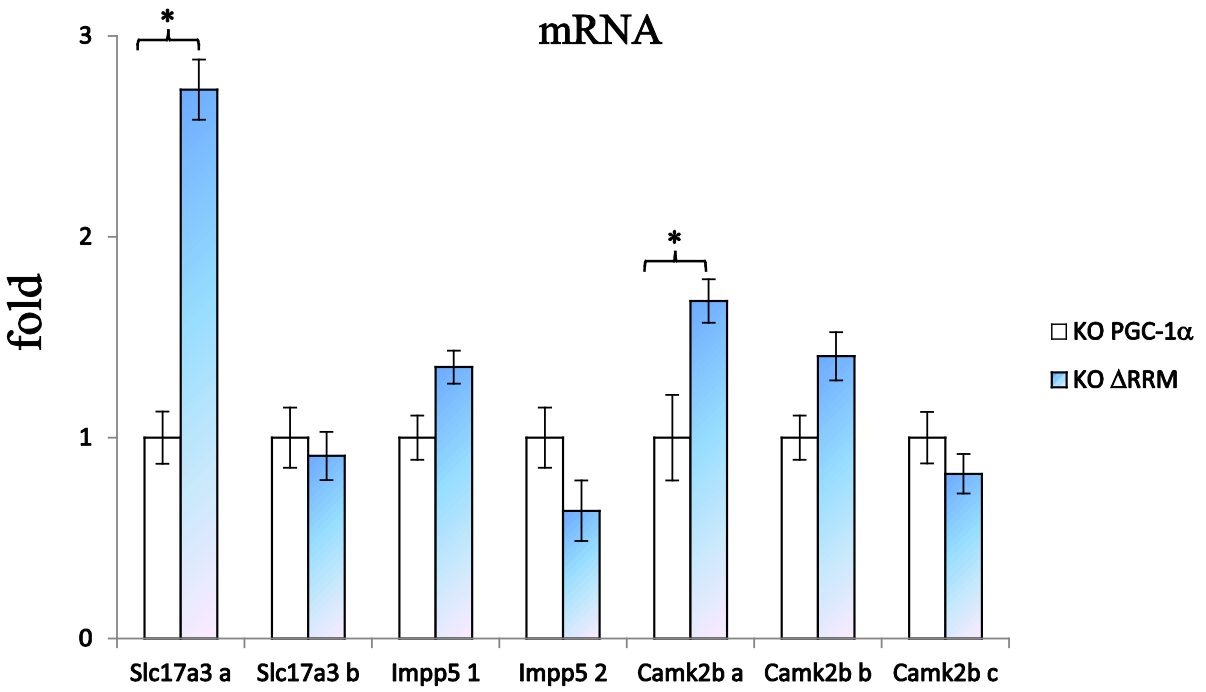

***Figure 2.26**: PGC-1α and PGC-1α-ΔRRM differentially regulate 3'UTR selection. qRT-PCR analysis of slc17a3, Impp5 and Camk2b gene expression in PGC-1α$^{-/-}$ hepatocytes that were infected with PGC-1α or PGC-1α-ΔRRM. mRNA expression is shown as the fold induction above the level in cells infected with control adenovirus. Control samples were assigned the value of 1. Data are means +SD. *P< 0.05.*

All together, the results support the notion of the RRM playing a functional role in PGC-1α target gene regulation. Furthermore, they show that RRM requirement is gene specific, playing a regulatory role for specific target genes. Finally, they suggest that PGC-1α activity may relate to the stabilisation of the transcript either by facilitating elongation/termination or by directly regulating RNA stability through the binding of UTR regions. PGC-1α has a RNA recognition motif (RRM) whose deletion abolishes some of the transactivation capacity of PGC-1α.

The second aim of this work was to study the functionality of the RRM motif in the specific context of regulating antioxidant genes. The results showed that some genes are more sensitive to the absence of RRM than others. To have a global overview of the genomic functionality of the RRM, a complete genome microarray expression analysis comparing wild-type PGC-1α protein to the PGC-1α protein lacking the RRM was performed. The observation that the deletion of the PGC-1α RRM differentially affects genes regulated by PGC-1α suggests that the RRM could be involved in selection of 3'UTR and as a consequence modify RNA transcripts.

3. Identification of PGC-1α ligand RNAs

In order to get insight into the mechanisms involved in RNA recognition motif (RRM) dependent regulation of gene expression, it was decided to investigate whether or not this domain showed RNA binding activity and if so to identify the ligand RNAs.

3.1. PGC-1α RNA binding activity

To investigate the basis of the RRM function it was first tested whether PGC-1α can actually bind RNA in cells. Therefore, a combination of UV crosslinking with specific antibody immunoprecipitation was performed as previously described (Greenberg JR 1979, Wagenmakers AJ *et al.* 1980, Choi YD and Dreyfuss G 1984).

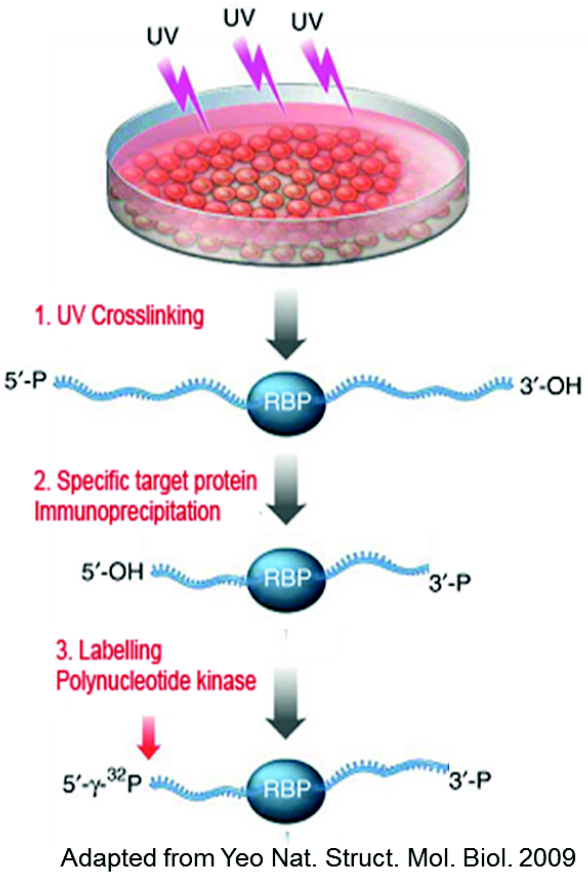

***Figure 2.28**: CrossLinked ImmunoPrecipitation (CLIP) Process (adapted from Yeo GW et al. 2009).*

As PGC-1α is composed of several domains and RRM is involved in regulation of mRNA, the assay was performed with the Carboxyl terminal domain (CTD) construct. The CTD is composed of the Arginine/Serine (RS) domain and the RRM until the C-terminal region of the protein.

PGC-1α or its C-terminal mutants was transiently transfected in HEK 293T cells. 24 h post transfection cells were UV irradiated in order to crosslink proteins to neighboring nucleic acids. Whole cell extracts (WCE) were prepared and PGC-1α was immunoprecipitated (IP). The

immunprecipitated crosslinked oligonucleotides were labelled with ^{32}P, using T4 polynucleotide kinase.

^{32}P labelled PGC-1α was separated by SDS-PAGE gel separation (Figure 2.29.) and subsequently detected. The result showed that PGC-1α can be cross-linked to nucleic acid in cells.

PGC-1α-ΔRS mutant that retained the RRM was specifically labelled, suggesting that the RRM of PGC-1α was actually used to bind nucleic acid.

All mutants tested that lacked the RRM, including PGC-1α-ΔCTD, the PGC-1α-ΔRRM/ΔSR mutant and PGC-1α-ΔRRM gave only a background signal. A hypothesis to explain the background binding is a hetero-dimerisation of PGC-1α with a mutant form lacking the RRM.

To identify the nature of the nucleic acid bound to PGC-1α, the labelled band was excised from the gel, protein was removed by protease K treatment, the remaining nucleic acid was incubated with either RNase A or DNase I enzymes. The material was analysed in a urea-denaturing gel. The result shown on Figure 2.29. illustrate the finding that the isolated nucleic acid was sensitive to RNase A treatment and resistant to DNase I. The result is supporting the idea that PGC-1α was binding an RNA molecule.

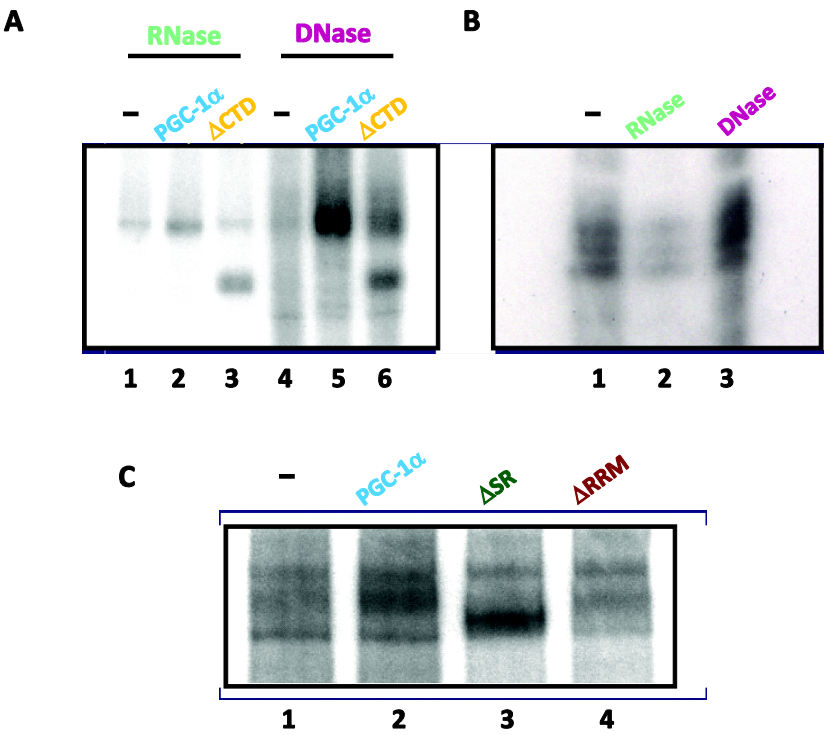

***Figure 2.29**: PGC-1α associates with RNA in cells. 70% confluent 293T cells (10 cm Ø plates) were transfected with 12.5 µg of 3.1-Flag-PGC-1α, and C-terminal alleles, 24h posttransfection, cells were UV treated to crosslink nucleic acids to proteins. PGC-1α was IP from WCE, and polynucleotides in the immunoprecipitates were end-labeled with ^{32}P. (A-C) The PGC-1α labeled polynucleotide complex was resolved on a 7.5% PAGE-SDS gel. As indicated extracts were treated with RNase A1 or DNase I. (B)The labeled material was excised from the gel, digested with proteinase K, recovered by ethanol precipitation, divided into three aliquots that were subjected to repeat digestion with RNAse A1 or DNAse I and resolved on a 20%-7 M urea gel.*

An alternative approach was used to confirm the nature and specificity of the identified material. WT PGC-1α or PGC-1α-ΔCTD mutant were UV crosslinked to the bound nucleic acid and immunoprecipitated. The immunoprecipitated material was incubated with RNAseA or DNAse I, labelled and analysed by SDS-PAGE separation and radiodetected. The only material associated with WT PGC-1α was sensitive to RNAse treatment, while the signal associated with PGC-1α-ΔCTD mutant was insensitive to both RNAse and DNAse I treatment. The result suggests that the background signal was not derived from a bound nucleic acid.

In order to determine the nature of the RNAs that PGC-1α binds in vivo, it was first investigated whether PGC-1α would remain stably associated with RNA during standard immunoprecipitation conditions. The experimental design was as follows. PGC-1α or the mutants PGC-1-ΔRRM, -ΔSR, -ΔCTD, -ΔSRΔRRM were transiently transfected into HEK 293T cells and immunoprecipitated with a specific PGC-1α antibody. Isolated RNA from the immunoprecipitated material was analysed under native acrylamide gels stained with EtBr.

RNAs were detected in the immunoprecipitates of PGC-1α and PGC-1α-ΔSR but not in the immunoprecipitates of those PGC-1α alleles that lack the RRM (Figure 2.30.). Therefore, it was possible to purify the RNAs bound to PGC-1α containing the RRM. It was observed that while the PGC-1α-ΔSR mutant was still able to associate with RNA, the ΔRRM deletion mutant was not (Figure 2.30.). Thus it is possible to conclude that stable RNA binding was mediated by the RRM.

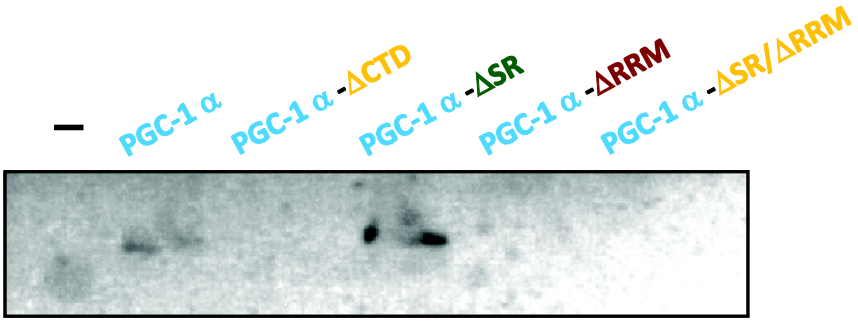

***Figure 2.30**: RNA associates with PGC-1α harboring the RRM. 70% confluent 293T cells were transfected with 3.1-Flag-PGC-1α WT, the indicated C-terminal mutants, or the corresponding empty vector. 24 h post-transfection, cells were harvested and PGC-1α was IP from DNase I treated WCE. RNA was extracted with Trizol from the immunoprecipitates, and analysed on a native acrylamide gel stained with EtBr.*

Aiming to identify the nature of those RNAs, the RNA present in the immunoprecipitates was retrotranscribed and the resulting cDNA was randomly amplified. The quality of the amplification reaction was determined by analysing the amplified DNA in an agarose gel stained with EtBr (Figure 2.31. A.). To control the reaction, the immunoprecipitated protein was monitored by western blotting (Figure 2.31. B.). The result is showing equal amount of protein PGC-1α and PGC-1α-ΔRRM immunoprecipitated.

To further evaluate the reaction, in parallel to the PGC-1α material immunoprecipitated by the specific antibody in the WCE, cells were transfected only with the vehicle plasmid, with PGC-1α-ΔRRM and analysed. The amount of amplified material in the control reactions was always much smaller than in the PGC-1α lane. A smear of nucleic acid was only observed in the amplification from WCE containing the wild type PGC-1α, suggesting the presence of a population of different RNAs in the starting material. In summary, it was possible to amplify several type of RNAs bound to PGC-1α containing the RRM suggesting that not only one type, or size of RNA is bound to the RRM of PGC-1α in vivo.

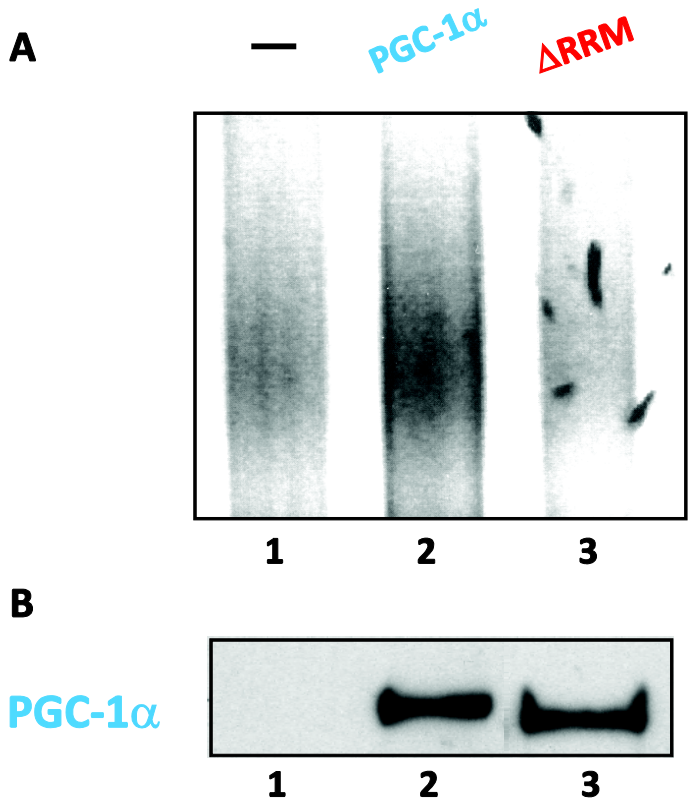

***Figure 2.31**: RNA binding to PGC-1α in vivo. 70% confluent 293T were transfected with 3.1-Flag-PGC-1α WT, 3.1-Flag-PGC-1α-ΔCTD, or the corresponding empty vector. Panel A: 24 h posttransfection, cells were harvested and PGC-1α was IP from DNase I treated WCE. RNA was extracted with Trizol from the immunoprecipitates, subjected to RT and random PCR amplification. RT was performed using primer Round A as template (5'-GTTTCCCAGTCACGATCNNNN NNNNNN-3'), followed by 20 cycles of PCR amplification with primer Round B (5'-GTTTCCCAGTCACGATC-3'). Panel B shows the control IP-western.*

To further investigate whether RRM of PGC-1α interaction with RNA is active and functional, an in vitro Glutathion S-Transferase (GST) pull down assay was designed. The assay incorporated a double stranded DNA (dsDNA) as negative control and two single stranded RNAs (ssRNA). The nucleic acid interaction with GST- PGC-1α-CTD was assayed (Figure 2.32.). The results of this assay showed that dsDNA did not bind to GST-CTD construct. This observation confirms the former findings of specific interaction of PGC-1α with RNA (Figure 2.29.)

The two RNA species tested were the E2 snoRNA situated in intron 4 (RNA1) and 1.7 kb of the pre-mRNA LR-1 fragment (RNA2) (Nag MK *et al.* 1993). The 1.7 kb of the pre-mRNA LR-1 fragment was selected because it contained the E2 coding intron together with putative regulatory mRNA processing sequences. The association between immobilized GST fusion protein for PGC-1α-CTD and

the two in vitro transcribed ^{32}P-labeled RNAs, one with a strong hair pin structure, a spliced form (E2: RNA1) and a pre-RNA fragment with an extended structure from the gene LR-1, an immature form (RNA2) was assayed. As expected, PGC-1α-CTD could bind the two ^{32}P-labeled RNAs (Figure 2.32.).

In order to evaluate the strength and specificity of the binding of the RNAs to the CTD domain, the assay design incorporate competition with non-specific cold RNAs (tRNA) at increasing concentration. The results show that increasing concentrations of non-specific cold RNAs competed more efficiently PGC-1α-CTD binding to RNA1 (Fig. 2.32., right pane: lanes 1-4) than to the 3' 1.7 kb LR-1 pre-mRNA fragment (RNA2; Figure 2.32.) as the labelled RNA1 was displaced more efficiently. In summary, since the two RNAs have different affinities, the binding of LR-1 pre-RNA (RNA2) is more efficient than the E2 snoRNA (RNA1).

In addition to the selective binding to RNA versus DNA, the last observation suggests that the RRM has some target specificity that could be sequence or structure dependent.

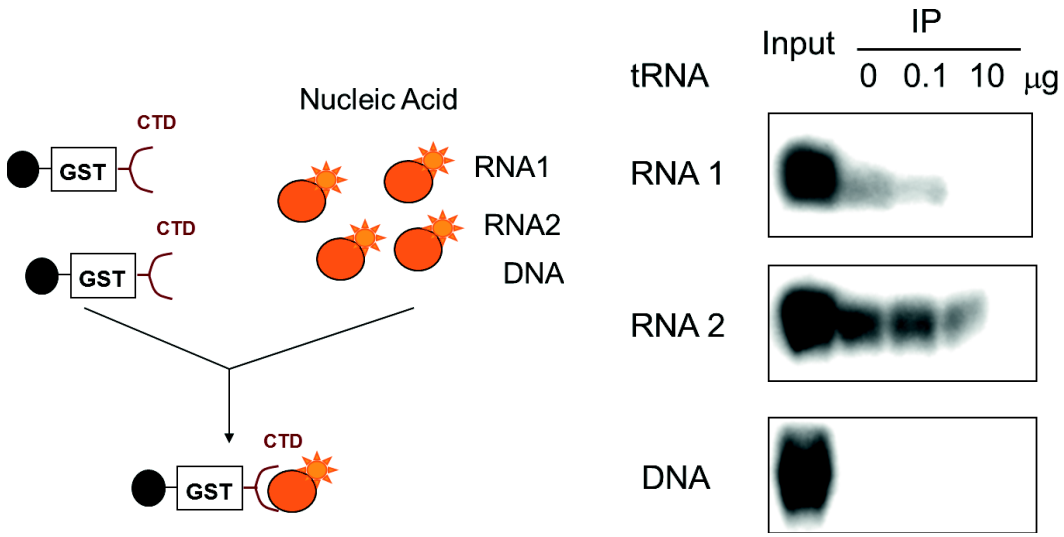

***Figure 2.32**: PGC-1α-CTD can interact preferentially with ssRNA in vitro. (A) Purified GST-CTD immobilized on glutathione beads were incubated with the indicated polynucleotide. LR-1 CDS: RNA1 or 3' LR-1 pre-RNA (1.7 kb) E2: RNA2, or DNA. (B) The preparation (GST/polynucleotide) was incubated in the presence of 0, 0.1 or 10 µg of tRNA, used as non-specific competitor. ^{32}P labeled polynucleotides were extracted and detected by autoradiography following separation on 1% agarose gels and autoradiography.*

LR-1 pre-RNA still has to be processed during it life cycle, which is not the case for E2 RNA. This enhanced affinity could suggest a preferential binding to immature RNA to the CTD domain of PGC-1α. The data also supports the idea of a direct interaction between PGC-1α and a pre-mRNA. From the results obtained, a specific sequence is supposed to be bound by PGC-1α protein therefore at least one binding site should be present in LR-1, 1.7 kb fragment. The results would therefore be consistent with the possibility of PGC-1α binding specific RNAs in vivo.

Both RNA species (RNA1 and RNA2) are displaced by increasing amount of tRNA. This observation shows a dynamic process of binding, suggesting an adaptation if environmental conditions changes.

The result supports the hypothesis of regulatory choice in which PGC-1α-CTD domain could be involved in vivo.

This result is consistent with studies from other RNA binding proteins. As a rule, RNA binding tends to be less sequence specific than DNA binding and relies to large extends on the recognition of particular secondary structures and/or hybridization to other nucleic acid.

The data also shows a preference of binding to RNA versus DNA, and moreover to immature, unprocessed RNA.

3.2. Identification of RNA species bound by PGC-1α

3.2.1. RNA Preparation

Since the discovery of the first small silencing RNA (siRNA) in 1993, a wide variety of new RNA types have been identified (Ghildiyal M and Zamore PD 2009). Technical improvements have allowed the identification of siRNA and their functional characterisation. This was an insight into many RNA activities, eg. RNA nature, genomic localisation,... Furthermore, starting with the identification of Argonaute and miRNA processing machinery (Zisoulis DG *et al.* 2010) major efforts have focused on the development of techniques that facilitate the identification of specific protein-bound RNA molecules. A combination of UV crosslinking with specific antibody immunoprecipitation (CLIP), followed by amplification and high throughput sequencing (HTS-CLIP) has become a standard method to identify novel RNA proteins ligands Figure 2.33. (Licatalosi et al 2008, Yeo et al 2009, Sanford et al 2009, Granneman et al 2009, Guil and Caceres 2007, Chi et al 2009).

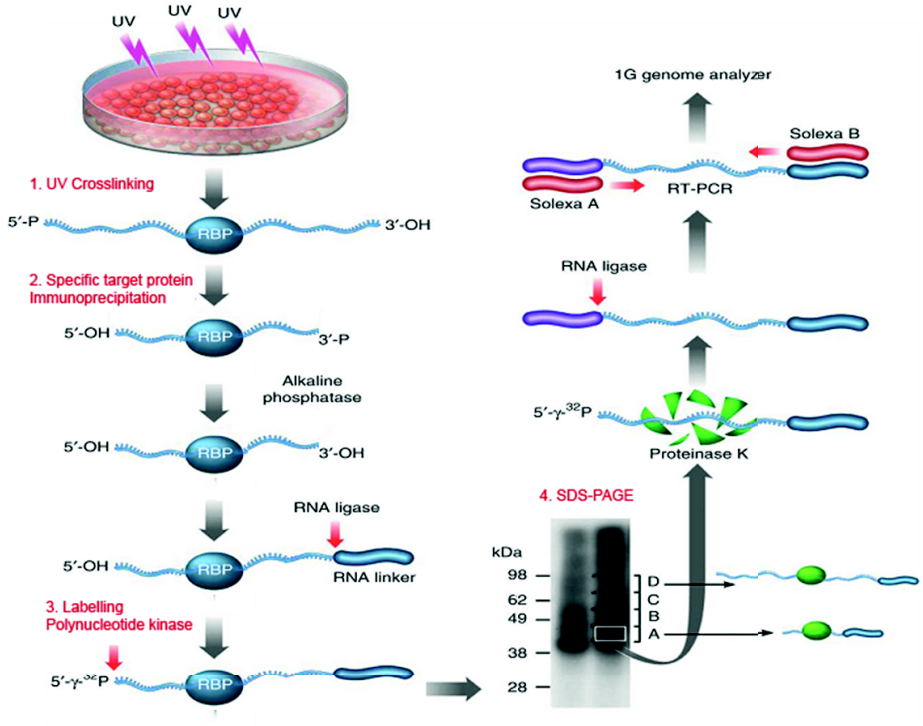

***Figure 2.33**: High Throughput Sequencing Cross-linked immunoprecipitation: HTS-CLIP*

In order to identify the PGC-1α ligand RNAs, CLIP assay was carried out in a functionally relevant cell type. The cell type used was rat hepatoma cells (FAO), because they preserve the hepatocyte structure and most of their functions. To that end, the cells were infected with Adenovirus coding for HA-PGC-1α. Following UV crosslinking and immunoprecipitation, the ligand RNA was radiolabeled and revealed by western blot and autoradiography (Figure 2. 34.). First, the identification of RNA-PGC-1α complex was confirmed in FAO.

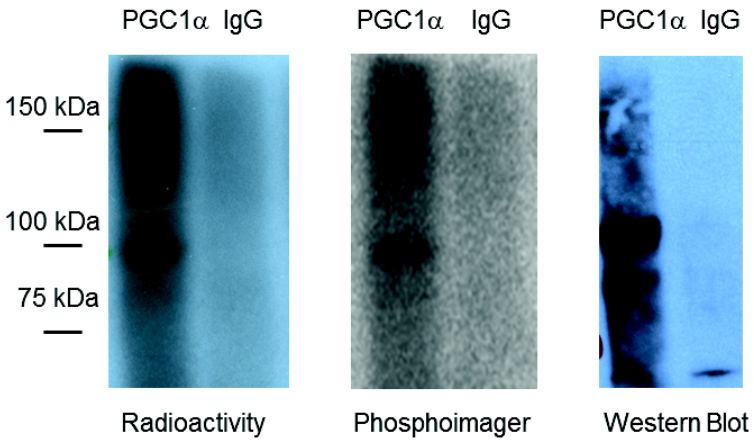

***Figure 2.34**: Crosslink and immunoprecipitation steps of CLIP. FAO cells were infected with Ad-HA-PGC-1α. 24h postinfection, cells were UV treated to crosslink nucleic acids to proteins. PGC-1α was IP from DNase I treated WCE, and polynucleotides in the immunoprecipitates were end-labeled with ^{32}P. The PGC-1α labeled polynucleotide complex was resolved on a 7.5% SDS-PAGE gel and revealed by western blot and autoradiography.*

To isolate the bound RNA following UV crosslinking of the protein of interest and immunoprecipitation of the protein-RNA complex, the protein was digested with proteases and the remaining RNA was purified. The RNA sample was 3' ligated to a 19 mer linker and 5' labelled with ^{32}P-γATP, using the oligomers indicated in Figure 2.35.

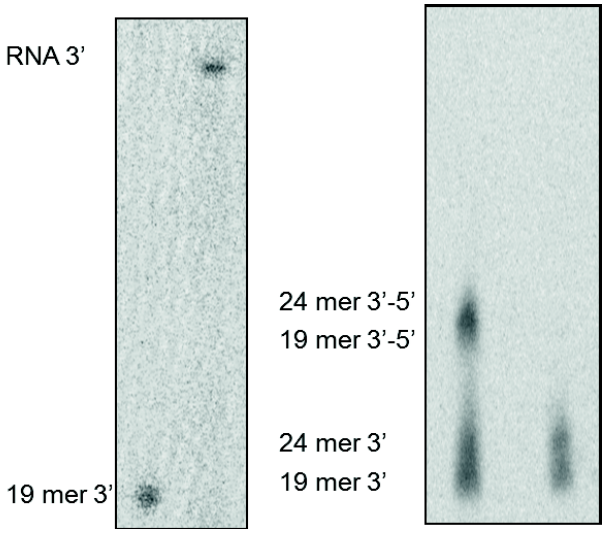

***Figure 2.35**: 3'ligation PGC-1α ligand RNA following. Left panel: FAO cells were infected with Ad-HA-PGC-1α, cells were UV treated to crosslink nucleic acids to proteins. PGC-1α was IP and polynucleotides in the immunoprecipitates were end-labelled with ^{32}P. The PGC-1α labelled polynucleotide complex was protease digested. The isolated RNA was 3' labelled. Right panel: Two controls (19 mer and 24 mer) were subjected to 3' and 5' ligation. The RNA species were resolved on native PAGE and revealed by phosphoimager.*

To boost the ligation efficiency a modified version of the T4 RNA ligase (T4 RNA ligase 2 truncated) first developed in Dr. Tuschl's laboratory was used (Rajasethupathy P *et al*. 2009). Labelled RNA was analysed by PAGE. Several experiment carried out could consistently identify a 3' end labelled RNA of around 60 nucleotides, suggesting that PGC-1α could bind RNAs about 40 nt long (Fig. 2.35).

The labelled RNA was excised from the gel and RNA was recovered by electro-elution and precipitation. Following Dr. Tuschl's protocol it was initially aimed to construct RNA libraries where the extracted RNA would be ligated with specific oligonucleotides at both 3' and 5' ends that introduced sequencing bar codes and then to analyse them by mass sequencing. However, the amount of gel-recovered material was too low to further proceed and the library preparation strategy had to be changed.

3.2.2. RNA amplification and library preparation

As indicated above, the initial studies used FAO cells. At this point primary hepatocytes were used to further elucidate PGC-1α mechanism of action. The primary hepatocytes were used because they are not transformed and respond more efficiently than immortalized cell lines to metabolic regulators like PGC-1α. Furthermore, not only WT hepatocytes but also PGC-1α KO hepatocytes were used, facilitating the background correction and the analysis of PGC-1α ΔRRM mutants that would be expressed using adenoviral infection. Hence, wild type and PGC-1α KO hepatocytes were infected with adenoviral vectors that coded for HA-tagged PGC-1α or HA-tagged ΔRRM-PGC-1α.

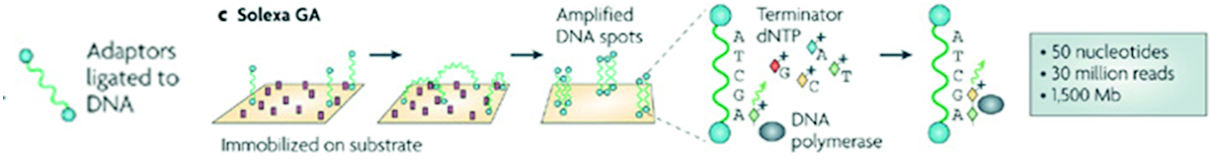

***Figure 2.36**: Summary of the different cluster amplification steps. Immobilisation is followed by bridging, amplification and a reading step.*

As in section 3.2.1., the CLIP workflow was used as previously indicated (Figure 2.33.) but instead a commercially available kit was used and an additional amplification step was introduced before the reverse transcription. In short, following stabilisation of *in vivo* protein-RNA interactions by UV irradiation, and antibody-mediated enrichment of specific RNA-protein complexes (anti-HA monoclonal antibody 12CA5), gel electrophoresis was used to isolate protein-RNA adducts 3' RNA linker ligation and 5' labelling using ^{32}P-γATP. Recovered RNA was ligated to 3' and 5' adapters sequentially introduced before amplification by RT-PCR (TruSeq small RNA: RS-930-1012). RT-PCR was performed to produce a stable DNA Adapter library. The final step was a PCR amplification introducing the index sequence. These index sequences bind the flow cell and allow amplification during the preliminary step of the RNA sequencing (Figure 2.36). RNA libraries were analyzed by mass sequencing using an Illumina platform.

In order to control for specificity, several libraries were constructed. Primary hepatocytes were infected with the HA-shuttle (empty) adenovirus or the HA-ΔRRM-PGC-1α adenovirus. As already explained (Section 3.1.), the deletion of the RRM makes the protein unable to bind RNA, and hence it was used as an additional control for nonspecific binding. Non-denaturing polyacrylamide gel analysis of the final amplification products are shown in Figure 2.37. The amplified bands (cDNA) were isolated and analysed by mass sequencing.

It was anticipated that if the amplified material from the RT-PCR reaction derived from a PGC-1α specific RNA ligand, it should not be present in the shuttle nor in the ΔRRM-PGC-1α samples because this structure do not contain RRM able to bind RNA. The only band present would be background random amplification signals of the adapters. Furthermore, the band derived from a PGC-1α specific RNA ligand was expected to have a size of approximatively 140-150 bp, or its concatemers, since in the previous assay a 60 nt labelled band was consistently identified before (Figure 2.35.). However, the major amplified DNA band in HA-shuttle or HA-ΔRRM-PGC-1α had a size of about 125 bp and was present in the control reactions. A major drawback in preparing nucleic acid fragment libraries by ligation of adapters to the ends of template nucleic acid fragments is the formation of adapter-dimers. Adapter-dimers are formed by the ligation of two adapters directly to each other such that they do not contain a nucleic acid template fragment as an insert. A minor band with the expected size of adapter dimers (size 120-125 nt) and a major band with the size of a predictable concatamer (size from 130-135 nt) were present in the control reaction. Nevertheless, no other contaminants could be detected; suggesting that the reaction was well controlled (Figure 2.37.).

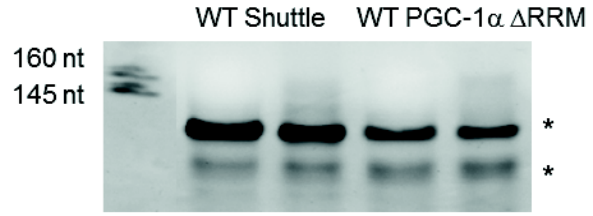

***Figure 2.37**: Library control. RT-PCR amplification products from WT-shuttle and WT-ΔRRM-PGC-1α were resolved on an agarose gel. The preparation was applied in duplicate. (*) indicate the non-specific amplification products.*

Additional internal controls for the RT and PCR reactions were included using the 19-mer and 24-mer oligonucleotides as templates. In Figure 2.38, the 19-mer and 24-mer band ligated to the 3' and 5' oligonucleotides are clearly identified.

As already mentioned, if a specific product had been ligated between the specific 3'-5' oligos and indexes, it should appear as a band of around 140-150 nt or its concatemers, since in the previous assay a 60 nt labelled band was consistently identified before (2.35.). In the preparation derived from WT and KO PGC-1α hepatocytes infected with HA-PGC-1α adenoviruses a product band of the expected size was identified (140-150 nt).

When low amounts of starting material were used (as was the case for the 19 mer- WT PGC-1α reaction), the proportion of adapters dimers was higher (amplified band size 120-125 nt). This band could be discriminated from the "specific" cDNA product. Another background band, attributed to the formation of adapter concatamers (size from 130-135 nt), could be observed directly below the specific PGC-1α RNA ligand band as in 19 mer amplification. The 130-135 nt band was more clearly visible in the samples derived from KO PGC-1α hepatocytes and was less evident in the 24 mer control reaction than in the KO HA-PGC-1α reaction. This effect could be related to the relatively lower amount of starting material present in the KO HA-PGC-1α and 19 mer preparations.

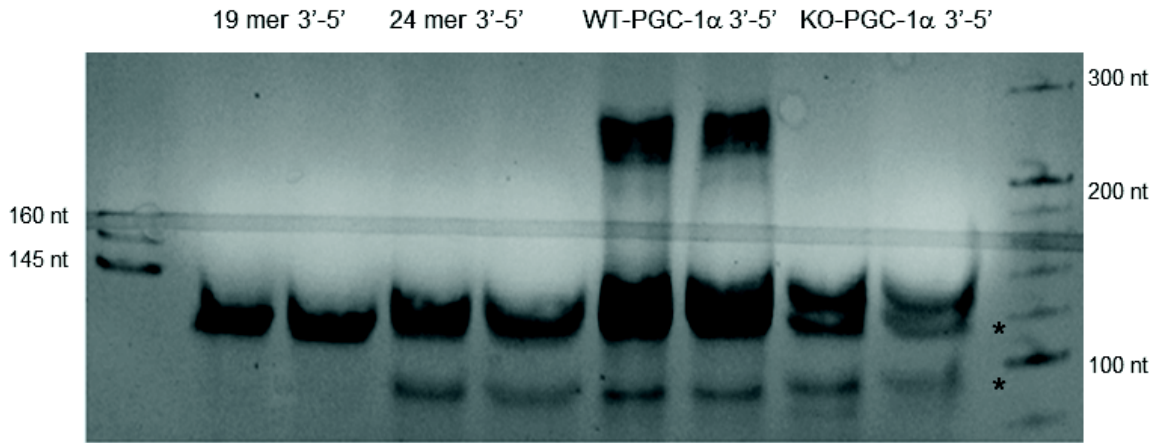

***Figure 2.38**: RT-PCR amplification products. Hepatocytes were transfected, crosslinked. The specifically bound RNA was isolated and RT-PCR protocol was performed allowing insertion of specific code bare. The products were resolved on an agarose gel. 19 mer, 24 mer, WT-PGC-1α and KO-PGC-1α preparations are presented in duplicate. (*) indicate the non-specific amplification products.*

The specific cDNA product was difficult to separate during the isolation process from the adapter concatamer bands and was later taken into account for the analysis of the reads.

Bands corresponding to approximately 150-155 nt are described as pre-miRNA or piRNA in the commercially available kit. No such bands were present in our preparations allowing concluding that the RNA identified is neither a pre-miRNA nor piRNA.

Preparations derived from WT hepatocytes infected with HA-PGC-1α adenovirus showed additional bands of >200 nt, that could derive from a 2x concatemer of the ligand RNA or from amplified tRNA molecules. The two sets of bands (140-150 bp and >200 nt) were excised from the gel, eluted and precipitated.

The integrity of the material following gel extraction was evaluated using a bioanalyzer; the High Sensitivity DNA Chip from Agilent Technologies 2100 Bioanalyser. This instrument validates the size of the bands extracted from the gels and showed a single size material (only one band was identified). Based on these results it was decided to use these samples for mass sequencing analysis.

3.3. Target Identification

3.3.1. Data analysis

Sequencing on Solexa was performed at the genomic unit at "Centro Nacional de Investigacion Cardiovascular (CNIC)", as described in Material and Method and following the guidelines from Illumina.

In order to obtain complete sequence coverage from the 212 nt preparation a pair-end sequencing run was performed allowing to read approximately half of the sequence in both directions. The small size preparations were sequenced using a single-end sequencing set-up. Since control samples had different barcodes, it was possible to mix them in a single flow cell.

Control samples

The presence of the adaptor-concatamers was a major drawback in the analysis. These molecules are undesirable, because adapter-concatamers are generally smaller than the fragments contained in the libraries and therefore they amplify and accumulate at a faster rate. This reduces the efficiency of the amplification reaction by limiting amplification of the library fragments because of depletion of components in the amplification reaction, such as for example dNTP's and primers. Another, more serious concern is that, when such amplified fragments are sequenced they do not give useful sequence information since they contain no insert. Thus, the preparation of libraries with a low level of adaptor-concatamers is highly advantageous in the sequencing of polynucleotides. Although the Bioanalyser did not show these bands, after cleaning the control data sets, a large proportion of reads bearing the adaptor code were found.

For each of the datasets mentioned above, the Illumina-Solexa small RNA sequencing data was filtered by eliminating low quality reads, adaptor sequences and adaptor contaminants in order to generate clean reads using Cutadapt 1.0. The control samples (constructs: HA-Shuttle, or HA-ΔRRM PGC-1α) showed very low amounts of counts after cleaning (around 0.2 million reads).

Specific RNA identification

A total of around 35 million reads for the pair-end sequencing run and 12 million reads for the single-end sequencing were obtained after cutadapt treatment for the specific preparation suggesting a specific amplification of ligand RNA. None of the identified sequences showed similarities with the control samples, demonstrating specificity in amplification.

Around 33% of these reads from WT or KO cells infected with HA-PGC-1α adenovirus were very short fragments of 12 to 24 nt. Surprisingly, the results of the pair-end sequencing run did not give longer nucleotide length. In fact, less than 1% showed a length of over 75 nt. It was hypothesised that these sequences were the result of the concatamerisation of the barcode-target-barcode, and not the

described tRNA sequences. This may also explain the observed DNA ladder now attributable to several concatemerisation levels.

Another relevant observation was the presence in the main data (33% sequences) of the 8 bp target sequence of the restriction enzyme PmeI (GTTT^AAAC). This sequence is present in the adenoviral vector and apparently was enriched and amplified specifically in the HA-PGC-1α samples, and not in the other samples, possibly suggesting some grade of sequence specificity. These sequences were part of the 12 to 24 nt long pool.

3.3.2. Identification of target sequences

The sequences identified in the samples from WT and KO hepatocytes infected with Ad-HA-PGC-1α were mainly 12 to 24 nt long. In order to identify clusters from the 12 to 24 nt long sequences, the ClustalW software was used. These sequences or reads, were mainly variants of a consensus sequence with one or more mismatches, short insertions or deletions. The identified sequences were aligned to the mouse reference genome (NCBI v37, mm9) using Integrative Genomics Viewer (IGV). The clean reads that could be perfectly aligned were considered as mapped reads, and the remainders were considered as unmapped reads. Most sequences mapped to noncoding intergenic regions that might be tentatively considered promoter/regulatory regions.

The chromosomal localization of the BLAST sequence was zoomed-in on the aligned reads on the mouse genome. To test the specificity of the read the graphic includes the HA-shuttle and HA-PGC-1α results. As a representative example, the chromosomal context of the hits found in chromosomes 17 and 5 are shown in Figures 2.39 and 2.40.

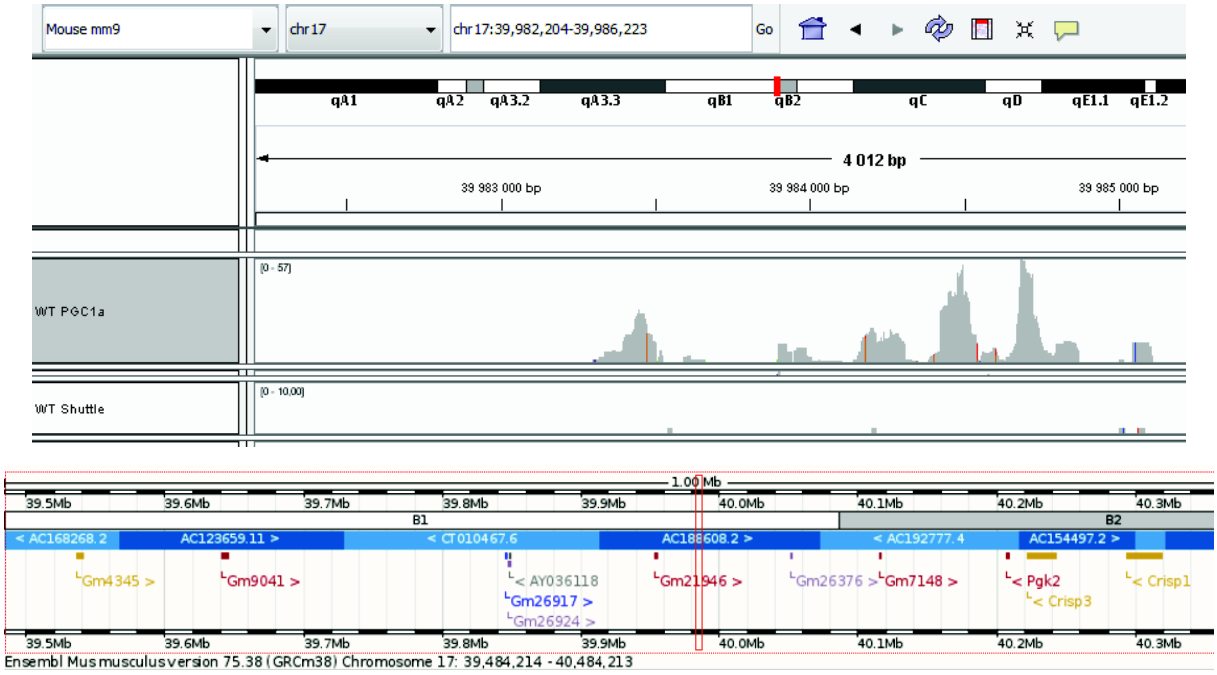

***Figure 2.39**: Integrative Genomics Viewer on Chromosome 17 regions. RNA sequencing signal on chromosome 17 with the corresponding genome localization.*

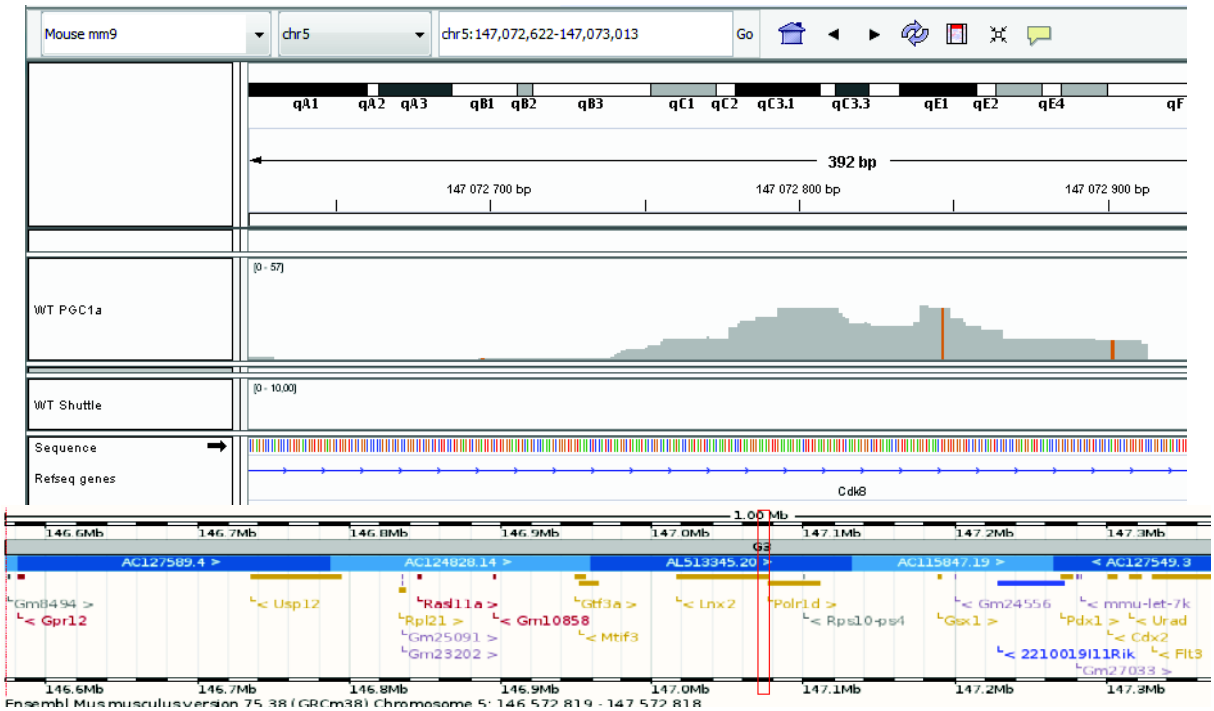

***Figure 2.40**: Integrative Genomics Viewer on Chromosome 5 regions. RNA sequencing signal on chromosome 5 with the corresponding genome localization.*

Validation of targets: RNA immunoprecipitation

In order to validate the results, and confirm the identified sequences as true targets of the PGC-1α RRM, RNA immunoprecipitation analysis was carried out.

FAO cells were infected with the following adenoviral vectors: HA-shuttle, HA-PGC-1α and HA-ΔRRM PGC-1α. WCE were used for specific anti-HA immunopericipitation of the targeted proteins. Agarose beads were linked to the specific antibody (HA). The complexed beads were incubated with total RNA from FAO cells, and washed. The bound RNA fraction was then extracted from the complex bound beads following a standard RNA purification protocol. Non-specific binding was avoided by restrictive binding conditions. The recovered RNA was analyzed by qRT-PCR using oligonucelotides designed to the putative target sequences identified in the HIT-CLIP assay. Selected chromosome sequences are located in chromosomes 1-2-5-6-10-15 and 17.

Specific binding should result in the specific amplification of the tested region. Of all the chromosomal regions tested, only one set of primers targeting chromosome 17 showed significant specific amplification on the immunoprecipitated fraction. This region is part of a predicted gene Gm21946, also identified as Esp38: Exocrine gland secreted peptide 38 present in the extracellular space and bearing pheromone activity. This approach is limited by the short sequence and the difficulties to design specific oligonucleotides. A possible alternative approach is proposed in the discussion.

GeneChip targets

In order to gather further functional insight on the function of the PGC-1α RRM a group of genes was selected that showed marked significant gene expression differences for the contrast PGC-1α/PGC-1α-ΔRRM (section 2.5.) and scanned them for putative CLIP hits. The genes *Camk2b, Cyp2b13, Cxcr7, Cxcl1, Slc17a3, Cy2b10* included putative specific RNA ligated sequences were found as derived from an IGV analysis of the CLIP results. This preliminary data further support the notion of the specific binding of PGC-1α to ligand RNA sequences.

In summary, these results support the idea that PGC-1α binds RNA in a sequence specific manner. Further validation of targets and mechanisms are however still necessary to understand the functional relevance of the ligated RNAs.

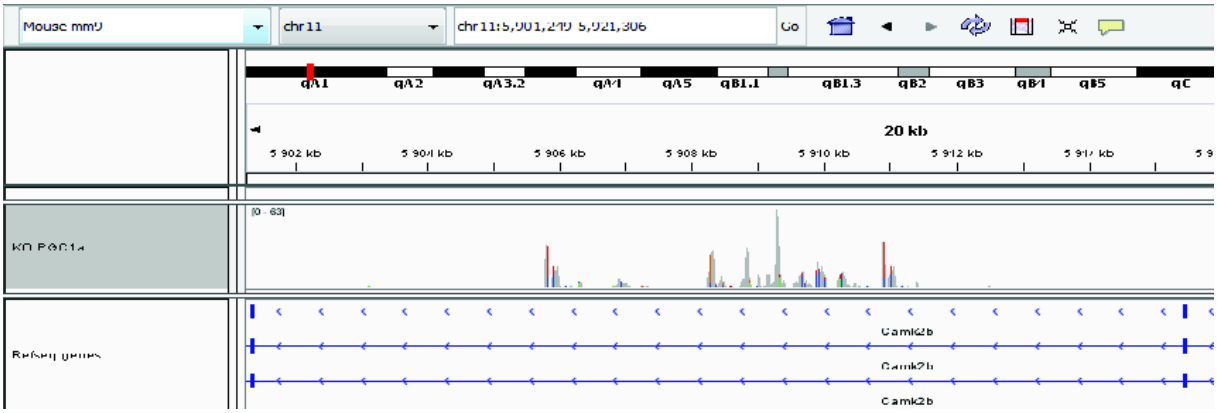

***Figure 2.41**: Integrative Genomics Viewer on GeneChip targets. RNA sequencing signal on Camk2b with the corresponding genome localisation.*

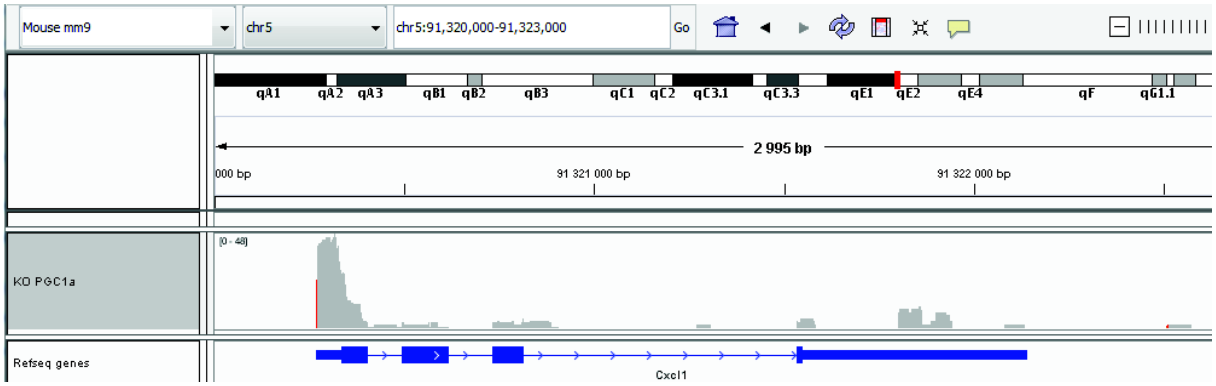

***Figure 2.42**: Integrative Genomics Viewer on GeneChip targets. RNA sequencing signal on Cxcl1 with the corresponding genome localisation.*

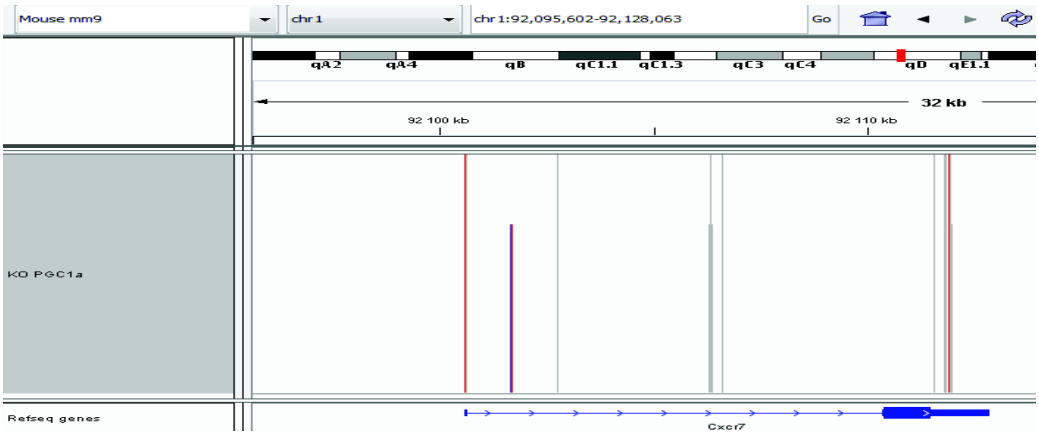

***Figure 2.43**: Integrative Genomics Viewer on GeneChip targets. RNA sequencing signal on Cxcr7 with the corresponding genome localisation.*

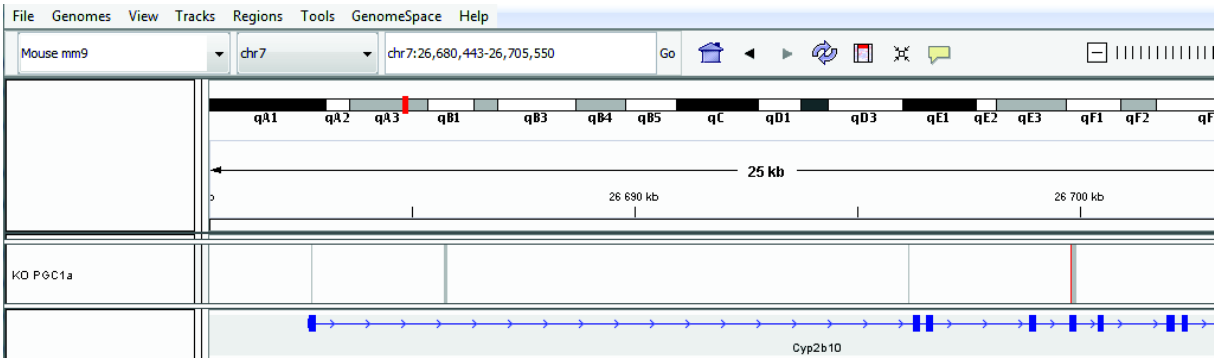

***Figure 2.44**: Integrative Genomics Viewer on GeneChip targets. RNA sequencing signal on Cy2b10 with the corresponding genome localisation.*

The final aim of this study was to confirm and identify RNA species binding to PGC-1α RRM. The technique applied to confirm and identify these RNA species was high throughput cross-linked immuno-precipitation (HIT-CLIP). The use of HIT-CLIP confirmed binding of RNA to PGC-1α. The presence of RRM suggests preferential transcription of some protein isoforms. The combination of the obtained results from array and RNA sequencing support this hypothesis.

In summary, this study not only gives detailed information about ROS detoxification gene regulation by PGC-1α but also allowed the identification of new mechanisms of action for SirT1 and PGC-1α.

Discussion

Discussion

All cellular processes such as cell development, differentiation, growth and metabolism are tightly regulated at different levels. Importantly, transcriptional regulation is the first limiting step in the control of any cellular process. Transcription is a highly dynamic process involving several steps, each one subject to regulation. Through alternative exon use, transcriptional regulator can also impact protein diversity without increasing gene number. Furthermore, not only is mRNA continuously being processed, it is also continuously being degraded. As a consequence mRNA can be regarded as a short-term memory for biological information. The complexity and tight regulation of the transcriptional process makes necessary the participation of a vast array of proteins with many different functions (Orphanides G and Reinberg D 2002). RNA polymerase II (RNAP II) transcribes all mRNA genes and a wide array of long and short non-coding RNAs, making it an essential component in gene expression control. Regulatory factors are often combined, in complex ways, into multiple layers of regulation and frequently can be either transcriptional activators or repressors, depending on the context.

Both the temporal and quantitative pattern of gene expression are subject to stringent control, which is essential for all cell processes (such as metabolism, proliferation, differentiation and the response to environmental signals). One example of a specific context is the mitochondrial content and respiration efficiency. The great variability from cell type to cell type from mitochondrial content and respiration efficiency reflect the physiological status of the cell (Moyes CD and Hood DA 2003). In this complex process, Peroxisome proliferator-activated receptor gamma (PPARγ)-coactivator 1 alpha (PGC-1α) has been described as a key player. PGC-1α coordinates expression of mitochondrial and nuclear encoded proteins activated in response to increased demand of mitochondrial output. In addition to the regulation of genes encoding mitochondrial biogenesis and mitochondrial respiratory activity, PGC-1α regulates other general or tissue specific genes involved in metabolic control. This includes gluconeogenesis in the mammalian liver, adaptive thermogenesis in brown adipose tissues, preferential fatty acid utilization and oxidation in the heart. Furthermore, PGC-1α regulates the expression of antioxidant genes, preventing excessive reactive oxygen species (ROS) accumulation in conditions of increased electron transport chain (ETC) activity. PGC-1α works as a transcriptional coactivator that must integrate several metabolic signals and interact with many transcription factors and co-factors to provide both gene specific and tissue specific transcriptional regulation. The mechanisms involved in PGC-1α transcriptional control are the focus of the presented study. The results obtained can be discussed under three main sections:

A ternary complex formed by SirT1, FoxO3a and PGC-1α is recruited to the promoter of antioxidant genes to control gene expression

The identification of the key transcriptional factors involved in the regulation of oxidative stress defence mechanisms is of great importance in the context of the vascular endothelium, where high ROS levels play a determinant role in endothelial dysfunction and therefore in the appearance and progression of atherosclerosis as well as in the control of the angiogenesis processes. This study shows that SirT1 positively regulates the expression of a group of oxidative stress protection genes in vascular endothelial cells and provide evidence that at least for some of this group of genes this effect is likely to be mediated by the SirT1 regulation of the PGC-1α/FoxO3a transcriptional complex.

Previous work had shown that PGC-1α is recruited to the promoter regions of the regulated antioxidant genes in endothelial cells (Valle I *et al.* 2005). Furthermore, later studies had identified the Forkhead class O protein 3a (FoxO3a), as the DNA binding transcriptional factor that drives the recruitment of PGC-1α to the promoter of antioxidant genes (Olmos Y *et al.* 2009). Aiming to identify additional cofactors, it was noted that both PGC-1α and FoxO3a have been shown to be targeted by the deacetylase SirT1, and that both proteins were acetylated in response to oxidative stress (van der Horst A *et al.* 2004, Kobayashi Y *et al.* 2005, Rodgers JT *et al.* 2008). Importantly, SirT1 is induced by NAD^+, acting as a sensor of the cellular redox and nutritional status. Therefore, the hypothesis in this work is that SirT1 could be a relevant regulatory player of antioxidant gene expression, activating PGC-1α and FoxO3a in response to oxidative stress and reduced availability of reducing equivalents. Later analysis demonstrated that overexpression of SirT1 induced the expression of antioxidant genes in a PGC-1α and FoxO3a dependent manner, further supporting the hypothesis of SirT1 regulatory role in the antioxidant gene expression. The tested of the effect of SirT1 depletion on antioxidant gene expression confirmed the involvement of SirT1 in antioxidant gene expression.

To further support the hypothesis, it was investigated how SirT1 deacetylation of both FoxO3a and PGC-1α could play a role in SirT1 induction of antioxidant genes. The tested effect of SirT1 on formation of the FoxO3a/PGC-1α complex was found to be an increased formation of the PGC-1α/FoxO3a complex in the presence of SirT1. It was proposed that SirT1 could work through two alternate mechanisms. SirT1 could deacetylate FoxO3a and PGC-1α independently and the deacetylated proteins could have an enhanced affinity for each other. Alternatively, SirT1 could be part of a ternary complex recruited to the target promoters. To challenge this hypothesis, it was tested whether FoxO3a and PGC-1α could modulate each other's level of acetylation. The finding is that PGC-1α decreases FoxO3a acetylation and FoxO3a reduces PGC-1α acetylation when present. As none of the two proteins bare deacetylation activity, the data is supporting the notion that SirT1 is part of a ternary complex together with PGC-1α and FoxO3a.

Since previously demonstrated in that FoxO3a and PGC-1α form a complex that is recruited to antioxidant gene promoters (Olmos Y *et al.* 2009), hypothesis of SirT1 as partner of the recruited regulatory complex have been made. To test this idea, ChIP analysis was used. The outcome was that SirT1 associates with the regulatory regions of a panel of antioxidant genes consolidating the approach. Important information about SirT1 binding was its association with reduced H4K16Ac, a hallmark of SirT1 activity. It is generally considered that reduced acetylation is associated with gene silencing. However, a number of studies carried out mainly in yeast, have shown that histone deacetylation and in particular H4K16 deacetylation can play a positive role in gene expression regulation (Skurk C *et al.* 2004). SirT1 mechanisms of action on chromatin described so far, involve the deacetylation of histones within the coding regions of active genes to ensure proper transcription initiation, by repressing aberrant initiation within the coding region (Kim MJ *et al.* 2009). This type of promoter specific effects are still poorly characterised (Sharma VM *et al.* 2007). The results show that SirT1 deacetylation of H4K16 is accompanied by a general reduction in RNAP II levels in the promoter proximal regions but this does not result in decreased gene expression. Importantly, finding that SirT1 recruitment was associated with increased levels of elongating RNAPII is suggesting that SirT1 activity might be contributing to repressing aberrant initiation and/or increased recruitment of elongation factors.

Although the mechanisms involved in the transcriptional activation by histone deacetylases are still unclear, there is some evidence that the lysine specificity of the deacetylase may be a critical determinant. In particular, H4K16 appears to be an important target for deacetylases playing an activating role (Wang A *et al.* 2002). It appears that unacetylated H4K16, in the context of acetylation at other epigenetic sites is important for transcription, but unacetylated H4K16 in the context of other unacetylated residues is important for heterochromatin formation. The complexity of epigenetic code and collaborative signals is highlighted. So far, the only characterised example in mammals in which H4K16Ac is linked to gene silencing is rDNA cluster regulation (Zhou Y and Grummt I 2005). A recent study has shed some light on the mechanism through which acetylated H4K16Ac plays a dual role in gene silencing: it recruits Sir2-4 and repels Sir3. (Oppikofer M. *et al*. 2011). Therefore, acetylation would serve to recruit SirT1 to the target gene and this recruitment may result in enhanced or decreased transcription depending on whether or not additional silencing/activating factors are subsequently recruited. Experimental evidence for this type of regulation in mammals is however missing. To gain a global view of the events, further experiments have been designed combining ChIP of different protein involved in gene transcription initiation.

The results suggest that SirT1 is likely to act, at least in part, by directly binding to promoter target genes, probably recruited through its interaction with transcription factors. Although SirT1 acts

predominantly as a co-repressor, there is evidence that SirT1 can also serve as a co-activator. For example, SirT1 recycles Tat to its unacetylated form and acts as a transcriptional co-activator during Tat transactivation (Pagans S. *et al.* 2005).

Monsalve and co-workers (Monsalve M *et al.* 2000) demonstrated PGC-1α N-terminal domain interacts with pre-initiation complex (PIC) RNAP II CTD serine-5 phosphorylated while PGC-1α C-terminal domain interacts with elongating RNAP II CTD serine-2 phosphorylated. An interesting possibility is that SirT1 may regulate the interaction of PGC-1α with the elongation complex. Moreover, FoxO3a also interacts with PGC-1α through its C-terminal domain and could also contribute to the transition between the initiation and elongation complexes.

FoxO3a has been shown to work as a priming factor, able to interact with target promoter sites even when chromatin is in a relative compact state, or hypo-acetylated (Matsuzaki H *et al.* 2005) suggesting that FoxO3a DNA binding activity to antioxidant genes may not be negatively affected by SirT1 deacetylation of nearby histones.

It should also be noted that the results are the first to demonstrate that SirT1 can have a transcriptional activation activity upon recruitment to chromatin sites. It is also the first piece of work to demonstrate a site-specific regulatory activity on a panel of antioxidant genes rather than a general silencing effect on all the transcription system. Furthermore, the results are the first to elucidate a mechanism in mammals through with deacetylation does not result in transcriptional silencing.

However, the mechanistic details of how SirT1 induces the transition from the initiation to the elongation complex remain to be elucidated. The transcription initiation process is complex and well regulated. The earliest stages of transcription are marked by instability of the transcription complex and a pronounced tendency to release short pieces of RNA (2-5mers) in a transcriptional phase, which is termed “abortive initiation”. Stabilization of early elongation complexes is observed when the DNA-RNA hybrid reaches 8 bases in length (Kireeva ML *et al.* 2000). RNA synthesis can be interrupted by pausing and/or arrest, which occurs with a backward movement of the RNAPII, termed “backtracking” (Figure 1.4). Of importance, it has been noted that unidirectional transcription is no longer the only way to proceed for RNAP II (Seila AC *et al*. 2008) at many, if not all, transcription sites. During the unstable phase, RNAP II can start transcription in both directions, in a process called divergent transcription (Seila AC *et al*. 2008). Transcription proceeds until the machinery encounters additional signals that enforce the selection of one direction..

The initiation process culminates with the recruitment of the positive transcription elongation factor b (P-TEFb). Once recruited, P-TEFb phosphorylates RNAP II at its serine 2 residue, releasing it from its

paused status (Lis JT *et al.* 2000, Ni Z *et al.* 2008). After RNAPII is released from its paused state, RNAP II proceeds into productive transcription elongation and completes transcription of genes (Figure 1.4). The events leading up to polymerase pause release often includes the covalent modifications of nucleosome barriers near the pausing event (Kireeva ML *et al.* 2005, Bondarenko VA *et al.* 2006, Li CF et al. 2006).

The results presented in this work in chapter 2, suggest that SirT1 recruitment with concomitant histone deacetylation and reduced RNAP II serine-5 recruitment does not necessarily cause a reduction in mRNA levels but instead it is associated with an increase in gene expression. The fact that SirT1 is present upstream of the core promoter could also be consistent with the hypothesis of SirT1 forming a barrier in one direction. This barrier could be one of the signals driving transcription machinery from divergent to unidirectional transcription. SirT1 could also foster access downstream to sequence specific binding transcription factors. An example of mechanism could be by promoting upstream closing of the chromatin thereby hindering access to the underlying sequences.

Recruitment of P-TEFb during pausing to facilitate polymerase pause release can be elicited through several alternative mechanisms, the two most common being its recruitment by factors that bind chromatin by transcription factors (Peterlin BM and Price DH 2006). An illustrative example of P-TEFb recruitment is provided in the study performed by Zippo A *et al.* 2009. This study discovered that the bromodomain containing 4 (BRD4) protein could bind to the acetylated H4K16 and H3K9 and recruit P-TEFb to facilitate polymerase pause release. Other studies have found that P-TEFb could be recruited to regions of active transcription by transcription factors like c-Myc (Eberhardy SR and Farnham PJ 2002). This emerging data from this study support the findings presented by Eberhardy SR and Farnham PJ of an alternative complex, interactive, regulation of transcription. The results add supporting data to the diversity developed by the transcription machinery and build argument to a generally used pausing process.

Taken together, the findings highlight the complexity of the pausing event as well as important roles for chromatin in regulating eukaryotic transcription the formation of barrier elements for the transcriptional machinery and specific complex formation (SirT1/PGC-1α/FoxO3a) with posttranslational modification as regulator of affinity.

Functional characterisation of PGC-1α RRM

After having been focusing on the transcription initiation, detoxification genes promoter regulation, PGC-1α complex formation and regulation, the second part of the work is focusing on PGC-1α specific domain features.

Drug targeted proteins are generally enzymes, whose activity is regulated by drugs, most of which get incorporated into the ligand binding pocket and consequently modify the enzymes proof of activity. PGC-1α is not an enzyme, but it possesses a putative targetable domain, the RRM. The use of this domain to modulate PGC-1α requires a characterisation of its functional role, and the demonstration that RNA binding actually modifies its activity. These two key issues are addressed in the present study.

The previous results from our laboratory (Monsalve M *et al*. 2000) had shown that deletion of the RRM decreased the capacity of PGC-1α to induce mitochondrial biogenesis. In this study the ability of ΔRRM mutants to induce antioxidant gene expression was tested. The finding was that the ΔRRM mutant had a reduced capacity to induce several, but not all, antioxidant genes, identifying that RRM is playing a role in antioxidant gene expression and suggesting that the dependency on the RRM is gene specific. Importantly, PGC-1α co-activator TLS, previously has been shown to co-regulate PGC-1α activity on antioxidant genes, but not in mitochondrial biogenesis genes. The experiments performed in the study, used PGC-α-ΔRRM and TLS this combination could boost PGC-α-ΔRRM activity at some genes but not others (Figures 2.18. and 2.19.). For the present study, one of the antioxidant genes was selected (*ucp-2*) for further evaluation and using reporter gene assays demonstrate that the proximal promoter region (200 bp) was enough to confer RRM specificity to the TLS-PGC-1α regulation of UCP-2 . This result suggested that RRM dependent activity does not have sequence requirements beyond that region, at least for the *ucp-2* gene even though the additional regulatory elements cannot be ruled out.

Taking into account the results that the RRM activity seemed to be gene specific, the next step was to carry out a genome wide transcriptional analysis to identify other specific genes regulated by PGC-1α RRM. The cellular model of choice was primary hepatocytes. These cells were selected because the liver is the central organ in metabolic control in the organism and functional relevance of PGC-1α in the liver is well established. Furthermore, primary hepatocytes from both WT and PGC-1α KO mice were isolated, facilitating the functional analysis of the ΔRRM mutant on a PGC-1α null background.

First, validation of the model was performed to ensure that adenoviral driven expression of PGC-1α WT in KO hepatocytes resulted in the expected up-regulation of known PGC-1α target genes. Next, whole genome gene expression microarrays was used to compare gene expression in WT vs KO PGC-

1α hepatocytes. In addition to previously reported PGC-1α regulated genes, additional gene families were found that could be targeted by PGC-1α, in particular 7 members of the Cyp2 P450 family and solute carriers. These two families of genes are involved in detoxification of natural compounds and xenobiotics, their activity is crucial to prevent drug induced liver toxicity but they also limit the bioavailability of therapeutic drugs, including those used in tumor chemotherapy (Konno Y *et al.* 2009, Horvath HC *et al.* 2010).

The cyp2 gene cluster on chromosome 19q13.2 includes several genes and pseudogenes from the *cyp2A, cypB, and cyp2F* subfamilies. *Cyp2b13/Cyp2b9* work synergistically and are known to be regulated in a coordinate fashion.

slc30a10 is a solute carrier family member, identified as a PGC-1α regulated gene. Interestingly, two exon probes were differentially expressed; possibly suggesting that PGC-1α could be involved in an alternative splicing event. The available genomic information found in databases is also consistent with the existence of alternatively spliced transcript variants. *Slc30a10* is highly expressed in liver, its protein product appears to be critical in maintaining intracellular manganese (Mn) levels. Mn is a cofactor of several important enzymes, including the mitochondrial superoxide dismutase, MnSOD. Loss of function mutations results in a pleomorphic phenotype, including dystonia and adult-onset Parkinsonism; conditions otherwise related to poor mitochondrial function.

In order to elucidate the functional role of PGC-1α RRM at a genome wide level, whole genome gene expression microarrays was used to compare gene expression in *PGC-1α*$^{-/-}$ primary hepatocytes infected with adenovirus driving the expression of WT PGC-1α or PGC-1α-ΔRRM Deletion of the RRM was found to largely phenocopies the full KO, with a general reduction in the activation of PGC-1α target genes. Still, significant gene specific differences were noted among the two groups (PGC-1α KO and PGC-1α-ΔRRM). The twenty top genes up-regulated and down-regulated as annotated by the contrast ΔRRM/WT within the assay are listed in Table 1.3. Technical validation of the array results by q-RT-PCR supported the identification of RRM dependent PGC-1α targets.

Three genes identified in the WT/KO microarray analysis as novel PGC-1α regulated genes were also clearly identified as dependent on the activity of the RRM in the second microarray analysis for the contrast ΔRRM/WT, namely: Cytochrome P450 family 24 subfamily a polypeptide 1 (*Cyp24a1)*, *C-X-C chemokine receptor type 7* (*Cxcr7)* and *calcium/calmodulin-dependant protein kinase II beta* (*Camk2b*). Interestingly, of all the P450 genes regulated by PGC-1α, *Cyp24a1* is the only member whose regulation required the RRM. This observation suggests different regulation of the family members and different ways PGC-1α can regulate genes (RRM or other domains and cofactor binding). Cyp24a1 is localised in the inner mitochondrial membrane and is involved in vitamin D_3

degradation, downstream of Cyp2r1 and Cyp27b1. A particular characteristic of this protein is that is generally present at low levels in the cells but undergoes rapid induction in response to elevated concentrations of vitamin D_3. High levels of Cyp24a1 in colorectal cancer have been described as associated with more aggressive tumors (Horvath HC *et al.* 2010). However, the transcriptional regulators involved in the control of its expression were so far unknown.

The Calcium/Calmodulin dependent protein kinase II beta (*Camk2b*) gene has a variety of splicing forms and codes for a number of alternatively processed transcripts. In the presence of Ca^{2+}, CAMK2b is activated and binds PGC-1α, forming a complex that is recruited to *pgc-1α* promoter to regulate its expression (Czubryt MP *et al.* 2003, Handschin C *et al*. 2003). The microarray analysis for the WT/ΔRRM contrast showed that deletion of PGC-1α RRM resulted in decreased levels of *Camk2b* gene for tags located in the 3'UTR region. This observation can reflect both inefficient termination and/or inefficient elongation in the absence of the RRM. Furthermore, this regulatory event evidences the existence of a retro-regulatory loop of PGC-1α on CAMK2b. However, supporting evidence would require further investigation such as luciferase assay or co-immunoprecipitation.

After looking into the up-regulated genes, the focus was given to genes that have been detected to be down-regulated by *PGC-1α* in a RRM dependent manner in our data set. Three selected examples are *Solute carrier family 17 (organic anion transporter), member 3 (Slc17a3), inositol polyphosphate-5-phosphatase J (Inpp5j)* and *chemokine (C-X-C motif) ligand 1 (Cxcl1)* genes.

Slc17a3 (npt4) was identified as a PGC-1α regulated gene in the two independent microarray assays. Exon analysis showed that while some gene regions did not evidence significant variations in gene expression for the contrast WT/ΔRRM, the region encompassing exons 9 to 11 is more expressed in ΔRRM PGC-1α hepatocytes, while the 3' UTR expression does not seem to be highly significantly modified by the presence or the absence of PGC-1α. Genomic information available in relevant databases indicates that this gene codes for four alternatively spliced mRNAs. These two observations might be indicative of an alternative splicing event regulated by PGC-1α in a RRM dependent manner. Evidence to support the theory of alternative splicing connected to the PGC-1α-RRM could be provided by further testing (Section Results 2.5.).

Taken together, these observations support the idea that deletion of the RRM results both in a general reduction in PGC-1α activity and a gene specific alteration in PGC-1α function. This gene specific modification seems to involve additional cofactors, like TLS and may be relevant in transcripts where alternative processing is involved. Importantly this regulation affects both types of genes, those that are positively regulated by PGC-1α and negatively regulated. The evidence accumulated so far suggests that promoter sequences are enough to provide RRM dependent

regulation by PGC-1α, although other regulatory regions are still possible (Figure 2.19). Elucidation of the mechanistic details on how the RRM domain impacts on PGC-1α activity would require further investigation. An approach has been selected and is described in Section 3 Results of this study.

Identification of PGC-1α ligand RNAs

Once the functional relevance of PGC-1α RRM was established, the aim was to determine if it actually function as an RNA binding domain. Most RNA binding proteins have two RRM in tandem. One of the RRM provides affinity and the other sequence specificity. PGC-1α has a single RRM. Therefore it was unclear whether it was a functional domain and if so, whether it could bind RNA in a sequence specific manner. It was found that in cells PGC-1α was bound to a nucleic acid that further identified as RNA based on its insensitivity to degradation by DNase I. Binding to RNA was abrogated by deletion of the RRM, suggesting that PGC-1α was in fact a RNA binding protein (Figure 2.30.).

As an initial test on the capacity of this RRM to bind RNA in a sequence specific manner, we tested in vitro the binding affinity of the PGC-1α-CTD for several DNA and RNA molecules. Finding that PGC-1α-CTD would preferentially bind ssRNA, and would bind RNAs with different affinities, could give support to consider PGC-1α as a general RNA-binding protein. The next aim was to establish a protocol that would enable the identification of the ligand RNAs. First UV-crosslinking followed by RNA labeling and purification was used. As a result, the length of the ligand RNAs of approximately 40 nt could be defined. . Following adapter ligation and RT-PCR amplification, the purified samples were analysed by deep sequencing with a Solexa/Illumina system. This is a variant of the shotgun sequencing approach that provides short reads 25-50 nucleotides long. The Illumina sequencing approach is built on a very large number of short-sequence reads. The technical challenge was to apply this technique to RNA isolated from a protein not previously identified as involved in RNA regulation. The first published examples of this type of approach, involved proteins like Dicer and Argonaute. These proteins are involved in binding a large number of RNA and involved in major processing steps.

The output of the RNA-seq experiment suggested that PGC-1α ligand RNAs mapped to several sites on the mouse genome, and showed a partial sequence homology. Application of bioinformatics tools such as ClustaW, BlastN and further Integrative Genomics Viewer (IGV) were used to identify the specific genomic locations of the identified RNAs on the mouse genome. Specific targeted regions were found on chromosomes 1-2-5-6-10-15 and 17. An RNA-immunoprecipitation assay, followed by qRT-PCR, was set up to validate the identified RNAs as specific PGC-1α ligands. Specificity was confirmed for the RNA that maps in chromosome 17. Attempts to confirm other locations failed due to the technology limitation of small length specific oligonucleotide design to amplify regions surrounded by unspecific sequences. The identified sequences are particularly high in CG and bear a

small specific signature just 12-25 nt long. To overcome these problems, a novel amplification strategy had to be envisioned, similar to the approach used for the specific quantitation of siRNAs. Nevertheless, the results clearly suggest that PGC-1α binds not one single but several RNAs molecules and does so with restrictive sequence specificity.

To get further insight into the regulatory mechanisms involved, analysis of genes whose regulation by PGC-1α was particularly sensitive to the presence of the RRM was performed. The genes were deduced from the array experiments. The presence of CLIP sequences using IGV was performed on these particular genes. Interestingly, sequence hits could be identified; possibly suggesting that non-coding snRNA from these positions would modulate PGC-1α activity on the coding gene. However this model assumption would require further validation.

In summary, the work presented here supports the hypothesis that PGC-1α can regulate gene expression not only modulating the efficiency of transcription initiation but can have an impact on transcription elongation, RNA processing and UTR selection. These alternative regulatory events can be mediated through the interaction with other factors like SirT1 and TLS but can also be the direct consequence of PGC-1α activity modulated by the ligand RNAs. Functional validation of the identified ligand RNAs and their impact on specific genes regulated by PGC-1α would decide whether modification of PGC-1α activity with synthetic ligand RNAs can have a therapeutic potential in metabolic diseases where PGC-1α inactivation has been shown to be a relevant feature.

Future development

To vision future developments in the field one must first look back 20 years ago and briefly analyse how the area of whole genome analysis has evolved. The microarray development could be used as a case study. The array technology has almost twenty years of development and had to deal with previously unforeseen challenges of changing experimental design, the need for improvements in standardisation, accuracy and precision, statistical analysis and the requirement for storage of huge amounts of data. All these challenges were faced by the more recently developed mass technologies such as ChIP-on-chip and HTS-CLIP. As already mentioned, HTS-CLIP (Jensen KB and Darnell RB 2008) was first used successfully in 2008 and has since then been applied to a plethora of well characterised RNA binding proteins. The main laboratories (Darnell RB, Tuschl T, Hafner M) that have implemented the HTS-CLIP technology have only recently been able to elaborate bioinformatics tools to properly analyse the data. The software designs are multiple and have focused on the particular experiment requirements for which they were developed. The experiments from the presented study, here mentioned, could only be analysed partially by the bioinformatics software available, being especially difficult to make a good background correction of the readings. Still, the major

drawback of a CLIP assays is the stepwise optimisation of the purification protocol and the low yields of material obtained.

However, the potential of these technological approaches has fostered novel improvements on the sample preparation and analysis tools. The most recent technology that deserves to be taken into consideration for analysis is the droplet barcoding for single-cell transcriptomics (Klein AM *et al.* 2015). The power of analysing a single cell and getting real-time transcription dynamic information is about to become a reality. The improvement in RNA sequencing combined with global transcription profiling at the single cell level is a tool that can be used to allow RNA inventory at the single-cell level. However, although a complete picture of the cell state is not obtained; information about cell heterogeneity and dynamic variation can be captured. This method could overcome artificial interactions, low reaction efficiency, as antibody epitope obstacle and could show specific binding sites with high accuracy. This approach could be used to analyse the response to stress of cells that express wild-type PGC-1α protein. The data could be compared to the ones obtained with the protein lacking the RRM under the same stress condition. The information could complete the picture of 3'UTR selection and RNA transcripts modulation which was obtained during the present study.

Nevertheless, the novelty of the technique implies that the analysis tools are not yet ready to cope with the challenges provided. Additional concerns come from the problem of storing huge sets of data for long periods of time. Awareness of this uprising concern is crystalizing in the setting up of bioinformatic centers in the hope to provide a global solution.

An important discovery from this work is the inter-connection of transcription pausing and epigenetic and RNA maturation events. Recent publications support this new concept, in particular it has been demonstrated that long non-coding RNA can regulate gene expression. A particularly relevant example, among others, is the PRC2 complex which is regulated by ncRNAs and the histone code (Zhao J *et al*. 2010).

Since the discovery of regulation by siRNAs, a plethora of studies have aimed to develop RNA based therapies, unfortunately, serious technical problems have so far hampered the successful launching of therapies based on small RNAs. Still, the huge potential to develop modulated treatment to a broad range of diseases (http://ranarx.com) by targeting regulatory regions or proteins using RNA has boosted new technical developments based on targeted delivery. In order to apply the findings to the therapeutic market, development of the guidelines by regulatory authorities for biotechnology has to be carried out in parallel.

Therefore work is ongoing on guidelines for new technologies (ncRNA therapy and clinical testing) and the scientific community also saw the birth of new scientific journals focusing on these types of

therapeutic technologies, for example EMBO Molecular Medicine (Dimmeler S 2011). Prominent scientists like Dr. S. Dimmeler stressed at the recent congress of Standardisation of thrombosis and haemostasis the importance of ncRNAs as key tools for future developments in cardiovascular regenerative medicine.

Figure 2.45.: Model of mechanism:

Normal conditions

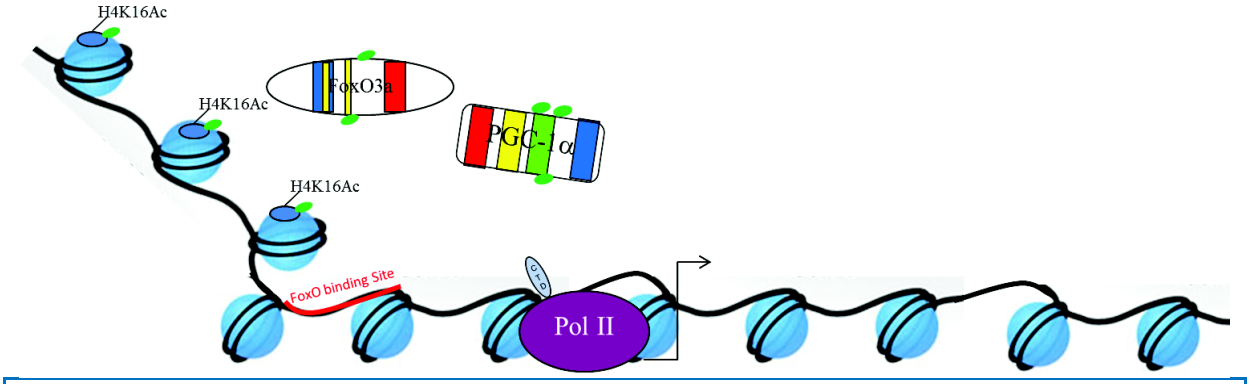

Pre-initiation complex under serum starvation conditions

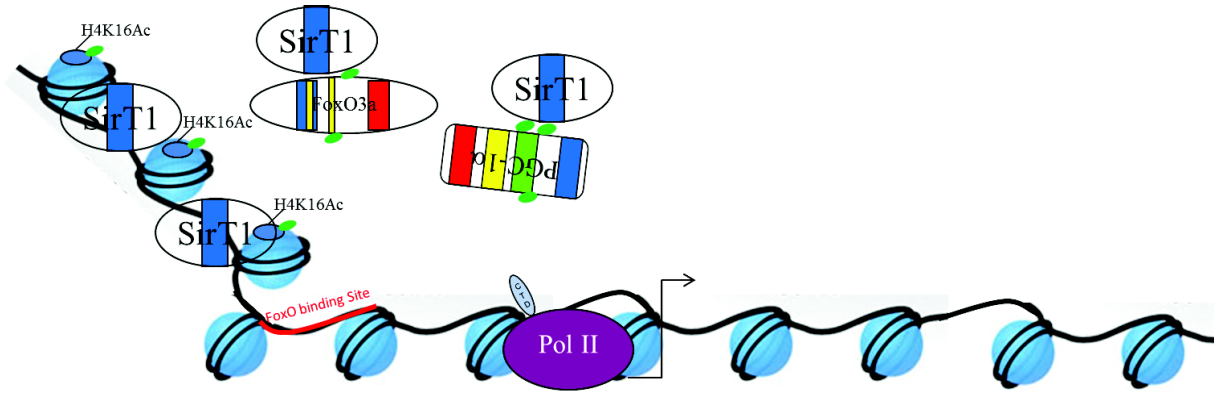

Initiation complex under serum starvation conditions

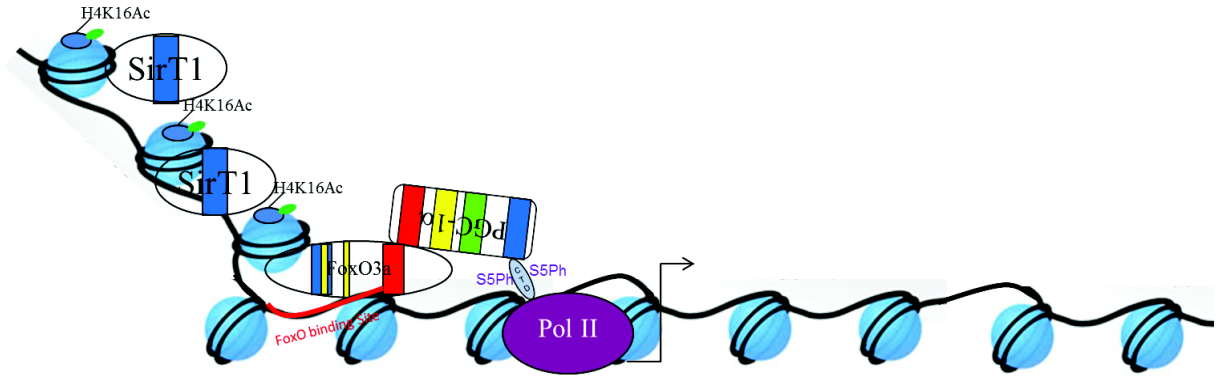

Elongation complex under serum starvation conditions

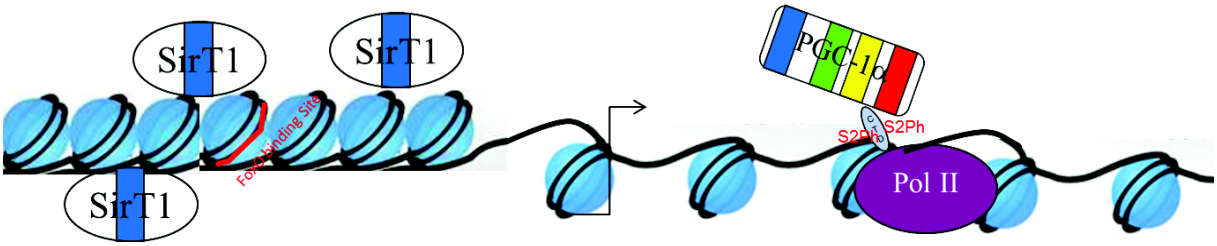

Conclusions

Conclusions

1. SirT1 regulates acetylation level, expression and stability of PGC-1α and FoxO3a in endothelial cells.
2. Under oxidative stress conditions SirT1 associates to FoxO3a and PGC-1α to form a ternary complex.
3. The ternary complex associates to specific sites on the promoter regions of the regulated genes.
4. SirT1 incorparation results in deacetylation of specific promoter regions.
5. This complex promotes the formation of the RNA PII elongation complex and thereupon gene expression of the target genes under oxidative stress conditions.

6. In the absence of PGC-1α RRM domain, expression of some PGC-1α reguated detoxification enzymes is decreased.
7. Analysis at the genomic level indicate selective gene transcription when PGC-1α RRM domain is absent.
8. PGC-1α RRM domain is binding to RNA on specifc sequences.
9. The estimated size of PGC-1α RRM domain bound RNAs is about 40 nucleotides after being isolated via the HITS-CLIP method.
10. The bound and isolated RNAs preferably locate in intronic regions.

Conclusiones

11. SirT1 regula el estado de acetilación, la expresión y la estabilidad de PGC-1α y de FoxO3a en células endoteliales.
12. En situaciones de estrés oxidativo SirT1 forma con FoxO3a y PGC-1α un complejo terciario.
13. El complejo se incorpora a las regiones promotoras de los genes regulados.
14. La incorporación de SirT1 tiene como resultado la desacetilación de la región promotora.
15. Este complejo facilita la formación del complejo de elongación y por tanto la expresión del gen diana en situaciones de estrés oxidativo.

16. En ausencia del dominio RRM de PGC-1α la expresión de algunas de las enzimas de detoxificación reguladas por PGC-1α esta disminuida.
17. El análisis a nivel genómico indica una selección de transcritos diferente en ausencia del RRM de PGC-1α.
18. El dominio RRM de PGC-1α se une a RNA de manera específica de secuencia.
19. El tamaño estimado de los RNA ligados de PGC-1α aislados por HITS-CLIP es de próximamente 40 nucleótidos.
20. Los RNA ligados identificados se localizan preferentemente en regiones intrónicas.

Bibliography

Akoulitchev S *et al.* (1995). Akoulitchev S, Mäkelä TP, Weinberg RA, Reinberg D. Requirement for TFIIH kinase activity in transcription by RNA polymerase II. *Nature*. *377*(6549):557-60.

Alcendor RR et al. (2007). Alcendor RR, Gao S, Zhai P, Zablocki D, Holle E, Yu X, Tian B, Wagner T, Vatner SF, Sadoshima J. Sirt1 regulates aging and resistance to oxidative stress in the heart. *Circ Res.* **100**(10):1512-21.

Andersson U and Scarpulla RC (2001). Pgc-1-related coactivator, a novel, serum-inducible coactivator of nuclear respiratory factor 1-dependent transcription in mammalian cells. *Mol Cell Biol*. **21**(11):3738-49.

Arndt KM and Kane CM (2003). Running with RNA polymerase: eukaryotic transcript elongation. *Trends Genet.* **19**(10):543-50.

Bahjat FR et *al.* (2000). Bahjat FR, Dharnidharka VR, Fukuzuka K, Morel L, Crawford JM, Clare-Salzler MJ, Moldawer LL. Reduced susceptibility of nonobese diabetic mice to TNF-alpha and D-galactosamine-mediated hepatocellular apoptosis and lethality. *J Immunol.* **165**(11):6559-67.

Blackledge NP and Klose R (2011). CpG island chromatin: a platform for gene regulation. *Epigenetics* **6**(2):147-52.

Boeger H *et al.* (2004). Boeger H, Griesenbeck J, Strattan JS, Kornberg RD. Removal of promoter nucleosomes by disassembly rather than sliding in vivo. *Mol Cell.* **14**(5):667-73.

Boehm AK *et al.* (2003). Boehm AK, Saunders A, Werner J, Lis JT. Transcription factor and polymerase recruitment, modification, and movement on dhsp70 in vivo in the minutes following heat shock. *Mol Cell Biol.* **23**(21):7628-37.

Bolstad BM et *al.* (2003). Bolstad BM, Irizarry RA, Astrand M, Speed TP. A comparison of normalization methods for high density oligonucleotide array data based on variance and bias. *Bioinformatics.* **19**(2):185-93.

Bondarenko VA *et al.* (2006). Bondarenko VA, Steele LM, Ujvári A, Gaykalova DA, Kulaeva OI, Polikanov YS, Luse DS, Studitsky VM. Nucleosomes can form a polar barrier to transcript elongation by RNA polymerase II. *Mol Cell*. **24**(3):469-79.

Borniquel S et *al*. (2006). Borniquel S, Valle I, Cadenas S, Lamas S, Monsalve M. Nitric oxide regulates mitochondrial oxidative stress protection via the transcriptional coactivator PGC-1alpha. *FASEB J*. **20**(11):1889-91.

Bregman DB *et al.* (2000). Bregman DB, Pestell RG, Kidd VJ. Cell cycle regulation and RNA polymerase II. *Front Biosci*. **5**:D244-57.

Brenner S *et al.* (1961). Brenner S, Jacob F, Meselson M. An unstable intermediate carrying information from genes to ribosomes for protein synthesis. *Nature* **190**: 576-581.

Brownell JE *et al* (1996). Brownell JE, Zhou J, Ranalli T, Kobayashi R, Edmondson DG, Roth SY, Allis CD. Tetrahymena histone acetyltransferase A: A homolog to yeast Gcn5p linking histone acetylation to gene activation. *Cell* 84: 843–851.

Brueckner F *et al.* (2008). Brueckner F, Armache KJ, Cheung A, Damsma GE, Kettenberger H, Lehman n E, Sydow J, Cramer P. Structure–function studies of the RNA polymerase II elongation complex. *Acta Crystallogr D Biol Crystallogr.* **65**(Pt 2): 112–120.

Brunet A *et al.* (2004). Brunet A, Sweeney LB, Sturgill JF, Chua KF, Greer PL, Lin Y, Tran H, Ross SE, Mostoslavsky R, Cohen HY, Hu LS, Cheng HL, Jedrychowski MP, Gygi SP, Sinclair DA, Alt FW, Greenberg ME. Stress-dependent regulation of FOXO transcription factors by the SIRT1 deacetylase. *Science*. **303**(5666):2011-5.

Butler JE and Kadonaga JT (2002). The RNA polymerase II core promoter: a key component in the regulation of gene expression. *Genes Dev.* **16**(20):2583-92.

Carmeliet P and Jain RK (2000). Angiogenesis in cancer and other diseases. *Nature*. 407(6801):249-57.

Chen LI *et al*. (1994). Chen LI, Nishinaka T, Kwan K, Kitabayashi I, Yokoyama K, Fu YH, Grünwald S, Chiu R. The retinoblastoma gene product RB stimulates Sp1-mediated transcription by liberating Sp1 from a negative regulator. *Mol Cell Biol*. **14**(7):4380-9.

Chen Y *et al.* (2011). Chen Y, Yang M, Deng J, Chen X, Ye Y, Zhu L, Liu J, Ye H, Shen Y, Li Y, Rao EJ, Fushimi K, Zhou X, Bigio EH, Mesulam M, Xu Q, Wu JY. Expression of human FUS protein in Drosophila leads to progressive neurodegeneration. *Protein Cell.* **2**(6):477-86.

Cho EJ *et al.* (2001). Cho EJ, Kobor MS, Kim M, Greenblatt J, Buratowski S. Opposing effects of Ctk1 kinase and Fcp1 phosphatase at Ser 2 of the RNA polymerase II C-terminal domain. *Genes Dev.* **15**(24):3319-29.

Choi YD and Dreyfuss G (1984). Isolation of the heterogeneous nuclear RNA-ribonucleoprotein complex (hnRNP): a unique supramolecular assembly. *Proc Natl Acad Sci U S A.* **81**(23):7471-5.

Chuang JC and Jones PA (2007). Epigenetics and microRNAs. *Pediatr Res.* **61**(5 Pt 2):24R-29R.

Clayton AL *et al.* (2001). Clayton AL, Hazzalin CA, Mahadevan LC. Enhanced histone acetylation and transcription: A dynamic perspective. *Mol. Cell***. 23**:289-296.

Comoglio F *et al.* (2015). Comoglio F, Sievers C, Paro R. Sensitive and highly resolved identification of RNA-protein interaction sites in PAR-CLIP data. *BMC Bioinformatics.* **16**:32.

Cosma MP *et al*. (1999). Cosma MP, Tanaka T, Nasmyth K. Ordered recruitment of transcription and chromatin remodeling factors to a cell cycle- and developmentally regulated promoter. *Cell.* **97**(3):299-311.

Costa FF (2008). Non-coding RNAs, epigenetics and complexity. *Gene*. **410**(1):9-17.

Cramer P (2002). Common structural features of nucleic acid polymerases. *Bioessays*. **24**(8):724-9.

Crick F (1970). Central dogma of molecular biology. *Nature* **227** (5258):561-3.

Czubryt MP *et al.* (2003). Czubryt MP, McAnally J, Fishman GI, Olson EN. Regulation of peroxisome proliferator-activated receptor gamma coactivator 1 alpha (PGC-1 alpha) and mitochondrial function by MEF2 and HDAC5. *Proc Natl Acad Sci U S A.* **100**(4):1711-6.

Daitoku H *et al.* (2004). Daitoku H, Hatta M, Matsuzaki H, Aratani S, Ohshima T, Miyagishi M, Nakajima T, Fukamizu A. Silent information regulator 2 potentiates Foxo1-mediated transcription through its deacetylase activity. *Proc Natl Acad Sci U S A*. **101**(27):10042-7.

Dalma-Weiszhausz DD *et al.* (2002). Dalma-Weiszhausz DD, Chicurel ME, Gingeras TR. Microarrays and genetic epidemiology: a multipurpose tool for a multifaceted field. *Genet Epidemiol*. **23**(1):4-20.

de Ruijter AJ *et al.* (2003). de Ruijter AJ, van Gennip AH, Caron HN, Kemp S, van Kuilenburg AB. Histone deacetylases (HDACs): characterization of the classical HDAC family*. Biochem J.* **370**(Pt 3):737-49.

Deaton AM and Bird A (2011). CpG islands and the regulation of transcription. *Genes Dev* **25**(10):1010-22.

Delerive P *et al*. (2002). Delerive P, Wu Y, Burris TP, Chin WW, Suen CS. PGC-1 functions as a transcriptional coactivator for the retinoid X receptors. *J Biol Chem*. **277**(6):3913-7.

Denu JM (2005). The Sir 2 family of protein deacetylases. *Curr Opin Chem Biol.* **9**(5):431-40.

Dimmeler S (2011). An interview with Stefanie Dimmeler, Chief Editor. *EMBO Mol Med*. **3**(4):181-2.

Draker R *et al*. (2011). Draker R, Sarcinella E and Cheung P. USP10 deubiquitylates the histone variant H2A.Z and both are required for androgen receptor-mediated gene activation. *Nucleic Acids Res.* **39**(9): 3529–3542.

Eberhardy SR and Farnham PJ (2002). Myc recruits P-TEFb to mediate the final step in the transcriptional activation of the cad promoter. *J Biol Chem.* **277**(42):40156-62.

Ek J *et al*. (2001). Ek J, Andersen G, Urhammer SA, Gaede PH, Drivsholm T, Borch-Johnsen K, Hansen T, Pedersen O. Mutation analysis of peroxisome proliferator-activated receptor-gamma coactivator-1 (PGC-1) and relationships of identified amino acid polymorphisms to Type II diabetes mellitus. *Diabetologia.* **44**(12):2220-6.

Ekwall K (2005). Genome-wide analysis of HDAC function. *Trends Genet.* **21**(11):608-15.

Esnault C *et al*. (2008). Esnault C, Ghavi-Helm Y, Brun S, Soutourina J, Van Berkum N, Boschiero C, Holstege F, Werner M. Mediator-dependent recruitment of TFIIH modules in preinitiation complex. *Mol Cell*. **31**(3):337-46.

Esterbauer H *et al.* (1999). Esterbauer H, Oberkofler H, Krempler F, Patsch W. Human peroxisome proliferator activated receptor gamma coactivator 1 (PPARGC1) gene: cDNA sequence, genomic organization, chromosomal localization, and tissue expression. *Genomics.* **62**(1):98-102.

Farthing CR *et al***.** (2008). Farthing CR, Ficz G, Ng RK, Chan CR, Andrews S, Dean W, Hemberger M, Reik W. Global mapping of DNA methylation in mouse promoters reveals epigenetic reprogramming of pluripotency genes. *PLoS Genet* **4**(6):e1000116.

Felsenfeld G and Groudine M (2003). Controlling the double helix. *Nature* **421**(6921):448-53.

Finch JT and Klug A (1976). Solenoidal model for superstructure in chromatin. *Proc Natl Acad Sci USA.* **73**(6):1897-901.

Frye RA (1999). Characterization of five human cDNAs with homology to the yeast SIR2 gene: Sir2-like proteins (sirtuins) metabolize NAD and may have protein ADP-ribosyltransferase activity. *Biochem Biophys Res Commun.* **260**(1):273-9.

Fuda NJ *et al.* (2009). Fuda NJ, Ardehali MB, Lis JT. Defining mechanisms that regulate RNA polymerase II transcription *in vivo. Nature.* **461**(7261): 186–192.

Gerstberger S *et al.* (2014). Gerstberger S, Hafner M, Ascano M, Tuschl T. Evolutionary conservation and expression of human RNA-binding proteins and their role in human genetic disease. *Adv Exp Med Biol.* **825**:1-55.

Ghildiyal M and Zamore PD (2009). Small silencing RNAs: an expanding universe. *Nat Rev Genet.* **10**(2):94-108.

Giannakou ME and Partridge L (2004). The interaction between FOXO and SIRT1: tipping the balance towards survival. *Trends Cell Biol.* **14**(8):408-12.

Gilbert N and Ramsahoye B (2005). The relationship between chromatin structure and transcriptional activity in mammalian genomes. Brief Funct Genomic *Proteomic*. **4**(2):129-42.

Glass CK and Rosenfeld MG (2000). The coregulator exchange in transcriptional functions of nuclear receptors. *Genes Dev.* **14**(2):121-41.

Goodrich JA and Tjian R (1994). Transcription factors IIE and IIH and ATP hydrolysis direct promoter clearance by RNA polymerase II. *Cell.* **77**(1):145-56.

Goto M *et al.* (2000). Goto M, Terada S, Kato M, Katoh M, Yokozeki T, Tabata I, Shimokawa T. cDNA Cloning and mRNA analysis of PGC-1 in epitrochlearis muscle in swimming-exercised rats. *Biochem Biophys Res Commun.* **274**(2):350-4.

Graveley BR (2000). Sorting out the complexity of SR protein functions. *RNA*. **6**(9):1197-211.

Greenberg JR (1979). Ultraviolet light-induced crosslinking of mRNA to proteins. *Nucleic Acids Res*. **6**(2):715-32.

Grewal Sl and Moazed D (2003). Heterochromatin and epigenetic control of gene expression. *Science* **301**(5634):798-802.

Guil S and Caceres JF (2007). The multifunctional RNA-binding protein hnRNP A1 is required for processing of miR-18a. *Nat Struct Mol Biol*. **14**(7):591-6.

Gutierrez-Marcos JF and Dickinson HG (2012). Epigenetic reprogramming in plant reproductive lineages. *Plant Cell Physiol.* **53**(5):817-23.

Hafner M et *al*. (2008). Hafner M, Landgraf P, Ludwig J, Rice A, Ojo T, Lin C, Holoch D, Lim C, Tuschl T. Identification of microRNAs and other small regulatory RNAs using cDNA library sequencing. *Methods.* **44**(1):3-12.

Hafner M *et al.* (2010). Hafner M, Landthaler M, Burger L, Khorshid M, Hausser J, Berninger P, Rothballer A, Ascano M Jr, Jungkamp AC, Munschauer M, Ulrich A, Wardle GS, Dewell S, Zavolan M, Tuschl T. Transcriptome-wide identification of RNA-binding protein and microRNA target sites by PAR-CLIP. *Cell.* **141**(1):129-41.

Hahn S (2004). Structure and mechanism of the RNA polymerase II transcription machinery. *Nat Struct Mol Biol.* **11**(5):394-403.

Hall BD and Spiegelman S (1961). Sequence complementarity of T2-DNA and T2-specific RNA. *Proc Natl Acad Sci U S A.* **47**:137-63.

Hampsey M (1998). Molecular genetics of the RNA polymerase II general transcriptional machinery. *Microbiol Mol Biol Rev*. **62**(2):465-503.

Handel AE *et al***.** (2010). Handel AE, Ebers GC, Ramagopalan SV. Epigenetics: molecular mechanisms and implications for disease. *Trends Mol Med*. 2010 Jan;**16**(1):7-16.

Handschin C and Meyer UA (2003). Induction of drug metabolism: the role of nuclear receptors. *Pharmacol Rev*. **55**(4):649-73.

Handschin C *et al.* (2003). Handschin C, Podvinec M, Meyer UA. In silico approaches, and in vitro and in vivo experiments to predict induction of drug metabolism. *Drug News Perspect.* **16**(7):423-34.

Hara K *et al*. (2002). Hara K, Tobe K, Okada T, Kadowaki H, Akanuma Y, Ito C, Kimura S, Kadowaki T. A genetic variation in the PGC-1 gene could confer insulin resistance and susceptibility to Type II diabetes*. Diabetologia.* **45**(5):740-3.

Hartzog GA *et al.* (1998). Hartzog GA, Wada T, Handa H, Winston F. Evidence that Spt4, Spt5, and Spt6 control transcription elongation by RNA polymerase II in Saccharomyces cerevisiae. *Genes Dev.* **12**(3):357-69.

Hasegawa K et al. (2008). Hasegawa K, Wakino S, Yoshioka K, Tatematsu S, Hara Y, Minakuchi H, Washida N, Tokuyama H, Hayashi K, Itoh H. Sirt1 protects against oxidative stress-induced renal tubular cell apoptosis by the bidirectional regulation of catalase expression. *Biochem Biophys Res Commun*. **372**(1):51-6.

Hastings ML and Krainer AR (2001). Functions of SR proteins in the U12-dependent AT-AC pre-mRNA splicing pathway. *RNA*. **7**(3):471-82.

Hawkins GA *et al.* (2002). Hawkins GA, Cramer SD, Zheng SL, Isaacs SD, Wiley KE, Chang BL, Bleecker ER, Walsh PC, Meyers DA, Isaacs WB, Xu J. Sequence variants in the human 25-hydroxyvitamin D3 1-alpha-hydroxylase (CYP27B1) gene are not associated with prostate cancer risk. *Prostate*. **53**(3):175-8.

Herzig S *et al.* (2001). Herzig S, Long F, Jhala US, Hedrick S, Quinn R, Bauer A, Rudolph D, Schutz G, Yoon C, Puigserver P, Spiegelman B, Montminy M. CREB regulates hepatic gluconeogenesis through the coactivator PGC-1. *Nature*. **413**(6852):179-83.

Hewagama A and Richardson B (2009). The genetics and epigenetics of autoimmune diseases. *J Autoimmun.* **33**(1):3-11.

Hirose Y and Manley JL (2000). RNA polymerase II and the integration of nuclear events. *Genes Dev.* **14**(12):1415-29.

Hirose Y and Ohkuma Y (2007). Phosphorylation of the C-terminal domain of RNA polymerase II plays central roles in the integrated events of eucaryotic gene expression*. J Biochem.* **141**(5):601-8.

Hirst M and Marra MA (2009). Epigenetics and human disease*. Int J Biochem Cell Biol.* **41**(1):136-46.

Holstege FC *et al.* (1996). Holstege FC, van der Vliet PC, Timmers HT. Opening of an RNA polymerase II promoter occurs in two distinct steps and requires the basal transcription factors IIE and IIH. *EMBO J.* **15**(7):1666-77.

Hori YS et al. (2013). Hori YS, Kuno A, Hosoda R, Horio Y. Regulation of FOXOs and p53 by SIRT1 modulators under oxidative stress. *PLoS One.* **8**(9):e73875.

Horvath HC *et al* (2010). Horváth HC, Khabir Z, Nittke T, Gruber S, Speer G, Manhardt T, Bonner E, Kallay E. CYP24A1 splice variants-implications for the antitumorigenic actions of 1,25-(OH)2D3 in colorectal cancer. *J Steroid Biochem Mol Biol.* **121**(1-2):76-9.

Howitz KT *et al.* (2003). Howitz KT, Bitterman KJ, Cohen HY, Lamming DW, Lavu S, Wood JG, Zipkin RE, Chung P, Kisielewski A, Zhang LL, Scherer B, Sinclair DA. Small molecule activators of sirtuins extend Saccharomyces cerevisiae lifespan. *Nature.* **425**(6954):191-6.

Hubbert C *et al.* (2002). Hubbert C, Guardiola A, Shao R, Kawaguchi Y, Ito A, Nixon A, Yoshida M, Wang XF, Yao TP. HDAC6 is a microtubule-associated deacetylase. *Nature*. **417**(6887):455-8.

Hurwitz J *et al.* (1961). Hurwitz J, Furth JJ, Malamy M, Alexander M. The role of desoxyribonucleic acid in ribonucleic acid synthesis ,III. The inhibition of the enzymatice synthesis of ribonucleic acid and deoxyribuncleic acid by actinomycin D and proflavin. *Proc Natl Acad Sci U S A.* **48**(7): 1222–1230.

Huss JM and Kelly DP (2004). Nuclear receptor signaling and cardiac energetics. *Circ. Res*. **95**:568–78.

Iborra FJ *et al.* (1996). Iborra FJ, Pombo A, Jackson DA, Cook PR. Active RNA polymerases are localized within discrete transcription "factories' in human nuclei. *J Cell Sci.***109** (Pt 6):1427-36.

Imbalzano AN et al. (1994). Imbalzano AN, Kwon H, Green MR, Kingston RE. Facilitated binding of TATA-binding protein to nucleosomal DNA. *Nature.* **370**(6489):481-5.

Islam S *et al*. (2011). Islam S, Kjällquist U, Moliner A, Zajac P, Fan JB, Lönnerberg P, Linnarsson S. Characterization of the single-cell transcriptional landscape by highly multiplex RNA-seq. *Genome Res.* **21**(7): 1160–1167.

Jacob F and Monod J (1961). Genetic regulatory mechanisms in the synthesis of proteins. *J Mol Biol* **3**:318-56.

Jacobson MK and Jacobson EL (1999). Discovering new ADP-ribose polymer cycles: protecting the genome and more. Trends Biochem Sci. **24**(11):415-7.

Janzen WP *et al*. (2010). Janzen WP, Wigle TJ, Jin J, Frye SV. Epigenetics: Tools and Technologies. *Drug Discov Today Technol.* **7**(1):e59-e65.

Jensen KB and Darnell RB (2008). CLIP: Crosslinking and ImmunoPrecipitation of In Vivo RNA Targets of RNA-Binding Proteins. *Methods Mol Biol*. **488**: 85–98.

Jenuwein T and Allis CD (2001). Translating the histone code. *Science.* **293**(5532):1074-80.

Jiang Y and Gralla JD (1993). Uncoupling of initiation and reinitiation rates during HeLa RNA polymerase II transcription in vitro. *Mol Cell Biol*. **13**(8):4572-7.

Jimeno S *et al.* (2002). Jimeno S, Rondón AG, Luna R, Aguilera A. The yeast THO complex and mRNA export factors link RNA metabolism with transcription and genome instability. *EMBO J.* **21**(13):3526-35.

Jing E et al. (2007). Jing E, Gesta S, Kahn CR. SIRT2 regulates adipocyte differentiation through FoxO1 acetylation/deacetylation. *Cell Metab.* **6**(2):105-14.

Jona G *et al.* (2001). Jona G, Wittschieben BO, Svejstrup JQ, Gileadi O. Involvement of yeast carboxy-terminal domain kinase I (CTDK-I) in transcription elongation in vivo. *Gene* 267(1):31-6.

Kang J *et al.* (2005). Kang J, Chen J, Shi Y, Jia J, Wang Z. Histone hypoacetylation is involved in 1,10-phenanthroline-Cu^{2+}-induced human hepatoma cell apoptosis. *J Biol Inorg Chem*. **10**(2):190-8.

Kelley RL and Kuroda MI (2000). Noncoding RNA genes in dosage compensation and imprinting. *Cell*. **103**(1):9-12.

Keogh MC *et al.* (2003). Keogh MC, Podolny V, Buratowski S. Bur1 kinase is required for efficient transcription elongation by RNA polymerase II. *Mol Cell Biol.* **23**(19):7005-18.

Kim MJ *et al*. (2009). Kim MJ, Ahn K, Park SH, Kang HJ, Jang BG, Oh SJ, Oh SM, Jeong YJ, Heo JI, Suh JG, Lim SS, Ko YJ, Huh SO, Kim SC, Park JB, Kim J, Kim JI, Jo SA, Lee JY. SIRT1 regulates tyrosine hydroxylase expression and differentiation of neuroblastoma cells via FOXO3a. *FEBS Lett.* **583**(7):1183-8.

Kim TK *et al.* (2000). Kim TK, Ebright RH, Reinberg D. Mechanism of ATP-dependent promoter melting by transcription factor IIH. *Science.* **288**(5470):1418-22.

Kireeva ML *et al.* (2000). Kireeva ML, Komissarova N, Kashlev M. Overextended RNA:DNA hybrid as a negative regulator of RNA polymerase II processivity. *J Mol Biol.* **299**(2):325-35.

Kireeva ML *et al.* (2000). Kireeva ML, Komissarova N, Waugh DS, Kashlev M. The 8-nucleotide-long RNA:DNA hybrid is a primary stability determinant of the RNA polymerase II elongation complex. *J Biol Chem.* **275**(9):6530-6.

Kireeva ML *et al.* (2005). Kireeva ML, Hancock B, Cremona GH, Walter W, Studitsky VM, Kashlev M. Nature of the nucleosomal barrier to RNA polymerase II. *Mol Cell.* **18**(1):97-108.

Klein AM *et al.* (2015). Klein AM, Mazutis L, Akartuna I, Tallapragada N, Veres A, Li V, Peshkin L, Weitz DA, Kirschner MW. Droplet barcoding for single-cell transcriptomics applied to embryonic stem cells. *Cell.* **161**(5):1187-201.

Knutti D *et al.* (2000). Knutti D, Kaul A, Kralli A. A tissue-specific coactivator of steroid receptors, identified in a functional genetic screen. *Mol Cell Biol.* **20**(7):2411-22.

Knutti D *et al.* (2001). Knutti D, Kressler D, Kralli A. Regulation of the transcriptional coactivator PGC-1 via MAPK-sensitive interaction with a repressor. *Proc Natl Acad Sci U S A*. **98**(17):9713-8.

Kobayashi Y *et al.* (2005). Kobayashi Y, Furukawa-Hibi Y, Chen C, Horio Y, Isobe K, Ikeda K, Motoyama N. SIRT1 is critical regulator of FOXO-mediated transcription in response to oxidative stress. *Int J Mol Med.* **16**(2):237-43.

Konno Y *et al.* (2008). Konno Y, Negishi M, Kodama S. The roles of nuclear receptors CAR and PXR in hepatic energy metabolism. *Drug Metab Pharmacokinet.* **23**(1):8-13.

Konno Y *et al.* (2009). Konno Y, Kodama S, Moore R, Kamiya N, Negishi M. Nuclear xenobiotic receptor pregnane X receptor locks corepressor silencing mediator for retinoid and thyroid hormone receptors (SMRT) onto the CYP24A1 promoter to attenuate vitamin D3 activation. *Mol Pharmacol.* **75**(2):265-71.

Kornberg RD (1974). Chromatin structure: a repeating unit of histones and DNA. *Nature* **184** (4139): 868-71.

Kressler D *et al*. (2002). Kressler D, Schreiber SN, Knutti D, Kralli A. The PGC-1-related protein PERC is a selective coactivator of estrogen receptor alpha*. J Biol Chem.* **277**(16):13918-25.

Kuo MH *et al*. (1996). Kuo MH, Brownell JE, Sobel RE, Ranalli TA, Cook RG, Edmondson DG, Roth SY, Allis, CD. Transcription-associated acetylation of histones H3 and H4 at specific lysines by Gcn5p. *Nature* 383: 269–272.

Kwon H *et al.* (1994). Kwon H, Imbalzano AN, Khavari PA, Green MR, Kingston RE. Nucleosome disruption and enhancement of activator binding by a human SW1/SNF complex. *Nature.* **370**:477-481.

Lamas S et *al*. (1991). Lamas S, Michel T, Brenner BM, Marsden PA. Nitric oxide synthesis in endothelial cells: evidence for a pathway inducible by TNF-alpha. *Am J Physiol*. **261**(4 Pt 1):C634-41.

Lassar AB *et al.* (1983). Lassar AB, Martin PL, Roeder RG. Transcription of class III genes: formation of preinitiation complexes. *Science.* **222**(4625):740-8.

Lehman JJ *et al.* (2000). Lehman JJ, Barger PM, Kovacs A, Saffitz JE, Medeiros DM, Kelly DP. Peroxisome proliferator-activated receptor gamma coactivator-1 promotes cardiac mitochondrial biogenesis. *J Clin Invest.* **106**(7):847-56.

Li CF *et al.* (2006). Li CF, Pontes O, El-Shami M, Henderson IR, Bernatavichute YV, Chan SW, Lagrange T, Pikaard CS, Jacobsen SE. An ARGONAUTE4-containing nuclear processing center colocalized with Cajal bodies in Arabidopsis thaliana. *Cell.* **126**(1):93-106.

Licatalosi DD *et al.* (2008). Licatalosi DD, Mele A, Fak JJ, Ule J, Kayikci M, Chi SW, Clark TA, Schweitzer AC, Blume JE, Wang X, Darnell JC, Darnell RB. HITS-CLIP yields genome-wide insights into brain alternative RNA processing. *Nature*. **456**(7221):464-9.

Lin J *et al*. (2002). Lin J, Wu H, Tarr PT, Zhang CY, Wu Z, Boss O, Michael LF, Puigserver P, Isotani E, Olson EN, Lowell BB, Bassel-Duby R, Spiegelman BM. Transcriptional co-activator PGC-1 alpha drives the formation of slow-twitch muscle fibres. *Nature*. **418**(6899):797-801.

Lin J *et al.* (2004). Lin J, Wu PH, Tarr PT, Lindenberg KS, St-Pierre J, Zhang CY, Mootha VK, Jäger S, Vianna CR, Reznick RM, Cui L, Manieri M, Donovan MX, Wu Z, Cooper MP, Fan MC, Rohas LM, Zavacki AM, Cinti S, Shulman GI, Lowell BB, Krainc D, Spiegelman BM. Defects in adaptive energy metabolism with CNS-linked hyperactivity in PGC-1alpha null mice. *Cell*. **119**(1):121-35.

Lin J *et al.* (2005). Lin J, Handschin C, Spiegelman BM. Metabolic control through the PGC-1 family of transcription coactivators. *Cell Metab.* **1**(6):361-70.

Lin PS *et al.* (2003). Lin PS, Tremeau-Bravard A, Dahmus ME. The repetitive C-terminal domain of RNA polymerase II: Multiple conformational states drive the transcription cycle. *The chemical records* **3** (4):235-245.

Lin SJ and Guarente L (2003). Nicotinamide adenine dinucleotide, a metabolic regulator of transcription, longevity and disease. *Curr Opin Cell Biol.* **15**(2):241-6.

Lis JT *et al.* (2000). Lis JT, Mason P, Peng J, Price DH, Werner J. P-TEFb kinase recruitment and function at heat shock loci. *Genes Dev.* **14**(7):792-803.

Liszt G *et al.* (2005). Liszt G, Ford E, Kurtev M, Guarente L. Mouse Sir2 homolog SIRT6 is a nuclear ADP-ribosyltransferase. *J Biol Chem*. **280**(22):21313-20.

Lopez-Ongil S et *al*. (1996). López-Ongil S, Saura M, Rodríguez-Puyol D, Rodríguez-Puyol M, Lamas S. Regulation of endothelial NO synthase expression by cyclosporin A in bovine aortic endothelial cells. *Am J Physiol*. **271**(3 Pt 2):H1072-8.

Lovén J *et al.* (2012). Lovén J, Orlando DA, Sigova AA, Lin CY, Rahl PB, Burge CB, Levens DL, Lee TI, Young RA. Revisiting global gene expression analysis. *Cell*. **151**(3):476-82.

Mangelsdorf DJ et *al*. (1990). Mangelsdorf DJ, Ong ES, Dyck JA, Evans RM. Nuclear receptor that identifies a novel retinoic acid response pathway. *Nature.* 345(6272):224-9.

Martin C and Zhang Y (2005). The diverse functions of histone lysine methylation. *Nat Rev Mol Cell Biol.* **6**(11):838-49.

Matsuzaki H *et al.* (2005). Matsuzaki H, Daitoku H, Hatta M, Aoyama H, Yoshimochi K, Fukamizu A. Acetylation of Foxo1 alters its DNA-binding ability and sensitivity to phosphorylation. *Proc Natl Acad Sci U S A.* **102**(32):11278-83.

McKenna NJ *et al*. (1999). McKenna NJ, Lanz RB, O'Malley. BW Nuclear receptor coregulators: cellular and molecular biology. *Endocr Rev.* **20**(3):321-44.

Meissner A *et al***.** (2008). Meissner A, Mikkelsen TS, Gu H, Wernig M, Hanna J, Sivachenko A, Zhang X, Bernstein BE, Nusbaum C, Jaffe DB, Gnirke A, Jaenisch R, Lander ES. Genome-scale DNA methylation maps of pluripotent and differentiated cells. *Nature* **454**(7205):766-70.

Michael LF *et al.* (2001). Michael LF, Wu Z, Cheatham RB, Puigserver P, Adelmant G, Lehman JJ, Kelly DP, Spiegelman BM. Restoration of insulin-sensitive glucose transporter (GLUT4) gene expression in muscle cells by the transcriptional coactivator PGC-1. *Proc Natl Acad Sci U S A.* **98**(7):3820-5.

Mohn F *et al.* (2008). Mohn F, Weber M, Rebhan M, Roloff TC, Richter J, Stadler MB, Bibel M, Schübeler D. Lineage-specific polycomb targets and de novo DNA methylation define restriction and potential of neuronal progenitors. *Mol Cell.* **30**(6):755-66.

Monsalve M *et al.* (2000). Monsalve M, Wu Z, Adelmant G, Puigserver P, Fan M, Spiegelman BM. Direct coupling of transcription and mRNA processing through the thermogenic coactivator PGC-1. *Mol Cell.* **6**(2):307-16.

Mootha VK *et al.* (2003). Mootha VK, Lindgren CM, Eriksson KF, Subramanian A, Sihag S, Lehar J, Puigserver P, Carlsson E, Ridderstråle M, Laurila E, Houstis N, Daly MJ, Patterson N, Mesirov JP, Golub TR, Tamayo P, Spiegelman B, Lander ES, Hirschhorn JN, Altshuler D, Groop LC. PGC-1alpha-responsive genes involved in oxidative phosphorylation are coordinately downregulated in human diabetes. *Nat Genet.* **34**(3):267-73.

Moyes CD and Hood DA (2003). Origins and consequences of mitochondrial variation in vertebrate muscle. *Annu Rev Physiol.* **65**:177-201.

Naar AM *et al.* (2001). Näär AM, Lemon BD, Tjian R. Transcriptional coactivator complexes. *Annu Rev Biochem.* **70**:475-501.

Nag MK *et al.* (1993). Nag MK, Thai TT, Ruff EA, Selvamurugan N, Kunnimalaiyaan M, Eliceiri GL. Genes for E1, E2, and E3 small nucleolar RNAs. *Proc Natl Acad Sci U S A.* **90**(19):9001-5.

Nakagawa M *et al*. (2008). Nakagawa M, Koyanagi M, Tanabe K, Takahashi K, Ichisaka T, Aoi T, Okita K, Mochiduki Y, Takizawa N, Yamanaka S. Generation of induced pluripotent stem cells without Myc from mouse and human fibroblasts. *Nat Biotechnol.* **26**(1):101-6.

Nakayama J *et al.* (2001). Nakayama J, Rice JC, Strahl BD, Allis CD, Grewal SI. Role of histone H3 lysine 9 methylation in epigenetic control of heterochromatin assembly. *Science.* **292**(5514):110-3.

Nechaev S and Adelman K (2011). Pol II waiting in the starting gates: Regulating the transition from transcription initiation into productive elongation. *Biochim Biophys Acta.* **1809**(1):34-45.

Nemoto S *et al.* (2004). Nemoto S, Fergusson MM, Finkel T. Nutrient availability regulates SIRT1 through a forkhead-dependent pathway. *Science.* **306**(5704):2105-8.

Ni Z *et al.* (2008). Ni Z, Saunders A, Fuda NJ, Yao J, Suarez JR, Webb WW, Lis JT. P-TEFb is critical for the maturation of RNA polymerase II into productive elongation in vivo. *Mol Cell Biol*. (2008) **28**(3):1161-70.

Oberkofler H *et al.* (2003). Oberkofler H, Schraml E, Krempler F, Patsch W. Potentiation of liver X receptor transcriptional activity by peroxisome-proliferator-activated receptor gamma co-activator 1 alpha. *Biochem J.* **371**(Pt 1):89-96.

Ohkuma Y (1997). Multiple functions of general transcription factors TFIIE and TFIIH in transcription: possible points of regulation by trans-acting factors. *J Biochem*. **122**(3):481-9. Review.

Okano M *et al***.** (1999). Okano M, Bell DW, Haber DA, Li E. DNA methyltransferases Dnmt3a and Dnmt3b are essential for de novo methylation and mammalian development. *Cell* **99**(3):247-57.

Olmos Y *et al.* (2009). Olmos Y, Valle I, Borniquel S, Tierrez A, Soria E, Lamas S, Monsalve M. Mutual dependence of Foxo3a and PGC-1alpha in the induction of oxidative stress genes. *J Biol Chem.* **284**(21):14476-84.

Olmos Y *et al.* (2013). Olmos Y, Sánchez-Gómez FJ, Wild B, García-Quintans N, Cabezudo S, Lamas S, Monsalve M. SirT1 regulation of antioxidant genes is dependent on the formation of a FoxO3a/PGC-1α complex. *Antioxid Redox Signal*. **19**(13):1507-21.

Oppikofer M *et al.* (2011). Oppikofer M, Kueng S, Martino F, Soeroes S, Hancock SM, Chin JW, Fischle W, Gasser SM. A dual role of H4K16 acetylation in the establishment of yeast silent chromatin*. EMBO J.* **30**(13):2610-21.

Orphanides G *et al*. (1996). Orphanides G, Lagrange T, Reinberg D. The general transcription factors of RNA polymerase II. *Genes Dev*. **10**(21):2657-83.

Orphanides G and Reinberg D (2000). RNA polymerase II elongation through chromatin. *Nature*. **407**(6803):471-5.

Orphanides G and Reinberg D (2002). A unified theory of gene expression. *Cell.* **108**(4):439-51.

Ouyang J and Gill G (2009). SUMO engages multiple corepressors to regulate chromatin structure and transcription. *Epigenetics*. **4**(7):440-4.

Pagans S *et al.* (2005). Pagans S, Pedal A, North BJ, Kaehlcke K, Marshall BL, Dorr A, Hetzer-Egger C, Henklein P, Frye R, McBurney MW, Hruby H, Jung M, Verdin E, Ott M. SIRT1 regulates HIV transcription via Tat deacetylation. *PLoS Biol.* **3**(2):e41.

Pal M and Luse DS (2003). The initiation–elongation transition: Lateral mobility of RNA in RNA polymerase II complexes is greatly reduced at +8/+9 and absent by +23. *Proc Natl Acad Sci U S A*. **100**(10): 5700–5705.

Panning B and Taatjes DJ (2008). Transcriptional regulation: it takes a village. *Mol Cell.* **31**(5):622-9.

Patti ME *et al.* (2003).Patti ME, Butte AJ, Crunkhorn S, Cusi K, Berria R, Kashyap S, Miyazaki Y, Kohane I, Costello M, Saccone R, Landaker EJ, Goldfine AB, Mun E, DeFronzo R, Finlayson J, Kahn CR, Mandarino LJ. Coordinated reduction of genes of oxidative metabolism in humans with insulin resistance and diabetes: Potential role of PGC1 and NRF1. *Proc Natl Acad Sci U S A*. **100**(14):8466-71.

Pérez-Cadahía *et al*. (2010). Pérez-Cadahía B, Drobic B, Khan P, Shivashankar CC, Davie JR. Current understanding and importance of histone phosphorylation in regulating chromatin biology. *Curr Opin Drug Discov Devel.* **13**(5):613-22.

Peterlin BM and Price DH (2006). Controlling the elongation phase of transcription with P-TEFb. *Mol Cell.* **23**(3):297-305.

Peterson CL and Laniel MA 2004. Histones and histone modifications. *Curr Biol.* **14**(14):R546-51.

Peterson CL and Workman JL (2000). Promoter targeting and chromatin remodeling by the SWI/SNF complex. *Curr Opin Genet Dev.* **10**(2):187-92.

Pfluger PT et *al*. (2008). Pfluger PT, Herranz D, Velasco-Miguel S, Serrano M, Tschöp MH. SirT1 protects against high-fat diet-induced metabolic damage. *Proc Natl Acad Sci U S A*. **105**(28):9793-8.

Plas DR and Thompson CB. Akt activation promotes degradation of tuberin and FOXO3a via the proteasome. *J Biol Chem.* **278**(14):12361-6.

Pradhan S *et al***.** (1999). Pradhan S, Bacolla A, Wells RD, Roberts RJ. Recombinant human DNA (cytosine-5) methyltransferase. I. Expression, purification, and comparison of de novo and maintenance methylation. *J Biol Chem.* **274**(46):33002-10.

Proudfoot N (2004). New perspectives on connecting messenger RNA 3' end formation to transcription. *Curr Opin Cell Biol.* **16**(3):272-8.

Proudfoot N and O'Sullivan J (2002). Polyadenylation: a tail of two complexes. *Curr Biol.* **12**(24):R855-7.

Proudfoot NJ *et al.* (2002). Proudfoot NJ, Furger A, Dye MJ. Integrating mRNA processing with transcription. *Cell*. **108**(4):501-12.

Puigserver P and Spiegelman BM (2003). Peroxisome proliferator-activated receptor-gamma coactivator 1 alpha (PGC-1 alpha): transcriptional coactivator and metabolic regulator. *Endocr. Rev*. **24**:78–90.

Puigserver P *et al.* (1998). Puigserver P, Wu Z, Park CW, Graves R, Wright M, Spiegelman BM. A cold-inducible coactivator of nuclear receptors linked to adaptive thermogenesis. Cell. 1998 Mar 20;92(6):829-39.

Puigserver P *et al.* (2001). Puigserver P, Rhee J, Lin J, Wu Z, Yoon JC, Zhang CY, Krauss S, Mootha VK, Lowell BB, Spiegelman BM. Cytokine stimulation of energy expenditure through p38 MAP kinase activation of PPAR gamma coactivator-1. *Mol Cell.* **8**(5):971-82.

Qiang L *et al.* (2010). Qiang L, Banks AS, Accili D. Uncoupling of acetylation from phosphorylation regulates FoxO1 function independent of its subcellular localization. *J Biol Chem*. **285**(35):27396-401.

Rajasethupathy P *et al*. (2009). Rajasethupathy P, Fiumara F, Sheridan R, Betel D, Puthanveettil SV, Russo JJ, Sander C, Tuschl T, Kandel E. Characterization of small RNAs in Aplysia reveals a role for miR-124 in constraining synaptic plasticity through CREB. *Neuron*. **63**(6):803-17.

Rana B et *al*. (1994). Rana B, Mischoulon D, Xie Y, Bucher NL, Farmer SR. Cell-extracellular matrix interactions can regulate the switch between growth and differentiation in rat hepatocytes: reciprocal expression of C/EBP alpha and immediate-early growth response transcription factors. *Mol Cell Biol.* **14**(9):5858-69.

Ranish JA *et al.* (1999). Ranish JA, Yudkovsky N, Hahn S. Intermediates in formation and activity of the RNA polymerase II preinitiation complex: holoenzyme recruitment and a postrecruitment role for the TATA box and TFIIB. *Genes Dev.* **13**(1):49-63.

Reed R and Magni K (2001). A new view of mRNA export: separating the wheat from the chaff. *Nat Cell Biol.* **3**(9):E201-4.

Reymond J and Segrè D (2006). The effect of oxygen on biochemical networks and the evolution of complex life. *Science*. **311**(5768):1764-7.

Richmond TJ *et al.* (1984). Richmond TJ, Finch JT, Rushton B, Rhodes D, Klug A. Structure of the nucleosome core particle at 7 A resolution. *Nature.* 311(5986):532-7.

Rodgers JT et *al*. (2005). Rodgers JT, Lerin C, Haas W, Gygi SP, Spiegelman BM, Puigserver P. Nutrient control of glucose homeostasis through a complex of PGC-1alpha and SIRT1. *Nature.* **434**(7029):113-8.

Rodgers JT *et al.* (2008). Rodgers JT, Lerin C, Gerhart-Hines Z, Puigserver P. Metabolic adaptations through the PGC-1 alpha and SIRT1 pathways. *FEBS Lett.* **582**(1):46-53.

Roeder RG *et al.* (1974). Multiple forms of deoxyribonucleic acid-dependent ribonucleic acid polymerase in Xenopus laevis. Isolation and partial characterization. *J Biol Chem.* **249**(1):241-8.

Rondon AG *et al.* (2003). Rondón AG, Jimeno S, García-Rubio M, Aguilera A. Molecular evidence that the eukaryotic THO/TREX complex is required for efficient transcription elongation. *J Biol Chem*. **278**(40):39037-43.

Roth SY *et al.* 2001. Roth SY, Denu JM, Allis CD. Histone acetyltransferases. *Annu Rev Biochem.* **70**:81-120.

Sanchez-Ramos C et *al*. (2011). Sánchez-Ramos C, Tierrez A, Fabregat-Andrés O, Wild B, Sánchez-Cabo F, Arduini A, Dopazo A, Monsalve M. PGC-1α regulates translocated in liposarcoma activity: role in oxidative stress gene expression. *Antioxid Redox Signal.* **15**(2):325-37.

Sanford JR *et al.* (2009). Sanford JR, Wang X, Mort M, Vanduyn N, Cooper DN, Mooney SD, Edenberg HJ, Liu Y. Splicing factor SFRS1 recognizes a functionally diverse landscape of RNA transcripts. *Genome Res*. **19**(3):381-94.

Sarma K and Reinberg D (2005). Histone variants meet their match. *Nat Rev Mol Cell Biol.* **6**(2):139-49.

Saunders A et al. (2006). Saunders A, Core LJ, Lis JT. Breaking barriers to transcription elongation. *Nat Rev Mol Cell Biol.* 7(8):557-67.

Schwartz LB and Roeder RG (1974). Purification and subunit structure of deoxyribonucleic acid-dependent ribonucleic acid polymerase I from the mouse myeloma, MOPC 315. *J Biol Chem.* **249**(18):5898-906.

Seila AC and Sharp PA (2008). Small RNAs tell big stories in Whistler. *Nat Cell Biol*. **10**(6):630-3.

Seila AC *et al.* (2008). Seila AC, Calabrese JM, Levine SS, Yeo GW, Rahl PB, Flynn RA, Young RA, Sharp PA. Divergent transcription from active promoters. *Science.* **322**(5909):1849-51.

Serrano M *et al.* (1997). Serrano M, Lin AW, McCurrach ME, Beach D, Lowe SW. Oncogenic ras provokes premature cell senescence associated with accumulation of p53 and p16INK4a. *Cell.* **88**(5):593-602.

Sharma VM *et al.* (2007).Sharma VM, Tomar RS, Dempsey AE, Reese JC. Histone deacetylases RPD3 and HOS2 regulate the transcriptional activation of DNA damage-inducible genes. *Mol Cell Biol.* **27**(8):3199-210.

Sigova AA *et al.* (2013). Sigova AA, Mullen AC, Molinie B, Gupta S, Orlando DA, Guenther MG, Almada AE, Lin C, Sharp PA, Giallourakis CC, Young RA. Divergent transcription of long noncoding RNA/mRNA gene pairs in embryonic stem cells. *Proc Natl Acad Sci U S A*. **110**(8):2876-81.

Sims RJ 3rd *et al.* (2003). Sims RJ 3rd, Nishioka K, Reinberg D. Histone lysine methylation: a signature for chromatin function. *Trends Genet.* **19**(11):629-39.

Sims RJ 3rd *et al.* (2004). Sims RJ 3rd, Belotserkovskaya R, Reinberg D. Elongation by RNA polymerase II: the short and long of it. *Genes Dev.* **18**(20):2437-68.

Sinha I *et al.* (2005). Sinha I, Wirén M, Ekwall K. Genome-wide patterns of histone modifications in fission yeast. *Chromosome Res.* **14**(1):95-105.

Skurk C et *al*. (2004). Skurk C, Maatz H, Kim HS, Yang J, Abid MR, Aird WC, Walsh K. The Akt-regulated forkhead transcription factor FOXO3a controls endothelial cell viability through modulation of the caspase-8 inhibitor FLIP. *J Biol Chem.* **279**(2):1513-25.

Smith CL and Peterson CL (2005). ATP-dependent chromatin remodeling*. Curr Top Dev Biol.* **65**:115-48.

Smitten AL *et al.* (2008). Smitten AL, Simon TA, Hochberg MC, Suissa S. A meta-analysis of the incidence of malignancy in adult patients with rheumatoid arthritis. *Arthritis Res Ther*. **10**(2):R45.

Smyth GK (2004). Linear models and empirical bayes methods for assessing differential expression in microarray experiments. *Stat Appl Genet Mol Biol.* **3**:Article3.

Stiller JW and Hall BD (2002). Evolution of the RNA polymerase II C-terminal domain. *Proc Natl Acad Sci U S A.* **99**(9):6091-6.

St-Pierre J *et al*. (2003). St-Pierre J, Lin J, Krauss S, Tarr PT, Yang R, Newgard CB, Spiegelman BM. Bioenergetic analysis of peroxisome proliferator-activated receptor gamma coactivators 1alpha and 1beta (PGC-1alpha and PGC-1beta) in muscle cells. *J Biol Chem.* **278**(29):26597-603.

Strahl BD and Allis CD (2000). The language of covalent histone modifications. *Nature.* **403**(6765):41-5.

Strasser K *et al.* (2002) Strässer K, Masuda S, Mason P, Pfannstiel J, Oppizzi M, Rodriguez-Navarro S, Rondón AG, Aguilera A, Struhl K, Reed R, Hurt E. TREX is a conserved complex coupling transcription with messenger RNA export. *Nature.* **417**(6886):304-8. Epub 2002 Apr 28.

Strasser K et al. (2002). Strässer K, Masuda S, Mason P, Pfannstiel J, Oppizzi M, Rodriguez-Navarro S, Rondón AG, Aguilera A, Struhl K, Reed R, Hurt E. TREX is a conserved complex coupling transcription with messenger RNA export. *Nature.* **417**(6886):304-8. Epub 2002 Apr 28.

Svejstrup JQ and Reid J (2004). DNA damage-induced Def1-RNA polymerase II interaction and Def1 requirement for polymerase ubiquitylation in vitro. *J Biol Chem* **279**(29):29875-8

Tanno M *et al.* (2010). Tanno M, Kuno A, Yano T, Miura T, Hisahara S, Ishikawa S, Shimamoto K, Horio Y. Induction of manganese superoxide dismutase by nuclear translocation and activation of SIRT1 promotes cell survival in chronic heart failure. *J Biol Chem.* **285**(11):8375-82.

Taunton J *et al.* (1996). Taunton J, Hassig CA, Schreiber SL. A mammalian histone deacetylase related to the yeast transcriptional regulator Rpd3p. *Science.* 272(5260):408-11.

Tcherepanova I *et al.* (2000). Tcherepanova I, Puigserver P, Norris JD, Spiegelman BM, McDonnell DP. Modulation of estrogen receptor-alpha transcriptional activity by the coactivator PGC-1. *J Biol Chem.* **275**(21):16302-8.

Teixeira A *et al.* (2004). Teixeira A, Tahiri-Alaoui A, West S, Thomas B, Ramadass A, Martianov I, Dye M, James W, Proudfoot NJ, Akoulitchev A. Autocatalytic RNA cleavage in the human beta-globin pre-mRNA promotes transcription termination. *Nature.* **432**(7016):526-30.

Thieffry D and Sarkar S (1998). Forty years under the central dogma. *Trends Biochem Sci* **23**(8):312-6.

Tissenbaum HA and Guarente L (2001). Increased dosage of a sir-2 gene extends lifespan in Caenorhabditis elegans. *Nature.* **410**(6825):227-30

Tontononoz P et *al*. (1994). Tontonoz P[1], Hu E, Spiegelman BM. Stimulation of adipogenesis in fibroblasts by PPAR gamma 2, a lipid-activated transcription factor. *Cell.* **79**(7):1147-56.

Tsukada Y *et al.* (2006). Tsukada Y, Fang J, Erdjument-Bromage H, Warren ME, Borchers CH, Tempst P, Zhang Y. Histone demethylation by a family of JmjC domain-containing proteins. *Nature.* **439**(7078):811-6.

Tsukiyama T *et al.* (1994). Tsukiyama T, Becker PB, Wu C. ATP-dependent nucleosome disruption at a heat-shock promoter mediated by binding of GAGA transcription factor. *Nature.* **367**(6463):525-32.

Turner BM (2000). Histone acetylation and an epigenetic code. *Bioessays*. **22**(9):836-45.

Ueki N et *al*. (1998). Ueki N, Oda T, Kondo M, Yano K, Noguchi T, Muramatsu M. Selection system for genes encoding nuclear-targeted proteins. *Nat Biotechnol.* **16**(13):1338-42.

Ule J *et al.* (2003). Ule J, Jensen KB, Ruggiu M, Mele A, Ule A, Darnell RB. CLIP identifies Nova-regulated RNA networks in the brain. *Science.* **302**(5648):1212-5.

Valle I et *al*. (2005). Valle I, Alvarez-Barrientos A, Arza E, Lamas S, Monsalve M. PGC-1alpha regulates the mitochondrial antioxidant defense system in vascular endothelial cells. *Cardiovasc Res*. **66**(3):562-73.

van der Horst A *et al.* (2004). van der Horst A, Tertoolen LG, de Vries-Smits LM, Frye RA, Medema RH, Burgering BM. FOXO4 is acetylated upon peroxide stress and deacetylated by the longevity protein hSir2(SIRT1). *J Biol Chem*. **279**(28):28873-9.

van der Knaap JA *et al*. (2005). van der Knaap JA, Kumar BR, Moshkin YM, Langenberg K, Krijgsveld J, Heck AJ, Karch F, Verrijzer CP. GMP synthetase stimulates histone H2B deubiquitylation by the epigenetic silencer USP7. *Mol Cell.* **17**(5):695-707.

van der Knaap JA *et al.* (2010). van der Knaap JA, Kozhevnikova E, Langenberg K, Moshkin YM, Verrijzer CP. Biosynthetic enzyme GMP synthetase cooperates with ubiquitin-specific protease 7 in transcriptional regulation of ecdysteroid target genes. *Mol Cell Biol.* **30**(3):736-44.

Vaquero A *et al.* (2003). Vaquero A, Loyola A, Reinberg D. The constantly changing face of chromatin. *Sci Aging Knowledge Environ.* 2003(**14**):RE4.

Vaziri H *et al.* (2001). Vaziri H, Dessain SK, Ng Eaton E, Imai SI, Frye RA, Pandita TK, Guarente L, Weinberg RA. hSIR2(SIRT1) functions as an NAD-dependent p53 deacetylase. *Cell*. **107**(2):149-59.

Vega RB *et al.* (2000). Vega RB, Huss JM, Kelly DP. The coactivator PGC-1 cooperates with peroxisome proliferator-activated receptor alpha in transcriptional control of nuclear genes encoding mitochondrial fatty acid oxidation enzymes. *Mol Cell Biol.* **20**(5):1868-76.

Wagenmakers AJ *et al.* (1980). Wagenmakers AJ, Reinders RJ, van Venrooij WJ. Cross-linking of mRNA to proteins by irradiation of intact cells with ultraviolet light. *Eur J Biochem.* **112**(2):323-30.

Wang A *et al.* (2002). Wang A, Kurdistani SK, Grunstein M. Requirement of Hos2 histone deacetylase for gene activity in yeast. *Science.* **298**(5597):1412-4.

Wang F *et al.* (2012). Wang F, Chan CH, Chen K, Guan X, Lin HK, Tong Q. Deacetylation of FOXO3 by SIRT1 or SIRT2 leads to Skp2-mediated FOXO3 ubiquitination and degradation. *Oncogene.* **31**(12):1546-57.

Weake VM and Workman JL (2008). Histone ubiquitination: triggering gene activity. *Mol. Cell.* **29**(6):653-63.

Weber M *et al***.** (2007). Weber M, Hellmann I, Stadler MB, Ramos L, Pääbo S, Rebhan M, Schübeler D. Distribution, silencing potential and evolutionary impact of promoter DANN methylation in the human genome. *Nat Genet* **39**(4):457-66.

Weiss SB and Nakamoto T (1961). On the participation of DNA in RNA biosynthesis. *Proc Natl Acad Sci U S A.* **47**:694-7.

Wilkins RC and Lis JT (1997). Dynamics of potentiation and activation: GAGA factor and its role in heat shock gene regulation. *Nucleic Acids Res.* **25**(20):3963-8.

Wind M and Reines D (2000). Transcription elongation factor SII. *Bioessays.* **22**(4):327-36.

Wu CH *et al.* (2003). Wu CH, Yamaguchi Y, Benjamin LR, Horvat-Gordon M, Washinsky J, Enerly E, Larsson J, Lambertsson A, Handa H, Gilmour D. NELF and DSIF cause promoter proximal pausing on the hsp70 promoter in Drosophila. *Genes Dev*. **17**(11):1402-14.

Wu Z *et al.* (1999). Wu Z, Puigserver P, Andersson U, Zhang C, Adelmant G, Mootha V, Troy A, Cinti S, Lowell B, Scarpulla RC, Spiegelman BM. Mechanisms controlling mitochondrial biogenesis and respiration through the thermogenic coactivator PGC-1. *Cell.* **98**(1):115-24.

Yang L et *al.* (2000). Yang L, Embree LJ, Hickstein DD. TLS-ERG leukemia fusion protein inhibits RNA splicing mediated by serine-arginine proteins. *Mol Cell Biol.* **20**(10):3345-54.

Yeo GW *et al.* (2009). Yeo GW, Coufal NG, Liang TY, Peng GE, Fu XD, Gage FH. An RNA code for the FOX2 splicing regulator revealed by mapping RNA-protein interactions in stem cells. *Nat Struct Mol Biol.* **16**(2):130-7.

Yoon JC *et al*. (2001). Yoon JC, Puigserver P, Chen G, Donovan J, Wu Z, Rhee J, Adelmant G, Stafford J, Kahn CR, Granner DK, Newgard CB, Spiegelman BM. Control of hepatic gluconeogenesis through the transcriptional coactivator PGC-1. *Nature*. **413**(6852):131-8.

Yudkovsky N *et al.*, 2000; Yudkovsky N, Ranish JA, Hahn S. A transcription reinitiation intermediate that is stabilized by activator. *Nature.* **408**(6809):225-9.

Zawel L *et al.* (1995). Zawel L, Kumar KP, Reinberg D. Recycling of the general transcription factors during RNA polymerase II transcription. *Genes Dev.* **9**(12):1479-90.

Zhao J *et al*. (2010). Zhao J, Ohsumi TK, Kung JT, Ogawa Y, Grau DJ, Sarma K, Song JJ, Kingston RE, Borowsky M, Lee JT. Genome-wide identification of polycomb-associated RNAs by RIP-seq. *Mol Cell.* **40**(6):939-53.

Zhou Y and Grummt I (2005). The PHD finger/bromodomain of NoRC interacts with acetylated histone H4K16 and is sufficient for rDNA silencing. *Curr Biol.* **15**(15):1434-8.

Zippo A *et al.* (2009). Zippo A, Serafini R, Rocchigiani M, Pennacchini S, Krepelova A, Oliviero S. Histone crosstalk between H3S10ph and H4K16ac generates a histone code that mediates transcription elongation. *Cell*. **138**(6):1122-36.

Zisoulis DG *et al.* (2010). Zisoulis DG, Lovci MT, Wilbert ML, Hutt KR, Liang TY, Pasquinelli AE, Yeo GW. Comprehensive discovery of endogenous Argonaute binding sites in Caenorhabditis elegans. *Nat Struct Mol Biol*. **17**(2):173-9.